Transport of artificial virus-like nano-carriers via m cell mediated transcytosis

by

Tianjian Tong

A dissertation submitted to the graduate faculty

in partial fulfillment of the requirements for the degree of

DOCTOR OF PHILOSOPHY

Major: Agricultural and Biosystems Engineering

Program of Study Committee:
Chenxu Yu, Major Professor
Cathy L. Miller
Qun Wang
Adina Howe
Kurt Rosentrater

The student author, whose presentation of the scholarship herein was approved by the program of study committee, is solely responsible for the content of this dissertation. The Graduate College will ensure this dissertation is globally accessible and will not permit alterations after a degree is conferred.

Iowa State University

Ames, Iowa

2021

DEDICATION

Dedicated to my grand mom Xinzhen Qiao, my parents Man Jiang and Jin Tong, my hero Kobe Bryant, and my cat Wakanda!

TABLE OF CONTENTS

NOMENCLATURE

MRV	Mammalian orthoreovirus
GNC	Gold nanocages
HSS	Hollowed silica nanospheres
PLL	Poly-l-lysine
AVN	Artificial virus-like nanocarriers
M cells	Microfold cells
MALTs	Mucosal associated lymphoid tissues
Rank L	Receptor activator of nuclear factor kappa-B ligand

ACKNOWLEDGMENTS

I would like to thank my major professor, Dr Chenxu Yu, for his endless support and patience. We established a Phil Jackson-Kobe Bryant like relationship during my time in Iowa State University. Dr Yu hand-picked me to be his Ph.D. student and gave me both guidance and freedom. I would like to thank Dr Qun Wang for his help, guidance, and opportunities that he provided me. I would like to thank Dr Cathy L Miller for her taking me under her wing for almost 5 years. During my time in her lab, she treated me as one of her own, gave me patience and guidance. I would like to thank my committee members: Dr Kurt Rosentrater and Dr Adina Howe for their understanding and guidance. I would like to thank our department DOGE, Dr Freeman for his help and understanding.

In addition, I would like to thank my group members: Dr Shaowei Ding, Dr Chao Wang, Dr Qing He, Cheng Pan, Fouad Habib, Casey Nelson, and Jingyi Yang. Dr Sherry Qi from Dr Wang's group. Dr Miller's group members: Dr Luke Bussiere, Debarpan Dhar, Nicole Jandick and Dr Promisree Choudhury. My friends at Iowa State Dr Bowei Zhang, Dr Jiaxuan Wu, Dr Jiahao Chen, Dr Chenglong Wang, Dr Ran Li, Dr Guang Han, Without the help from these colleagues and good friends, I couldn't get to this point.

I would also like to thank all my haters, and the people who betrayed me. Without you guys, I wouldn't be this motivated to prove that all of you were wrong. I would also like to thank all the girls I loved and the girls I lost during my Ph.D. period for their love and time.

Special thanks: The Late Great Mr. Kobe Bean Bryant aka THE BLACK MAMBA for the inspiration he provided with his entire basketball career and his post basketball career. The Mamba Mentality inspired me during failure and frustration. I hope he can now rest in peace in heaven. Special thanks: Miss Zoey Jia, for her countless help on several prospects: business opportunities,

communication skills, and provided me a safe haven. Special thanks: Mr. Xiaoguang Qi, Mr. Pai Liu, Dr Tairan Wang, Mr. Yu Shi, Mr. Jingzhan Li, Mr. Zhipeng Liang, Dr Yuxuan Zhang, Mr. Wei Sun, Dr Ke Zhang and Dr Xu Wang for being my brothers from another mother.

Very special thanks: Miss Chenrui Niu, for cheering me up during my down time, and all the conversations and beautiful music & stories we shared during my time in Ames. Very special thanks: my cat “Wakanda”, he gives me lights, joy and protection during my time with him.

Last, but not least, I must express my gratitude for my grandparents Xinzhen Qiao and Duanfang Jiang, my parents Man Jiang and Jin Tong, my uncle Qing Jiang, my aunties Wu Jiang, Ping Yang and Shuyu Tong. I would also like to thank my cousins: Qinqin Jiang, Xiaoming Liu, John Lin, and Joanna Lin. None of my accomplishments as a graduate student would not have been possible without their unconditional love.

ABSTRACT

Compared with subcutaneous or intramuscular routes for vaccination, oral vaccination or vaccine delivery via gastrointestinal mucosa has tremendous potential as it is easy to administer and pain free. Robust immune responses can be triggered successfully once vaccine carried antigen reaches the mucosal associated lymphoid tissues (MALTs). However, the absence of an efficient delivery method has always been an issue for successful oral vaccine development. In our study, inspired by mammalian orthoreovirus (MRV) transport into gut mucosal lymphoid tissue via Microfold cells (M cells), artificial virus-like nanocarriers (AVNs, gold nanocages-based and hollowed silica nanospheres-based), consisting of gold nanocages/hollowed silica spheres functionalized with the σ1 protein from mammalian reovirus (MRV), were tested as an effective oral vaccine delivery vehicle utilizing M cell-mediated transcytosis pathway for effective transport of payloads. Poly-l-lysine's role as coating material for both AVNs was also tested. Gold AVN and Silica AVN were shown to have a significantly higher transport total compared to other experimental groups across M cell incorporated mouse organoid monolayers. Thus, we proved that with σ1 protein functionalization and poly-l-lysine (PLL) coating, a potentially highly effective transport system for oral vaccines can be developed that target M cell mediated transcytosis pathway to deliver vaccines to MALTs regardless of the type of nanoparticles.

CHAPTER 1. INTRODUCTION AND BACKGROUND

1.1 Type 1 Reovirus Adherence to M Cell Apical Surfaces: T1L σ1 Protein and α 2-3-Linked Sialic Acid

Mammalian reovirus (MRV) is a nonenveloped virus which has a size of around 85 nm. It can infect a host's Peyer's patch mucosa by specifically adhered to M cells and explore the M cells mediated transcytosis to go through the gastrointestinal epithelia [1,2]. Type 1 Lang (T1L) mammalian reovirus (MRV) can adheres to the apical surfaces of M cells but not the enterocytes (the gastrointestinal lining is mainly consisted of enterocytes) when in contact with an adult mice's intestinal lumens [3]. It has been previously reported that the in vivo infection of MRV requires proteolytic processing of the viral outer capsid by enzymes in the mice's intestinal lumen [4–6], which leads to the form of infectious subviral particles (ISVP) and results in a form of cleaved membrane penetration protein μ1 [6–8]. In addition, in this process, μ1 lost σ3 protein which can protect the μ1[7–9]. It was previously reported that in order for T1L MRV to adherence to M cells in mice, ISVP is the required form [1,3].

The MRV σ1 protein have played a critical role in mediating hemagglutination (HA) as viral version of adhesin, in addition, it can also bind to multiple types of cultured cells [3,10–18]. Tropisms of reovirus strains T1L and T3D in mice can be differed by σ1 protein [6,10,19–21]. Both T1L and T3D σ1 protein had a domain with lectin-like structure, however, the specificities of carbohydrate biding and the location of T1L and T3D in σ1 protein are different [3]. It has been previously reported that σ1 protein plays a significant role in HA activities[3]. Moreover, it is the α 2-3-linked sialic acid on the M cell surface are the one that adherence to σ1 protein[10,11,13–15,17,18,22,23]. MRVs can pass through the gastrointestinal epithelia by exploring selective adherence to M cells via the α 2-3-linked sialic acid[3].

Intestinal epithelial cells are very extreme, the two side of intestinal epithelia cells, apical membrane and basolateral membranes cannot be more different in their composition[3]. Vivo test showed that the epithelial tight junctions can keep its polarity, and force the MRV to contact to the apical side[3]. As we mentioned before, intestinal epithelial cells are polarized, on the basolateral membranes side, there is a receptor called the human and murein junction adhesion molecule (JAM-A)[3,10,24]. It is also reported that in an isolated enterocytes form, MRV can binds to basolateral cell surfaces due the JAM-A adherence[25,26]. JAM-A can link to both T1L and T3D MRV, but since it is at the basolateral membranes side, it is not available for the MRV to access in the intestinal lumen[3]. In Fig. 1, it showed that ISVP can adherence to the apical side of the epithelial cells, with M cells presence[3].

There is sufficient coating of glycoconjugates at the surface of apical membranes of gasttrointestinal epithelial cells[3]. To further confirm the adherences between T1L and T3D MRV and α 2-3-linked sialic acid, a test of rabbit Peyer's patch mucosal tissue binding to the viruses has been reported[3]. T1L MRV can bind to certain M cells but T3D cannot[3]. It was reported that adherence of T1L MRV and other type 1 isolates with apical side which have glycoconjugates consist of NeuAc α 2-3 are achievable[3]. Furthermore, lectins MAL-I and MAL-II can recognize the α 2-3-linked sialic acid[3]. After compare T1L MRV, T3D MRV, and the viral cores of both MRVs, T1L hemagglutinin σ1 is the key to the adherence of MRVs to M cells[3].

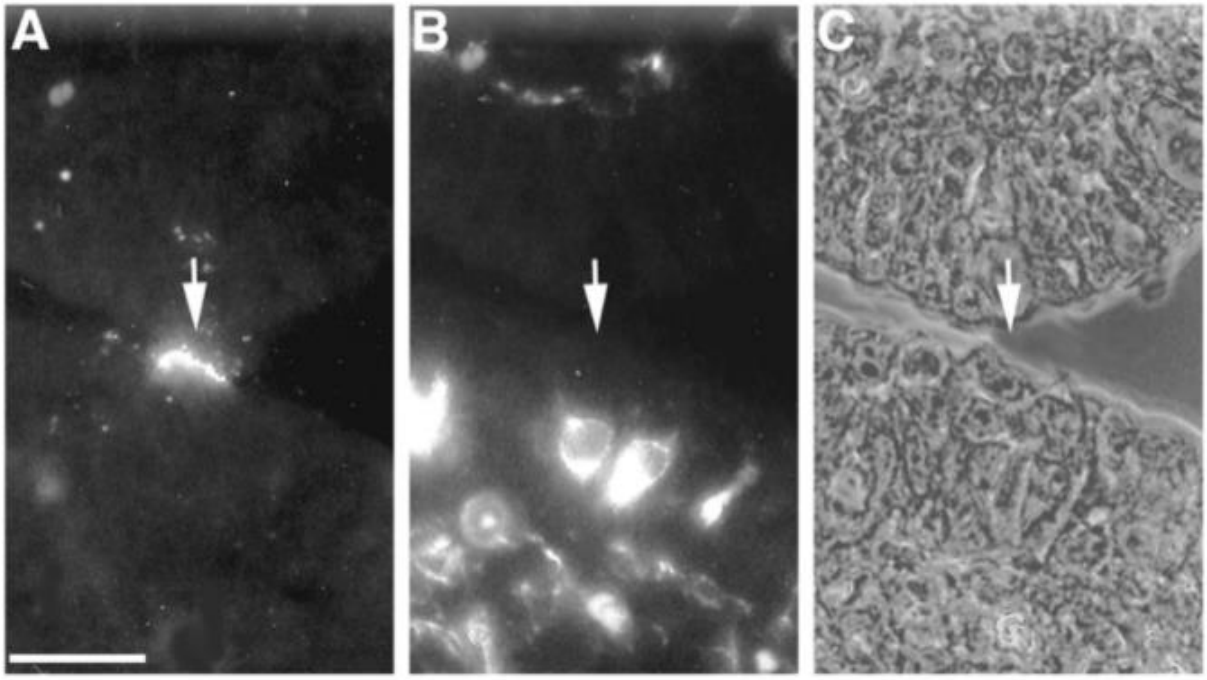

Fig 1.1 T1L MRV adherence to apical side of M cells of rabbit Peyer's patch in an overlay assay section. (A) fluorescence image of ISVP adhered to epithelial cells' apical side (B) fluorescence image of Mab specific vimentin dual labeling methods to confirm the presence of M cells; (C) phase-contrast image of the same section to show the M cell structures.[3]

1.2 M cells incorporated organoids

Ultimately, vaccine transport/delivery needs to be studied in vivo to properly evaluate the effectiveness of transport systems. However, *in vivo* testing is both time and cost consuming[31]. Hence, *in vitro* test models have been developed by growing small "mini-gut" type organoids out of gastrointestinal stem cells which have similar epithelial structures as actual gastrointestinal lining. Organoids is a 3D multicellular in vitro tissue that is constructed to mimic to it related in vivo organ[27]. Receptor activator of nuclear factor kappa-B ligand (Rank L) is a protein that affect the immune systems and manipulate the regeneration and remodeling of bone cells[28–31].

It is previously reported that by adding proper amount of Rank L, M cells can be induced in organoids[32]. This finding made M cell incorporated organoids a very useful tools as a platform

for testing the MRV-type transport of antigens as well as potential drug/vaccine delivery vehicles to MALTs [33-33]. It is previously reported that at the apical side of M cells from the mouse Peyer's patch, there are two receptors' expression which can be detected, C5a receptor and glycoprotein 2 receptor [34,35], that can be used as markers to identify the presence of M cells. In this study, both were utilized to demonstrate the successful conversion of stem cells in organoids into M cells.

In Fig. 1.2a, we can see that GP2 marker only expressed when Rank L is added. In contrast, the control group, which had no Rank L, there was no GP2 expression. In Fig 1.2b, at day 1 of Rank L addition, there was no GP2 expression, at day 3, GP2 expression was detected. In Fig. 1.2c & 2d, again, GP2 markers only showed up in Rank L treated groups.

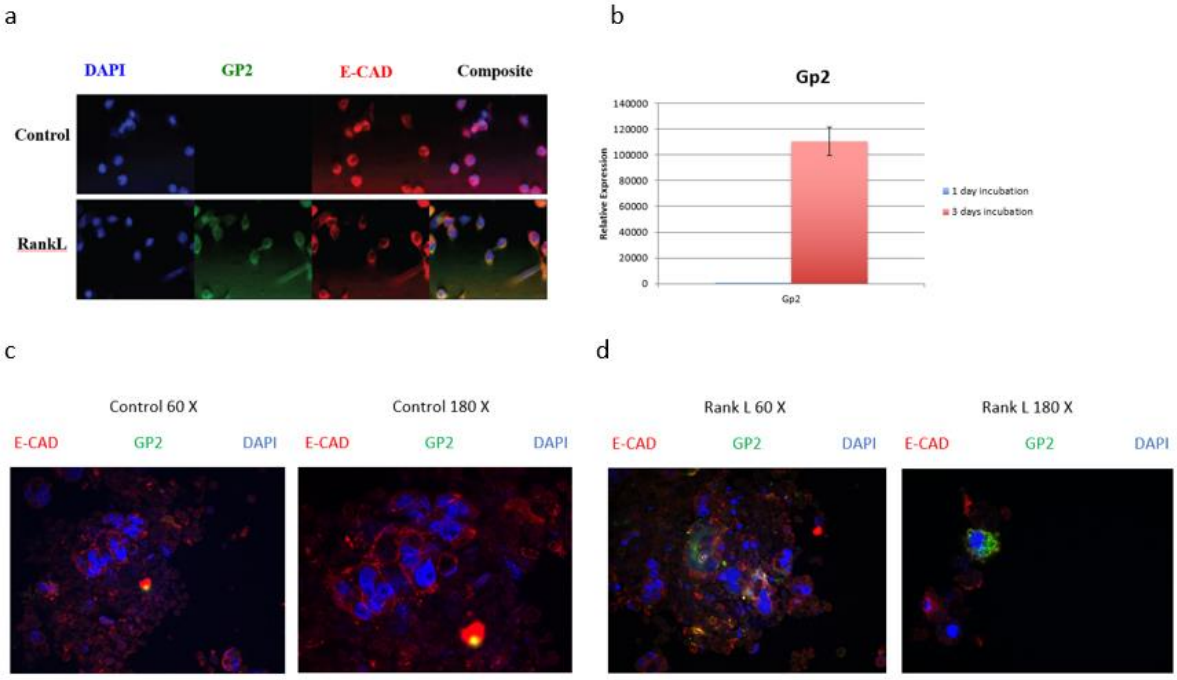

Fig 1.2 Detection of microfold cells in 3D mouse organoids and 2D organoid-derived monolayers. (a)Immunofluorescence images of untreated and three-day Rank L-treated 3D organoids stained with antibodies against GP2 (green) and E-Cadherin (red). Nuclei are stained with DAPI (blue). (b) RT-qPCR analysis for expression of GP2-specific mRNA isolated from untreated and Rank L-treated organoids. (c) Immunofluorescence images of untreated organoid monolayers stained with antibodies against GP2 (green) and E-cadherin (red). Nuclei are stained with DAPI (blue). (d) Immunofluorescence images of Rank L-treated organoid monolayers

stained with antibodies against GP2 (green) and E-cadherin (red). Nuclei are stained with DAPI (blue).

1.3 Oral drug/vaccine delivery

There are five major drug delivery methods: intravenous (IV), intranasal (IN), intramuscular (IM), intradermal (ID), and the key of this study, oral[36]. Oral delivery methods have several advantages compared to the other four drug delivery methods (IV, IN, IM, and ID): cost-efficiency, better safety, patient-friendly, and easier to administer [34,36]. Although oral drug/vaccine delivery methods are very promising and attractive, there are specific barriers and challenges that limited their application [34,36]. In additional, oral vaccine delivery methods are believed to be able to trigger both local and system immune responses[36]. In this section, we will discuss the major challenges of oral delivery methods.

The difficulties for oral drug delivery methods can be divided into two types: chemical and biological. We will focus on the biological challenges first.

1.3.1 Biological challenges

Oral vaccine delivery is happening in the gastrointestinal (GI) tract[36]. GI tract can be classified into the upper GI tract and the lower GI tract[36]. Upper GI tract includes duodenum (the inimical part of small intestine), pharynx, esophagus, and stomach [36]. Lower GI tract included jejunum, ileum, and the large intestine section including cecum rectum, and colon[36].

1) The lumen of the GI tract is covered by mucosa, sub-mucosa and muscularis mucosa[37]. These mucosal layers (mucosa, sub-mucosa, and muscularis mucosa) are mainly consisted of epithelial cells[34], which are significant for oral drug delivery vehicles to transport into mucosal space and trigger immune response[36]. In another word, lumen presents the first barrier for oral drug delivery.

2) Secondly, mucus proposes another biological challenge. Mucus is everyway in the GI tract, and the texture of mucus is viscous, elastic and even sticky to some extent[36], this texture will cause problems for the oral drug delivery vehicle itself[36]. The lumen challenge is attacking the payload, and the mucus, they are attacking the oral drug delivery vehicle. There are several more components inside the mucus, which are salts, bacteria, carbohydrates, antibodies and more[36].
3) Thirdly, gastric enzymes (gelatinase & pepsin) could degrade the payloads (i.e., the medically effective ingredients of a drug/vaccine)[36]. Furthermore, enzymes secreted in pancreas could enter the intestinal lumen which could also degrade payloads afterwards[36]

In order to have a successful oral vaccine delivery, the vehicles need to protect the payloads from degradation, they also need to find a way to transport the payloads through enterocytes to get to the mucosal space to trigger the immune response both local and systemic[34,36].

1.3.2 Chemical challenges

The harsh acidic condition of upper GI tract, especially in the stomach, can easily denature and degrade the payloads [35-38]. The oral delivery vehicles need to offer some protection against this low pH environment. From the synthetization point of view, what types of oral delivery vehicles to choose from could pose as another set of chemical challenges. This includes, types of materials, shape/size of the oral drug delivery vehicles, coating materials, and ways get them through the enterocytes. Another thing to consider is whether the delivery vehicle could provide some release control to facilitate more effective delivery of the payloads.

Materials: there are several types of materials have been studied for oral drug delivery vehicles: hydrogels[39–42], inorganic nanoparticles like gold nanoparticles[34], and silica nanoparticles[43],

polymers (nonhydrogels) [44,45]. As to how to protect the payload inside of the oral drug delivery vehicles, different types of materials have different answers.

1) Hydrogels: hydrogels have its own advantage of easy compositional control, tunable mechanical properties, and hydrophilic characteristics[36]. Porous hydrogel matrixes have been utilized widely for increasing the loading capacity for payloads inside the hydrogel systems [36]. Hydrogel platforms are typically micro-sized, it could provide slow release, but typically no targeted delivery.
2) Inorganic nanoparticles such as gold nanoparticles and silica nanoparticles. These inorganic nanoparticles are chemically inert; hence they are generally considered non-cytotoxic and could be safely administered to patients. To increase loading capacity of the inorganic oral drug delivery vehicles, hollowed structures are preferable[34, 46]. However, without protection, payloads can diffuse into the hollowed structures, they can also diffused out at a similar rate [34]. Thus, coating is becoming very important. Coating materials for the hollowed structure inorganic nanoparticle-based oral drug delivery vehicles can sever two purposes, one is to hold the payload inside the oral drug delivery vehicles during the transporting process, the other one is to provide protection for the payload [47].
3) Polymers (not including hydrogels): polymer oral drug delivery vehicle have its own advantages, as the polymers often time can serve as both payload carriers and protectors[44,45].

The next challenge is how to get through the enterocytes with effectiveness, which is the key focus of this research. We developed a novel way to get the oral delivery vehicles through the enterocytes. In this approach, we functionalized inorganic nanoparticles with σ1 protein on the

surface[34]. Inspired by how MRVs invade the M cells, we design this σ1 protein functionalized artificial virus-like nanocarriers (AVNs) to utilize the σ1 protein- α 2-3-linked sialic acid adhesion to explore the M cells transcytosis[34].

1.4 Dissertation organization

In Chapter 2, synthesis and functionalization of inorganic nanoparticles (i.e., gold nanocages, hollowed silica nanospheres) were discussed, and the extraction and purification of MRV T1L σ1 proteins were reported. In Chapter 3, we reported the results on σ1 protein functionalized gold nanocage AVNs and its transport performance of a model payload (R6G) was characterized on M cell incorporated organoid monolayer systems. In Chapter 4, a different AVN system (hollowed silica nanospheres, HSS) was investigated, and a poly-l-lysine coating procedure was implemented to provide payload protection and release control. In Chapter 5, the effects of microfold cell modulated by Rank L in intestinal monolayers affecting transport efficiency of sigma-1 functionalized nanocarriers were investigated. And, at last, Chapter 6 offered some thoughts on future directions.

1.5 References

[1] H. M. Amerongen, G. A. Wilson, B. N. Fields and M. R. Neutra, *J. Virol.*, , DOI:10.1128/jvi.68.12.8428-8432.1994.

[2] J. L. Wolf, D. H. Rubin, R. Finberg, R. S. Kauffman, A. H. Sharpe, J. S. Trier and B. N. Fields, *Science (80-.).*, , DOI:10.1126/science.6259737.

[3] A. Helander, K. J. Silvey, N. J. Mantis, A. B. Hutchings, K. Chandran, W. T. Lucas, M. L. Nibert and M. R. Neutra, *J. Virol.*, , DOI:10.1128/JVI.77.14.7964-7977.2003.

[4] Bass DM, Trier JS, Dambrauskas R and Wolf JL, *Lab. Investig.*, 1988, **58**, 226–235.

[5] D. K. Bodkin, M. L. Nibert and B. N. Fields, *J. Virol.*, , DOI:10.1128/jvi.63.11.4676-4681.1989.

[6] M. L. Nibert, D. B. Furlong and B. N. Fields, *J. Clin. Invest.*, , DOI:10.1172/JCI115369.

[7] R. D. Fraser, D. B. Furlong, B. L. Trus, M. L. Nibert, B. N. Fields and A. C. Steven, *J. Virol.*, , DOI:10.1128/jvi.64.6.2990-3000.1990.

[8] M. L. Nibert, T. S. Dermody and B. N. Fields, *J. Virol.*, , DOI:10.1128/jvi.64.6.2976-2989.1990.

[9] K. Dryden, G. Wang, M. Yeager, M. Nibert, K. Coombs, D. Furlong, B. Fields and T. Baker, *J. Cell Biol.*, , DOI:10.1083/jcb.122.5.1023.

[10] E. S. Barton, J. C. Forrest, J. L. Connolly, J. D. Chappell, Y. Liu, F. J. Schnell, A. Nusrat, C. A. Parkos and T. S. Dermody, *Cell*, , DOI:10.1016/S0092-8674(01)00231-8.

[11] E. S. Barton, J. L. Connolly, J. C. Forrest, J. D. Chappell and T. S. Dermody, *J. Biol. Chem.*, , DOI:10.1074/jbc.M004680200.

[12] K. Chandran, X. Zhang, N. H. Olson, S. B. Walker, J. D. Chappell, T. S. Dermody, T. S. Baker and M. L. Nibert, *J. Virol.*, , DOI:10.1128/JVI.75.11.5335-5342.2001.

[13] J. D. Chappell, J. L. Duong, B. W. Wright and T. S. Dermody, *J. Virol.*, , DOI:10.1128/JVI.74.18.8472-8479.2000.

[14] T. S. Dermody, M. L. Nibert, R. Bassel-Duby and B. N. Fields, *J. Virol.*, , DOI:10.1128/jvi.64.10.5173-5176.1990.

[15] M. L. Nibert, J. D. Chappell and T. S. Dermody, *J. Virol.*, , DOI:10.1128/jvi.69.8.5057-5067.1995.

[16] A. F. Pacitti and J. R. Gentsch, *J. Virol.*, , DOI:10.1128/jvi.61.5.1407-1415.1987.

[17] R. W. Paul and P. W. K. Lee, *Virology*, , DOI:10.1016/0042-6822(87)90351-5.

[18] D. H. Rubin, J. D. Wetzel, W. V Williams, J. A. Cohen, C. Dworkin and T. S. Dermody, *J. Clin. Invest.*, , DOI:10.1172/JCI116147.

[19] H. L. Weiner, M. L. Powers and B. N. Fields, *J. Infect. Dis.*, , DOI:10.1093/infdis/141.5.609.

[20] K. L. Tyler, M. A. Mann, B. N. Fields and H. W. Virgin, *J. Virol.*, , DOI:10.1128/jvi.67.6.3446-3453.1993.

[21] K. L. Tyler, H. W. Virgin, R. Bassel-Duby and B. N. Fields, *J. Exp. Med.*, , DOI:10.1084/jem.170.3.887.

[22] J. D. Chappell, E. S. Barton, T. H. Smith, G. S. Baer, D. T. Duong, M. L. Nibert and T. S. Dermody, *J. Virol.*, , DOI:10.1128/JVI.72.10.8205-8213.1998.

[23] J. D. Chappell, V. L. Gunn, J. D. Wetzel, G. S. Baer and T. S. Dermody, *J. Virol.*, , DOI:10.1128/jvi.71.3.1834-1841.1997.

[24] A. E. Prota, J. A. Campbell, P. Schelling, J. C. Forrest, M. J. Watson, T. R. Peters, M. Aurrand-Lions, B. A. Imhof, T. S. Dermody and T. Stehle, *Proc. Natl. Acad. Sci.*, , DOI:10.1073/pnas.0937718100.

[25] D. M. Bass, D. Bodkin, R. Dambrauskas, J. S. Trier, B. N. Fields and J. L. Wolf, *J. Virol.*, , DOI:10.1128/jvi.64.4.1830-1833.1990.

[26] D. B. Weiner, K. Girard, W. V. Williams, T. McPhillips and D. H. Rubin, *Microb. Pathog.*, , DOI:10.1016/0882-4010(88)90078-2.

[27] H. Clevers, *Cell*, , DOI:10.1016/j.cell.2016.05.082.

[28] B. R. Wong, J. Rho, J. Arron, E. Robinson, J. Orlinick, M. Chao, S. Kalachikov, E. Cayani, F. S. Bartlett, W. N. Frankel, S. Y. Lee and Y. Choi, *J. Biol. Chem.*, , DOI:10.1074/jbc.272.40.25190.

[29] D. M. Anderson, E. Maraskovsky, W. L. Billingsley, W. C. Dougall, M. E. Tometsko, E. R. Roux, M. C. Teepe, R. F. DuBose, D. Cosman and L. Galibert, *Nature*, , DOI:10.1038/36593.

[30] C. G. Mueller and E. Hess, *Front. Immunol.*, , DOI:10.3389/fimmu.2012.00261.

[31] T. Wada, T. Nakashima, N. Hiroshi and J. M. Penninger, *Trends Mol. Med.*, , DOI:10.1016/j.molmed.2005.11.007.

[32] M. B. Wood, D. Rios and I. R. Williams, *Am. J. Physiol. Physiol.*, , DOI:10.1152/ajpcell.00108.2016.

[33] S. Karandikar, A. Mirani, V. Waybhase, V. B. Patravale and S. Patankar, in *Nanostructures for Oral Medicine*, Elsevier, 2017.

[34] T. Tong, Y. Qi, L. D. Bussiere, M. Wannemuehler, C. L. Miller, Q. Wang and C. Yu, *Nanoscale*, , DOI:10.1039/D0NR03680C.

[35] S.-H. Kim, D.-I. Jung, I.-Y. Yang, J. Kim, K.-Y. Lee, T. Nochi, H. Kiyono and Y.-S. Jang, *Eur. J. Immunol.*, , DOI:10.1002/eji.201141592.

[36] B. Homayun, X. Lin and H.-J. Choi, *Pharmaceutics*, , DOI:10.3390/pharmaceutics11030129.

[37] H. Cheng, *Am. J. Anat.*, , DOI:10.1002/aja.1001410404.

[38] J. Huang, Q. Shu, L. Wang, H. Wu, A. Y. Wang and H. Mao, *Biomaterials*, , DOI:10.1016/j.biomaterials.2014.10.059.

[39] A. S. Hoffman, *Adv. Drug Deliv. Rev.*, , DOI:10.1016/j.addr.2012.09.010.

[40] J. Li and D. J. Mooney, *Nat. Rev. Mater.*, , DOI:10.1038/natrevmats.2016.71.

[41] E. Caló and V. V. Khutoryanskiy, *Eur. Polym. J.*, , DOI:10.1016/j.eurpolymj.2014.11.024.

[42] Q. Chai, Y. Jiao and X. Yu, *Gels*, , DOI:10.3390/gels3010006.

[43] H. Zhang, D. Liu, M.-A. Shahbazi, E. Mäkilä, B. Herranz-Blanco, J. Salonen, J. Hirvonen and H. A. Santos, *Adv. Mater.*, , DOI:10.1002/adma.201400953.

[44] S. Maghrebi, C. A. Prestidge and P. Joyce, *Expert Opin. Drug Deliv.*, , DOI:10.1080/17425247.2019.1605353.

[45] S. Rao and C. A. Prestidge, *Expert Opin. Drug Deliv.*, , DOI:10.1517/17425247.2016.1151872.

[46] N. Jatupaiboon, Y. Wang, H. Wu, X. Song, Y. Song, J. Zhang, X. Ma and M. Tan, *J. Mater. Chem. B*, , DOI:10.1039/C5TB00194C.

[47] C.-H. Ahn, S. Y. Chae, Y. H. Bae and S. W. Kim, *J. Control. Release*, , DOI:10.1016/j.jconrel.2004.04.002.

CHAPTER 2. GOLD NANOCAGES, HOLLOWED SILICA NANOSPHERS, AND T1L MRV SIGMA 1 PROTEIN

2.1 Gold nanocages

2.1.1 Background

The various applications of metal nanoparticles have been widely reported for their unique and tunable optical properties[1–3]. The size, shape, structure (solid or hollowed), and composition of metal nanoparticles can be custom made to impart desired properties [4–7]. Different shapes of nanoparticles has been reported as: nanowires[8], nano rods[9], nanospheres[10], nanoplates [11,12], nanocubes[13]. Galvanic replacement reactions have been reported that can introduce structural and compositional complexity[14]. The galvanic replacement reaction can be utilized to prepare hollowed metal nanoparticles[14]. The different electrochemical potential of the two metals involved are the driving force of this reaction[14]. One of the two metals serves as cathode and the other metal as anode[14]. Galvanic replacement reaction can happen at nano-size level and one metal nanostructures can be replaced by the other[14]. In this study, the synthesis of gold nanocages was achieved by utilizing silver nanocubes as the sacrificing template via the galvanic replacement reaction[14].

2.1.2 Materials and Methods

Materials

Ethylene glycol (Sigma-Aldrich), Polyvinylpyrrolidone (PVP) (Sigma-Aldrich), AgNO3 (Sigma-Aldrich), NaSO4 (Acros), HAuCl4 (Sigma-Aldrich), $HAuCl_4$ (Sigma-Aldrich), acetone, DI-water.

Methods

Ag nanocubes synthesis

1) Set up oil bath for Ag nanocubes synthesis: oil bath, 20 ml glass vile, stir bar (stir bar needs to be new or cleaned by soaking in 1:1 mixture of aqua regia and water for 2 hour or more, and then wash with DI-water), heating and stirring hotplate, and temperature thermocouple:
2) Put stir bar in the glass vial, then heat the oil bath and set the spin speed at 220 rpm, the oil bath should be heated to 160 ˚C;
3) After temperature of the oil bath is steady, add 6 ml of ethylene glycol (EG) into the glass vial, the cap of the glass vile should be loosely put on the top of the glass vial. This heating step requires one hour of time;
4) Prepare PVP in EG solution, by adding 0.07 g of PVP into 3.5 ml of EG solution, vortex for PVP/EG mixture for 20-30 minute to achieve complete solve of PVP into EG solution;
5) Prepare silver nitrate in EG solution, by adding 0.12 g of $AgNO_3$ into 2.5 ml EG solution, vortex the $AgNO_3$/EG mixture for 20-30 minute to achieve complete solve $AgNO_3$ of into EG solution;
6) Prepare 3mM sodium sulfide in EG solution, it is diluted from 30mM $NaSO_4$ EG solution, vertex for 20-30 minute;
7) After one-hour heating and stirring of the EG solution, take the loosely placed cap of the glass vial and continue the process for 10-15min. Then adding 70 μl of sodium sulfide solution to the heated and stirred EG solution;

8) After 10-15 minutes reaction, add 1.5 ml of PVP solution and 0.5 ml of $AgNO_3$ solution into the reaction;
9) After 10-15 minutes, end the reaction by take glass vial out of oil bath and added 6 ml of acetone

Ag nanocubes washing

1) Put the reaction vile into cold water bath to cool the reaction vial back to room temperature;
2) Transfer all the solution into 50 ml centrifuge tubes, centrifuge the tubes at 1,300 g for 30 minutes;
3) Get rid of supernatant and add 1 ml of DI-water, re-disperse the pellet in water by ultrasonication for one hour;
4) Transfer the solution to 2 ml centrifuge tubes, centrifuge at 9,000 g for 10 minutes;
5) Repeat step 3-4;
6) Store Ag nanocubes at 4 ˚C;

Gold nanocages synthesis

1) Synthesis set-up: glass vial, stir bar (stir bar needs to be new or cleaned by soaking in 1:1 mixture of aqua regia and water for 2 hour or more, and then wash with DI-water), heating and stirring hotplate;
2) Add 20 mg of PVP into 20 ml DI-water in a glass vial, heat the solution at 245 ˚C and stir at 220 rpm till boiling;
3) Make 10 mM $HAuCl_4$ solution and vortex for 10 minutes to complete solve in DI-water, then dilute the solution by 100 x to make 0.1 mM $HAuCl_4$ solution;

4) Add 200 μL of Ag nanocubes into the boiled solution, and keep the cap off the glass vial and let the solution boil for another 10 minutes;
5) Add 10 μL of $HAuCl_4$ into the Ag nanocubes at the time span of 2 minutes, until the desired dark blue or light blue color is reached, the total amount of $HAuCl_4$ added needs to be recorded;

Gold nanocages washing

1) Keep the heat and stir on to vaporize the DI-water and make sure the volume of the solution is down to 1-2 ml;
2) Add NaCl into the solution to make a saturated solution;
3) Pipetted all the solution out of the vial and transfer it into two 1 ml centrifuge tubes, make sure the weight is balanced;
4) Centrifuge at 2,000 g for 30 minutes and remove the supernatant;
5) Add 1 ml DI-water into each tube, and re-disperse the pellet by ultrasonication for one hour;
6) Centrifuge at 9,000 g for 10 minutes, and get rid of the supernatant;
7) Add 1 ml DI-water into each tube, and re-disperse the pellet by ultrasonication for one hour;
8) Repeat step 6-7;
9) Gold nanocages needs to be restored at 4 ˚C;

Table 2.1 Trouble shooting table[15]: three possible problems included. 1) The anticipated color changes for the silver (Ag) nanotubes synthesis were not observed. 2) Ag nanotubes appear to have rounded corners. 3) It is difficult to image samples by scanning electron microscope (SEM).

Step	Problem	Possible reasons	Solution
9	Anticipated color changes for the silver (Ag) nanocube synthesis were not observed	Stir bars were dirty	Buy new stir bars or clean using the procedure described in the text. After rinsing with copious amounts of water, check the pH of the stir bars to ensure sufficient rinsing
		Solutions were not made correctly or were not freshly made	Remake solutions and use immediately
		Reaction temperature too high or too low	Adjust the reaction temperature slightly (within 148–152 °C); slight temperature variations between reaction setups have yielded different results
		Reaction stir rate too high or too low	Adjust stir rate
		Ethylene glycol has absorbed too much water	Replace ethylene glycol
16	Ag nanocubes appear to have rounded corners	Sulfide concentration was too low or the solution was not made fresh	Try a wider range of sulfide volumes or remake sulfide solution
		Reaction was quenched too early or too late	Shorten or lengthen reaction time
		Reaction was allowed to sit too long without washing	Isolate Ag nanocubes immediately after synthesis
16 and 28	It is difficult to image samples by scanning electron microscope (SEM)	Excess poly(vinyl pyrrolidone) remains on the samples	Before SEM sample preparation, wash a small amount of product in a 1:1 ethanol to water mixture. Using this aliquot, proceed with sample preparation as described

2.1.3 Mechanism of gold nanocages synthesis

In the process of gold nanocages synthesis, Ag nanocubes are the first products we synthesize. It is in solid cube structure. And in the second step, the Ag nanocubes are used as the sacrificing template for gold to replace the silver out by the galvanic replacement reactions. This reaction can be described as an amount-controlled process. Since the gold was added slowly into the Ag nanocubes, the gold replacement of silver didn't happen just in a second. Starting from the first batch of the gold added in, through intermediate statew that both gold and silver are on the cubes together, silver is gradually replaced by gold. When the blue color (dark or light) shows up, all the silver has been replaced by the gold. And the Gold nanocages are formed.

2.1.4 Characterization of Gold nanocages

The gold nanocages were characterized by transmission electron microscopy (TEM) and UV-visible spectrometry; From Fig. 2.1a, we can see the size of gold nanocages we synthesized is around 40 nm with hollowed interior. In Fig. 2.1b, we can see that the absorption peak for this batch of gold nanocages are around 740 nm, which is size-dependent.

a b

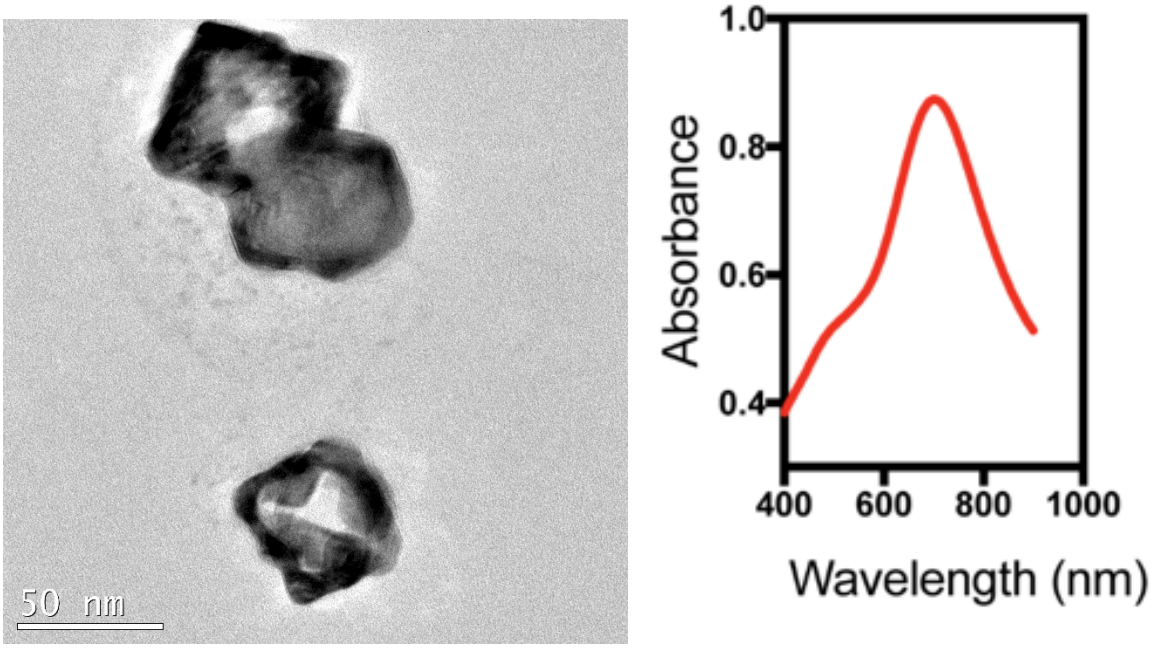

Fig 2.1 Characterization of Gold nanocages. (a) transmission electron microscopy (TEM) image; (b) UV-visible spectrometer showed the absorption of gold nanocages.[16]

2.1.5 Applications of Gold nanocages

1) Cancer treatment by gold nanocages: Gold nanocages have several characteristics that qualified them to become desirable drug delivery vehicles. First, gold nanocages are bioinert and very tough, they can survive the harsh gastric environment and protect the payload inside it[16]; Second, the structures of gold nanocages are favorable to load vaccine/ drug inside and can dramatically increase the amount of payload it can carry[16];

Third, the surface chemistry of gold nanocages allows it to cope with different coating materials, for example, poly-l-lysine, and poly (ethylene glycol) (PEG)[14,16]. With coating materials, the drug delivery vehicle can become bio-functional, and better protection of the payload and slow release control can be achieved[16].

2) Cancer diagnosis enhanced by gold nanocages: early detection of cancer is critical to protect people from suffering from cancer. Gold nanocages can play an important role in enhancing the traditional imaging techniques as the imaging enhancing agents[14]. The gold nanocages have the tunable size and absorption characteristics made this happen[14]. Both spectroscopic optical coherence tomography (SOCT) and optical coherence tomography (OCT) can be very useful in diagnosing early stage cancer as the no evading methods[14,17]
3) Photothermal therapy enhancement by gold nanocages: gold nanocages can crosslink and form large aggregates which can serve as photothermal therapeuticals. Once the crosslink of gold nanocages is triggered, the aggregates can absorb light and convert the light energy into heat, and results in a tune up of the local temperature to kill cancer cells[14].

2.2 Hollowed silica nanospheres

2.2.1 Background

Hollowed silica nanospheres (HSSs) have recently draw a lot of attention in several prospects including drug delivery[18,19], due to their unique hollowed structures and inert chemical properties [20]. They have been explored as delivery vehicles for vaccine/drug[21,22], nanoprobes for cancer diagnosis[23], and catalytic materials [24]. Traditional ways to synthesize hollowed structure nanoparticles required at least two steps to finish the reaction: soft/hard template methods[25], galvanic replacement[14,26], and hydrothermal methods[27]. Most hollowed silica nanospheres were

synthesized by soft/hard template methods[20,25]. These soft/hard template methods required the synthesis of the template first and then after the reaction, the extra template was removed, and this process could be time-consuming and expensive[20]. The template method needs to be controlled pretty precisely, and the size of hollowed silica nanospheres synthesized is limited to a very condensed size range[20]. If the desirable size of the hollowed silica nanospheres is less than 100 nm, the process to remove the core from the solid silica nanospheres could cause unnecessary conjugation and form undesired large particles if not properly controlled [20]. Large particles are not good candidates to be used as drug delivery vehicles, due to their poor water solubility and poor loading capacity[20]. Another approach to make hollowed silica nanoparticles was through a sol-gel process: a wet chemical process including several steps: hydrolysis, polycondensation, gelation, aging, drying, densification, and crystallization[28]. This sol-gel process was time-consuming, and the size of hollowed silica nanospheres was not uniform[20]. In order to acquire uni-sized hollowed silica nanospheres, Jatupaiboon et al. reported a novel method of one-step reverse microemulsion reaction system that includes: APS, Triton X-100, n-hexanol, cyclohexane and DI-water[20]. This reverse microemulsion process can be done in 24 hours and at room temperature[20]. We modified it to fit our needs to make hollowed silica nanospheres.

2.2.2 Materials and Methods

Materials

(3-aminopropyl) triethoxysilane (APS), tetraethylorthosilicate (TEOS), and Triton X-100 were purchased from Acros Organics. Cyclohexane was purchased from Fisher, DI-water

Methods

Synthesis of hollowed silica nanospheres

1) Water phase: Three different concentration of APS (1, 2, and 3 μL) added into 1.1 ml of DI-water;
2) Oil phase: mixing 14.5 of cyclohexane, 3,64 g of n-octanol and 4.47 g of Trition X-100, shake well on the vortexer;
3) Put oil phase into a 500 ml glass beaker with clean stir bar (stir bar needs to be new or cleaned by soaking in 1:1 mixture of aqua regia and water for 2 hour or more, and then wash with DI-water), set the speed at 600-700 rpm;
4) Add water phase (APS solution) into the oil phase and keep the spinning speed;
5) Add 200 μL of TEOS into 200 μL NH4OH and shake well on the vortexer;
6) Add TEOS and NH4OH mixture into the water/oil mixtures;
7) Let the reaction goes on at room temperature for 24 hours;
8) Add 60-80 ml of acetone to stop the reaction;

Wash step for hollowed silica nanospheres

1) Transfer the solution into clean 50 ml pipette tubes. Balance the pipette tubes and centrifuge at 10,000 rpm for 25 minutes;
2) Get rid of the supernatant and add 30 ml of ethanol, re-disperse the pellet by ultrasonication for 1 hour. Centrifuge at 10,000 rpm for 25 minutes;
3) Repeat step 2 for two more times;
4) Get rid of the supernatant and add 20 ml of DI-water, re-disperse the pellet by ultrasonication for 1 hour; Centrifuge at 10, 000 rpm for 20 minutes;
5) Repeat step 4 for two more times;
6) Hollowed silica nanospheres stored at 4 ˚C;

2.2.3 Mechanism of hollowed silica nanospheres synthesis

Uni-sized outlay and tunable hole size inside hollowed silica nanospheres were prepared by a one-step reverse microemulsion process at room temperature by less than 24 hours. Not only empty hollowed silica nanospheres, but also hollowed silica nanospheres encapsulated with iron oxide, FITC, Eu^{3+} – complexes, and serval drugs/vaccine could be achievable by this reverse microemulsion process[20].

2.2.4 Characterization of hollowed silica nanospheres

The hollowed silica nanospheres were characterized by transmission electron microscopy (TEM). In Fig. 2.2 we can see that the size of hollowed silica nanospheres were around 100 nm. With color difference between the shell and core, we can tell the hollowed structure has been achieved.

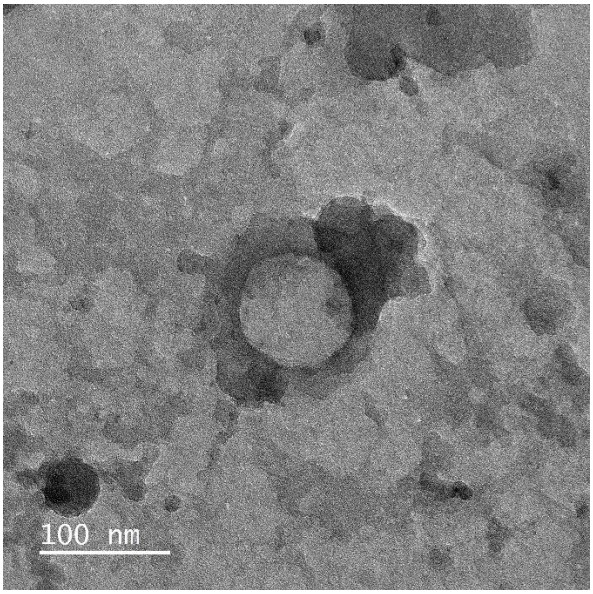

Fig 2.2 Transmission electron microscopy (TEM) of hollowed silica nanospheres showing an average diameter around 100 nm.

2.2.3 Applications of hollowed silica nanospheres

Different agents and chemical can be embedded into the core of silica nanospheres to make different types of hollowed silica nanospheres.

1) FITC- hollowed silica nanospheres
2) BHHCT-EU3+- hollowed silica nanospheres
3) Fe3O4- hollowed silica nanospheres
4) BHHCT-Eu3+@Fe3O4- hollowed silica nanospheres
5) Load vaccine/drug inside of hollowed silica nanospheres: we aim to use these hollowed silica nanospheres as vaccine delivery vehicles, more details of this effort are in Chapters 4 and 5. The hollowed silica nanospheres can be loaded with varies drugs and vaccines inside[20]. With proper coating materials, for example, poly-l-lysine, and poly (ethylene glycol) (PEG)[14,16], payloads loaded inside the core of the hollowed silica nanospheres can be protected against the harsh environment of intestinal mucosa.

2.3 T1L Sigma 1 protein

2.3.1 Background

T1L MRV is an 85 nm diameter, non-enveloped virus comprised of 5 structural proteins (λ1, λ2, λ3, σ2, and μ2) forming a core particle that encloses the virus genome, surrounded by 3 outer capsid proteins (σ1, μ1, and σ3) that play critical roles in virus cell entry[29]. Following oral inoculation, T1L MRV accesses mucosal associated lymphoid tissues (MALTs) by exploring the transcytosis through M cells, which are specialized cells located at follicle-associated epithelium (FAE) of Peyer's patches[30].

M cells are continuously sampling for foreign antigens within the lumen by endocytosing antigens suspended in fluid at the apical surface of the cell. These antigens are then transcytosed from the apical surface to the basolateral surface. Since there is a thick mucus layer on the apical surface of the enterocytes, viruses often exploit M cell sampling to gain access to the basolateral side of the enterocytes where infection can proceed. In the case of MRV, the outer capsid protein, σ1, adheres to α 2-3-linked sialic acids on the M cell apical surface, and is transcytosed across the M cell to the MALT where it can initiate infection of enterocytes on the basolateral surface of these cells[31]. This pathway is aimed in this study as a route to facilitate transport of orally-delivered vaccines to MALT for elevated vaccine efficacy.

2.3.2 Materials and Methods

2.3.2.1 Growth of sigma 1 protein via L929 cells

1) Begin L929 spinners by growing L929 cells in a three-layer flask and upon splitting the flask add all collected cells to a 1000ml round spinner flask (shown on the right) with a stir bar and fill up to 500ml with cMEM.
2) Put spinner flask within 37ºC bacteria incubator (no CO_2 tank attached) on top of the spinner plate and set the speed of the plate 3/4 of the way between “3” and “4” as shown below.
3) Allow the spinner flask to sit for 24 hours. Once the L929 spinner flask is started the cells will need to be counted every day. For the first few days the cells may not reach > $8x10^5$ cells/ml and therefore the cells should be left an additional 24 hours when they are counted again. Once the cells reach > $8x10^5$ cells/ml they will need to be split according to the calculations shown below which will leave $2.5x10^8$ cells behind and provide > or =

$2x10^8$ cells per day. Moving forward the cells must be counted and split every day to keep them from crashing.

4) Once the L929 spinner flask is established the cells can be utilized to growth large amounts of reovirus. Begin by splitting the L929 cells and putting all the collected L929 cells into a 225ml conical bottle. Make sure that there is > or = $4x10^8$ total cells (L929 cells > or = $1.3x10^6$ cells/ml) for maximum virus propagation.
5) Pellet the cells at 3000xg for 10 min and discard supernatant without disrupting pellet. Resuspend the pellet so the cells are at 2x107 cells/ml (20ml of cMEM for 4x108 cells), and then add all the P3 virus propagated in a T75 flask. Allow the virus to absorb for 1 hour at 37^{o}C with shaking every 20 mins.
6) While the cells are infecting add 800ml of cMEM to a 1000ml flask with a stir bar at the bottom and set up in the isotemp immersion circulator water bath (shown below). The water bath should have distilled water added so that the water level is up to the two screws (shown by the arrow) but below the small notches above the screws, and the water should be at 37^{o}C before beginning. Add small, white plastic balls to the water to stop evaporation. Make sure not to turn the machine on without the water filled as the machine fuse will trip, best case scenario, or the motor will burn and the machine will be broken if the fuse does not work, worst case scenario (the fuse has been modified after it tripped last time and it may not function correctly anymore).
7) Once the cells are infected for 1 hour add the cells and virus to the 1000ml flask in the hood and bring back to the water bath. At this point turn the magnetic spinner on at the level “3”.

8) Monitor the flask each day. The media should go from pink to orange to yellow and back toward orange/red. Usually after 4 days the media has gone through this cycle and is orange/red and the cell viability should be determined to decide if the cells and virus are collected. While it is suggested that the viability of the cells should be about 65%, I have determined when to stop the incubation based on when the media turned color which has been 4-5 days.
9) Harvest the cells by centrifuging the media at 3000xg for 10 min in two 225ml conical bottles. Remove the supernatant and once all the cells are pelleted resuspend the cells in 8ml of HO buffer and add to one of the two 225ml conical bottles. Freeze at -80 until ready for purification.

2.3.2.2 Purification of sigma 1 protein

1) Thaw cells at room temperature and place on ice until chilled, and then add to 25ml Corex tube.
2) Sonicate the cells twice with 20 sec pulses while keeping them on ice. Hold tubes near top so as not to deaden sonicator energy at the bottom of tube. Move tip around to distribute maximum energy. Do not touch sides of tube with tip.
3) Add 1/100th volume of 10% DOC (deoxcycholate) and swirl gently to mix. Incubate in ice for 30 min.
4) Add half a volume of Vertrel and emulsify by sonication as done in step 2.
5) Centrifuge the Corex tube at 7000 rpm for 10 min.
6) Put the aqueous phase in a clean Corex tube making sure not to take any of the pellet and add 4ml of Vertrel and sonicate twice with 20 sec pulses. Repeat the sonication step with an additional 4ml of Vertrel, and then centrifuge at 7000 rpm for 10 min.

7) Remove aqueous phase and layer gently over a CsCl gradient, 1.25-1.45 g/cc, in a SW32 tube (25x89mm). The gradient is made by adding 8 ml of 1.25g/cc CsCl to the SW32 tube and then using a syringe to gently add 8 ml of 1.45g/cc CsCl to the bottom of the of the tube.
8) Centrifuge at 23,000 rpm overnight and the next day collect the tube and set up on a ring stand to allow an 18 ½ g needle to pierce the bottom of the tube. Allow the liquid to drop into a waste container and collect the desired bottom and top band of the virus in separate tubes.
9) Load collected virus into properly prepared dialysis tubing and dialyze against 3 liter of dialysis buffer for 48 hours at 4^{o}C changing the buffer at 24 hours.
10) Collect the virus from the dialysis tubing and store at 4^{o}C in a glass 1 dram vial.

2.3.3 Characterization of Sigma 1 protein

As we can clear see in Fig.2.3, the western blot results on the left lane showed that T1L σ1 protein was successfully acquired and purified. The middle land is the solution go through the 30 KDa filter, there is no T1L σ1 protein at all, which indicated that all the T1L σ1 protein was kept in the filter and didn't go through. On the right land of this wester bolt, it's the pellet from the final step of the centrifuge, we solve the pellet and run it as the positive control. The pellet has all the MRV structural proteins.

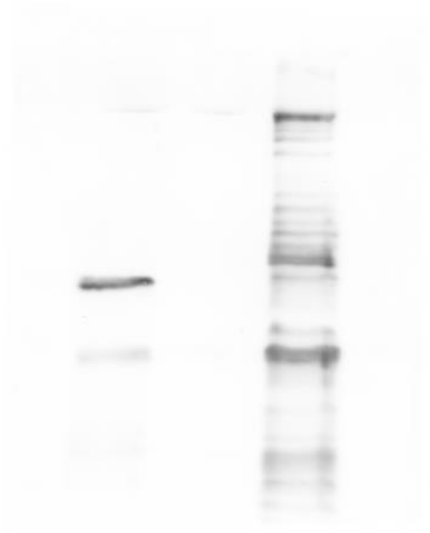

Fig 2.3 Western blot for pellets after last centrifugation, control group, and T1L σ1 protein (50 kDa). Following purification, T1L σ1 protein was concentrated using a 30 kDa filter (left). Filtrated solution (middle) and pellets (right) serve as the control.

2.3.4 Application of Sigma 1 protein

In this study, we aimed to utilize the T1L sigma 1 as a handle to facilitate transport of AVNs across M-cell mediated transcytosis pathways:

1) Functionalization of gold nanocages, σ1 protein will be on the surface of gold nanocages, our previous work showed with σ1 protein functionalization, we formed an artificial virus nanocarriers[16]. This artificial virus nanocarriers can mimic the T1L MRV and explore the M cells transcytosis;
2) Functionalization of hollowed silica nanospheres, and with poly-l-lysine coating. In this set up, we coating the hollowed nanospheres with poly-l-lysine, and then functionalize the HSS-PLL with σ1 protein. Now, we have a more complete artificial virus nanocarriers. Poly-l-lysine coating will provide a better protection of payload inside the hollowed silica nanospheres. Again, σ1 protein can guide the artificial virus nanocarriers through the M cells embedded monolayers via M cells transcytosis;

2.3.5 Other efforts toward acquiring Sigma 1 protein

In addition to the direct harvesting of sigma 1 proteins from cultivated T1L MRVs, we also explored other alternative methods to obtain histidine-tagged recombinant sigma 1 proteins.

2.3.5.1 Recombinant protein synthesis

Experiment design: We plan to use recombinant DNA methods to added a polyhistidine-tag (his-tag) on the tail of full-length σ1 and 1-169 base pairs cut off σ1 we named as "170 σ1". His-tag is known for its role in link protein onto gold nanoparticles[32]. To add full-length σ1 and 170 σ1 onto the vector with his-tag, we tried to use AfII and XbaI. Repeated testing over a year confirmed that 170 σ1 with his-tag could not be obtained with this method. We then focused on the full-length σ1. After mini-prep, transfect, and max-prep, the final results for full-length σ1 was again a no show.

2.3.5.2 Denatured sigma 1 proteins

The expression of full-length σ1 was not successful, thus, we tried to use the denaturation process to tackle this problem. Firstly, we tried the regular denaturation-renaturation method [33].

From Fig. 2.4, we can see that full-length σ1 protein lane does show some results. On the right lane, the denatured/ renatured σ1 proteins have a pale band, at least this is a progress compared to our previous methods. However, the amount of σ1 protein was way too low for us to get enough σ1 proteins for the subsequent functionalization of AVNs. We then aimed to increase the renature percentage of σ1 protein via renaturation.

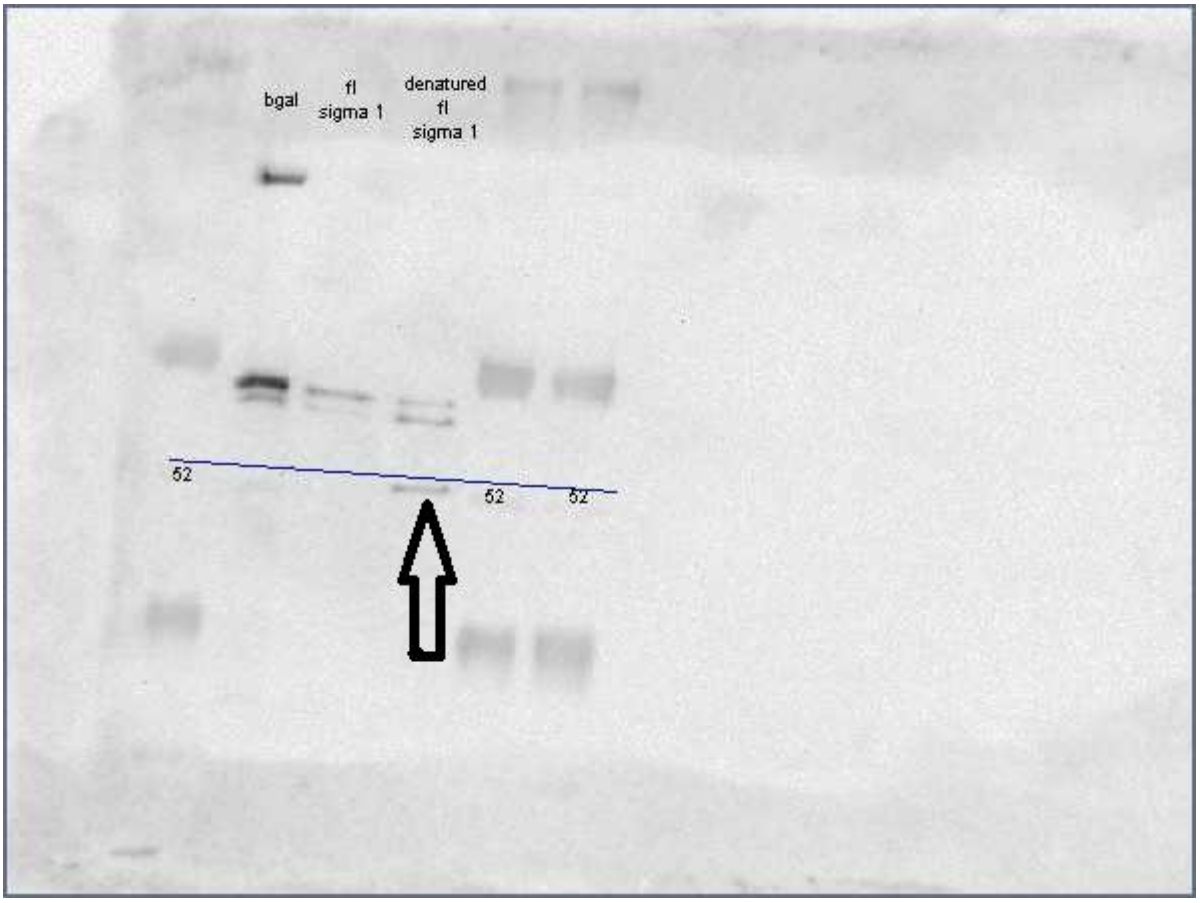

Fig 2.4 Western blot for σ1 protein prepared by regular denature-renature methods. Bgal on left lane, full-length σ1 on middle land and denatured full-length σ1 on the right lane.

2.3.5.3 Sigma 1 protein via TaKaRabio renature kit

Denature protocol

1) Suspend the target protein in an appropriate buffer and the concentration of target protein should not be more than 10 mg/ml;
2) Add 75 µl 8 M Guanidine Hydro-chloride and 1 µl of 4M DTT into the protein solution;
3) The reaction is carried at room temperature for 1 hour;

Renature protocol

1) Add 1.4 ml of +DL-Cystine as the surfactant solution to every 20 µl denature protein;
2) The reaction is carried at room temperature for 1 hour;

3) Add 3% CA solution into every 400 µl solution from step 2, then incubate the solution at room temperature for overnight;
4) Centrifuge the solution at 15, 000 rpm for 10 minutes and discard the pellet, then collect the supernatant;

The result from the renaturation protocol is shown in Fig.2.5, we got some positive results. Tween 40, CTAB, and SB3-14 surfactant groups of renatured σ1 had a positive yield. SB3-14 group had the best performance. Although the amount of σ1 protein was improving compared to regular denature-renature method, the amount was still not enough for us to continue our AVNs work. Given the cost/time consuming nature of this approach, we chose not to further invest in this pathway. However, these results did prove that the recombinant full-length σ1 proteins with his-tag could indeed be produced, which could be explored in the future.

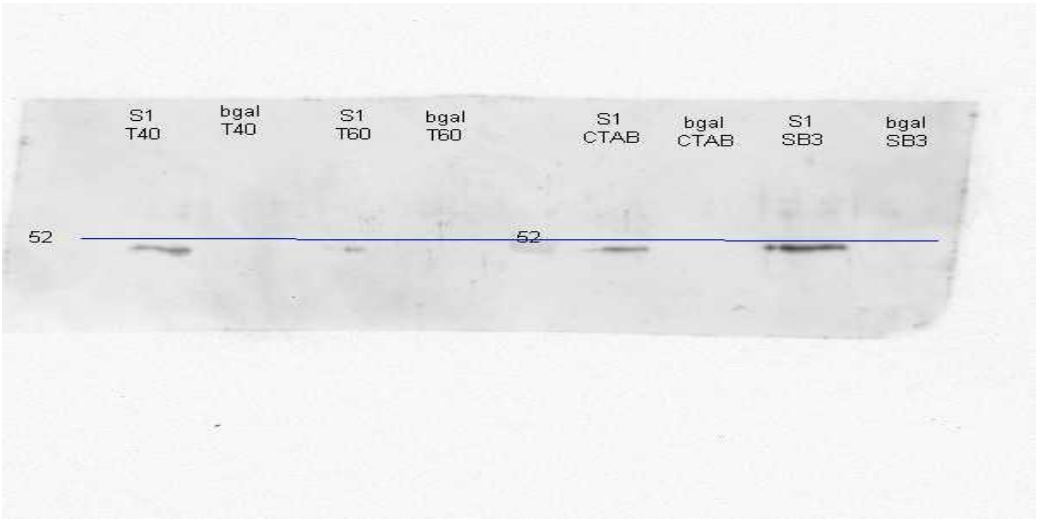

Fig 2.5 Western blot results for renature σ1 protein prepared by TaKaRabio nature kit with different surfactant solution (Tween 40, Tween 60, CTAB, and SB3-14). From left to right is σ1 protein with T40, bgal T40, σ1 protein T60, bgal T60, σ1 CTAB, bgal CTAB, σ1 SB3-14, and bgal SB3-14.

2.4 References

[1] A. N. Shipway, E. Katz and I. Willner, *ChemPhysChem*, , DOI:10.1002/1439-7641(20000804)1:1<18::AID-CPHC18>3.0.CO;2-L.

[2] C. J. Murphy, T. K. Sau, A. M. Gole, C. J. Orendorff, J. Gao, L. Gou, S. E. Hunyadi and T. Li, *J. Phys. Chem. B*, , DOI:10.1021/jp0516846.

[3] K. A. Willets and R. P. Van Duyne, *Annu. Rev. Phys. Chem.*, , DOI:10.1146/annurev.physchem.58.032806.104607.

[4] B. Wiley, Y. Sun and Y. Xia, *Acc. Chem. Res.*, , DOI:10.1021/ar7000974.

[5] C. Noguez, *J. Phys. Chem. C*, , DOI:10.1021/jp066539m.

[6] M. Hu, J. Chen, Z.-Y. Li, L. Au, G. V. Hartland, X. Li, M. Marquez and Y. Xia, *Chem. Soc. Rev.*, , DOI:10.1039/b517615h.

[7] M. A. El-Sayed, *Acc. Chem. Res.*, , DOI:10.1021/ar960016n.

[8] Y. Xia, P. Yang, Y. Sun, Y. Wu, B. Mayers, B. Gates, Y. Yin, F. Kim and H. Yan, *Adv. Mater.*, , DOI:10.1002/adma.200390087.

[9] N. R. Jana, L. Gearheart and C. J. Murphy, *J. Phys. Chem. B*, , DOI:10.1021/jp0107964.

[10] J. B. Jackson and N. J. Halas, *J. Phys. Chem. B*, , DOI:10.1021/jp003868k.

[11] Y. Sun and Y. Xia, *Adv. Mater.*, , DOI:10.1002/adma.200304652.

[12] S. Chen and D. L. Carroll, *Nano Lett.*, , DOI:10.1021/nl025674h.

[13] Y. Sun and Y. Xia, *Science (80-.).*, , DOI:10.1126/science.1077229.

[14] S. E. Skrabalak, J. Chen, Y. Sun, X. Lu, L. Au, C. M. Cobley and Y. Xia, *Acc. Chem. Res.*, , DOI:10.1021/ar800018v.

[15] S. E. Skrabalak, L. Au, X. Li and Y. Xia, *Nat. Protoc.*, , DOI:10.1038/nprot.2007.326.

[16] T. Tong, Y. Qi, L. D. Bussiere, M. Wannemuehler, C. L. Miller, Q. Wang and C. Yu, *Nanoscale*, , DOI:10.1039/D0NR03680C.

[17] J. G. Fujimoto, *Nat. Biotechnol.*, , DOI:10.1038/nbt892.

[18] J. Liu, F. Fan, Z. Feng, L. Zhang, S. Bai, Q. Yang and C. Li, *J. Phys. Chem. C*, , DOI:10.1021/jp804161f.

[19] R. M. Anisur, J. Shin, H. H. Choi, K. M. Yeo, E. J. Kang and I. S. Lee, *J. Mater. Chem.*, , DOI:10.1039/c0jm02647f.

[20] N. Jatupaiboon, Y. Wang, H. Wu, X. Song, Y. Song, J. Zhang, X. Ma and M. Tan, *J. Mater. Chem. B*, , DOI:10.1039/C5TB00194C.

[21] Y. Chen, H.-R. Chen and J.-L. Shi, *Acc. Chem. Res.*, , DOI:10.1021/ar400091e.

[22] F. Tang, L. Li and D. Chen, *Adv. Mater.*, , DOI:10.1002/adma.201104763.

[23] Y. Chen, H. Chen, Y. Sun, Y. Zheng, D. Zeng, F. Li, S. Zhang, X. Wang, K. Zhang, M. Ma, Q. He, L. Zhang and J. Shi, *Angew. Chemie Int. Ed.*, , DOI:10.1002/anie.201106180.

[24] C.-H. Lin, X. Liu, S.-H. Wu, K.-H. Liu and C.-Y. Mou, *J. Phys. Chem. Lett.*, , DOI:10.1021/jz201336h.

[25] M. Fuji, T. Shin, H. Watanabe and T. Takei, *Adv. Powder Technol.*, , DOI:10.1016/j.apt.2011.06.002.

[26] Y. Sun and Y. Xia, *J. Am. Chem. Soc.*, , DOI:10.1021/ja039734c.

[27] S. K. Das, M. K. Bhunia, D. Chakraborty, A. R. Khuda-Bukhsh and A. Bhaumik, *Chem. Commun.*, , DOI:10.1039/c2cc17181c.

[28] I. A. Neacşu, A. I. Nicoară, O. R. Vasile and B. Ş. Vasile, in *Nanobiomaterials in Hard Tissue Engineering*, Elsevier, 2016.

[29] L. D. Bussiere, P. Choudhury, B. Bellaire and C. L. Miller, *J. Virol.*, , DOI:10.1128/JVI.01371-17.

[30] M. Wang, Z. Gao, Z. Zhang, L. Pan and Y. Zhang, *Hum. Vaccin. Immunother.*, , DOI:10.4161/hv.36174.

[31] A. Helander, K. J. Silvey, N. J. Mantis, A. B. Hutchings, K. Chandran, W. T. Lucas, M. L. Nibert and M. R. Neutra, *J. Virol.*, , DOI:10.1128/JVI.77.14.7964-7977.2003.

[32] L. Torres-González, R. Díaz-Ayala, C. Vega-Olivencia and J. López-Garriga, *Sensors*, , DOI:10.3390/s18124262.

[33] Z. Yang, L. Zhang, Y. Zhang, T. Zhang, Y. Feng, X. Lu, W. Lan, J. Wang, H. Wu, C. Cao and X. Wang, *PLoS One*, , DOI:10.1371/journal.pone.0022981.

CHAPTER 3. TRANSP0ORT OF ARIFICIAL VIRUS-LIKE NANOCARRIES (AVN) THROUGH INTESTINAL MONOLAYER VIA MICROFOLD CELLS

Tianjian Tong[§], Yijun Qi[§], Luke D. Bussiere, Michael Wannemuehler, Cathy L. Miller, Qun Wang*, Chenxu Yu*

[1]Department of Agricultural Biosystem and Engineering, Iowa State University, Ames, Iowa

[2]Department of Chemical and Biological Engineering, Iowa State University, Ames, Iowa

[3]Department of Veterinary Microbiology and Preventive Medicine, College of Veterinary Medicine, Iowa State University, Ames, Iowa

[4]Interdepartmental Microbiology Program, Iowa State University, Ames, Iowa

Modified from a manuscript published in *Nanoscale*.

Abstract

Compared with subcutaneous or intramuscular routes for vaccination, vaccine delivery via gastrointestinal mucosa has tremendous potential as it is easy to administer and pain free. Robust immune responses can be triggered successfully once vaccine carried antigen reaches the mucosal associated lymphoid sites (e.g., Peyer's patches). However, the absence of an efficient delivery method has always been an issue for successful oral vaccine development. In our study, inspired by mammalian orthoreovirus (MRV) transport into gut mucosal lymphoid tissue via Microfold cells (M cells), artificial virus-like nanocarriers (AVN), consisting of gold nanocages functionalized with the σ1 protein from mammalian reovirus (MRV), were tested as an effective oral vaccine delivery vehicle targeting M cells. AVN was shown to have a significantly higher

transport compared to other experimental groups across mouse organoid monolayers containing M cells. These findings suggest that AVN has the potential to be an M cell-specific oral vaccine/drug delivery vehicle.

3.1 Introduction

Oral vaccination targeting the gastrointestinal (GI) mucosa layer is considered more patient-friendly to subcutaneous injection or intravenous injection with regards to induction of a protective immune response [1]. GI mucosal delivery of vaccines has additional practical advantages over vaccination by intravenous injection or subcutaneous injection, including both cost efficiency and increased safety [2]. While progress has been made substantially with the increased stability of and immune activation by mucosal vaccines, practical and effective oral vaccine delivery systems targeting GI mucosa remain to be developed due to poor understanding of specific and non-specific factors determining delivery, targeting, recognition and transport of vaccine/vaccine carriers across the GI mucosal epithelia. In this article, we aimed to validate the development of an artificial virus-like nanocarrier which specifically targets M cells for transcytosis providing a more effective strategy to deliver oral vaccines into mucosal associated lymphoid tissues (e.g., Peyer's patches) for enhanced vaccine efficacy.

Type 1 Lang mammalian reovirus (MRV) is an 85 nm diameter, non-enveloped virus comprised of 5 structural proteins (λ1, λ2, λ3, σ2, and μ2) forming a core particle that encloses the virus genome, surrounded by 3 outer capsid proteins (σ1, μ1, and σ3) that play critical roles in virus cell entry [3]. Following oral inoculation, T1L MRV accesses mucosal associated lymphoid tissue (MALT) by transcytosis through M cells, which are specialized cells located at follicle-associated epithelium (FAE) of Peyer's patches [4,5]. M cells are continuously sampling

for foreign antigens within the lumen by endocytosing antigens suspended in fluid at the apical surface of the cell. These antigens are then transcytosed from the apical surface to the basolateral surface. Since there is a thick mucus layer on the apical surface of the enterocytes, viruses often exploit M cell sampling to gain access to the basolateral side of the enterocytes where infection can proceed. In the case of MRV, the outer capsid protein, σ1, adheres to α 2-3-linked sialic acids on the M cell apical surface, and is transcytosed across the M cell to the MALT where it can initiate infection of enterocytes on the basolateral surface of these cells [6].

Taking inspiration from the natural pathway of MRV transcytosis across M cells (Fig. 3.1a), we hypothesized that artificial virus-like nanocarriers (AVNs), comprised of T1L σ1 conjugated gold nanocages would be able to effectively transcytosis through M cells. Hence, these AVNs can serve as effective transport vehicles for oral vaccines. AVN construction required purification of σ1, preparation of gold nanocages, and linkage of σ1 to the nanocage surface in an appropriate conformation where the head domain (C-terminal portion) [7] of σ1 can interact with α2-3 sialic acid located on the M cell apical surface [6].

With the nanocarriers being surface-functionalized T1L σ1, conventional 2-D spherical nanoparticles were not good candidates as the outer surface would no longer be available for payload loading. In this study, we chose gold nanocages (i.e., hollow nanocubes) as our base for nanocarrier development mainly due to their easiness to fabricate and their internal loading capacity. The nanocages had holes to allow loading/unloading of payloads. Coating could be added to cover the outer surface to further protect the payloads sealed inside for oral vaccine to survive the harsh gastric environment.

To test our hypothesis, a simple and effective testing platform was developed using M cell containing intestinal monolayers derived from mouse intestinal organoids in which M cell

differentiation was induced using recombinant RANK ligand (RankL) [8]. Compared with a monolayer of Caco-2 cells, the organoid monolayer contains various epithelial cell types, such as goblet cells, enteroendocrine cells, enterocytes and Paneth cells [9]. The development of an *ex vivo* intestinal mucosal system composed of a continuously expanding, self-organizing structure, reminiscent of normal intestinal epithelium, provides an alternative that bridges the gap between cell lines and in vivo animal models for the study of oral vaccines. Based on previous studies [10], the organoid generated monolayers are polarized as evidenced by the fact that they maintain apical and basally oriented membranes, which is a critical component of our model as MRV adheres to the apical membrane of M cells *in vivo* [11]. Additionally, from previous studies, M cells can be induced in both 2D and 3D organoid systems [12]. Our experimental setup used transwell plates containing an M cell embedded organoid monolayer mimicking an intestinal mucosal layer on the top inserts, with the bottom compartment mimicking a MALT site (Fig. 3.1b). Using this system, we examined the capacity of AVNs to exploit M cell-mediated uptake through interaction of σ1-conjugated AVNs with α 2-3 sialic acids followed by transcytosis through M cells.

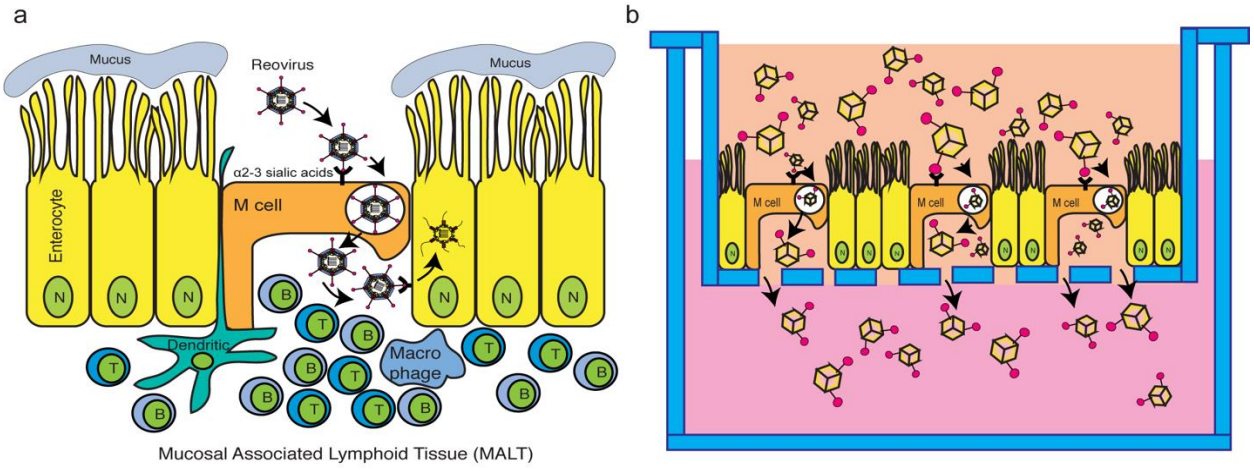

Fig 3.1 Scheme: T1L σ1 functionalized Gold nanocage explore M cell pathway. a, Model of MRV infection of enteric tissue. b, Experimental design to test the transport of σ1 functionalized AVNs through M cells incorporated to intestinal organoid monolayers.

3.2 Results and discussion

3.2.1 Artificial Virus-like Nanocarriers: Gold nanocages and MRV σ1

Gold nanoparticles are widely used in the drug/vaccine delivery field [13,14,15 ,16,17,18]. Gold nanocages (GNC) are 3D structures with a hollowed interior which allows a substantially increased loading capacity for payload (e.g., drugs or immunogens) when compared with 2D delivery vehicles. GNC were produced using a two-step galvanic replacement reaction [15,16]. In the first step, silver nanocubes were fabricated as sacrifice templates, and in the second step, a galvanic replacement reaction was utilized to replace silver with gold. 3D hollowed gold nanocages were obtained from this reaction with an average size of 40 nm (Fig. 3.2a). GNC utilized throughout our study had an absorption peak of around 760 nm (Fig. 3.2b). MRV σ 1 was harvested from purified MRV as previously described [19,20,21]. Presence of σ1 protein is confirmed by Western blot using the T1L virion antisera which recognizes σ1 along with other capsid proteins. In Fig. 3.2c, our Western blot analysis revealed one band at 50 kDa representing σ1 protein (right lane). No band was detected in filtered suspension (middle) indicating there was no unconjugated σ1 protein present, while in the post-purification pellet (left), all MRV structural proteins were revealed. EDC/NHS mediated conjugation was utilized to link σ1 proteins onto GNC [22,23] to produce AVNs. Conjugation success was confirmed by incubation of AVNs as well as GNC without σ1 conjugation (i.e., control) with gold nanospheres (GNS) conjugated with a σ1 specific monoclonal antibody (5C6). While the control-maintained absorption peaks representing free-floating GNC (760 nm) and GNS (550 nm), the (GNC- σ1) + (GNS-5C6) group showed no absorption indicating aggregation via σ1-5C6 crosslinking and confirming σ1 conjugation to GNC.

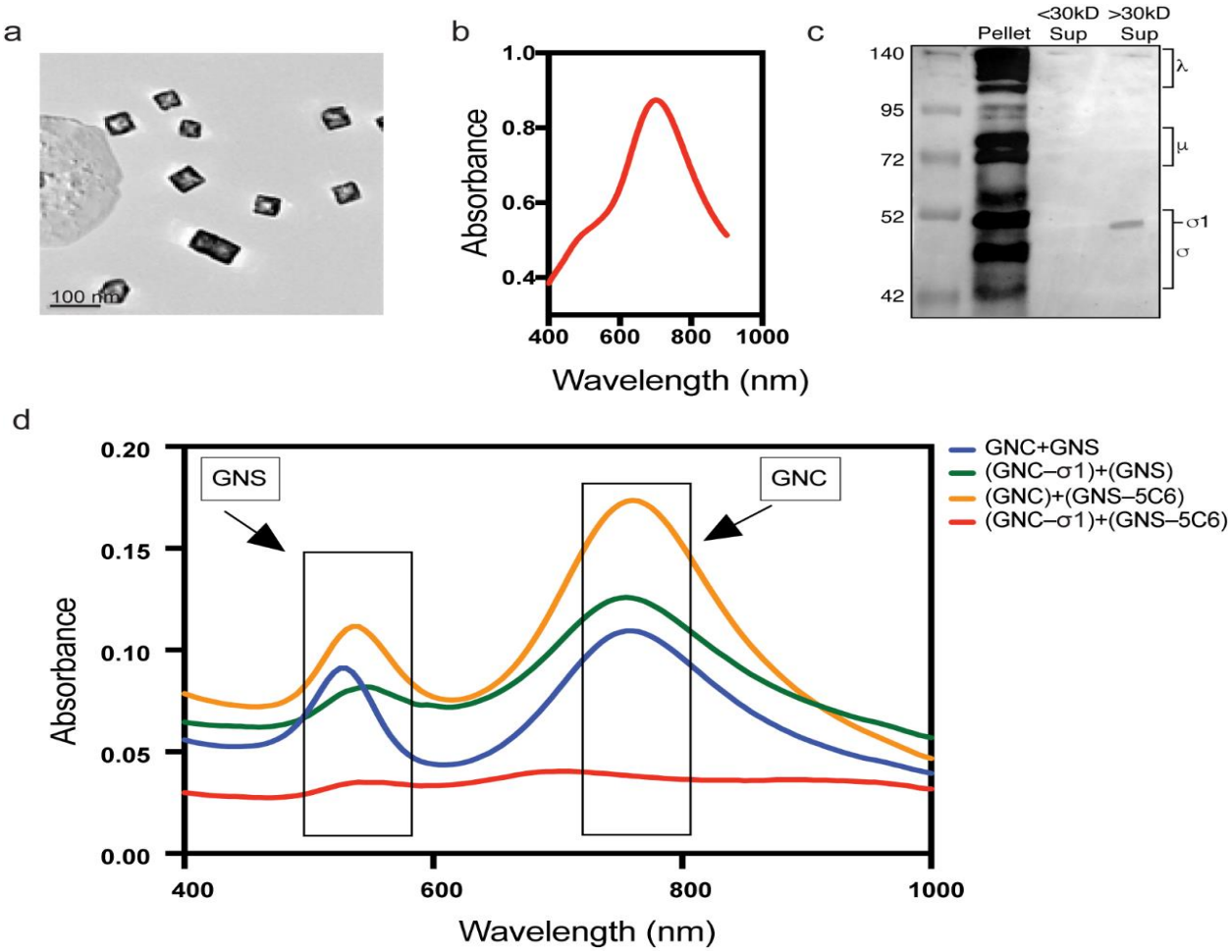

Fig 3.2: MRV σ1 functionalization of GNC a, TEM (Transmission Electron Microscopy) image of GNC showing 40 nm average size. b, UV (Ultraviolet) absorption of GNC shows characteristic peak at 760 nm. c, Western blot for pellet after last centrifuge, control group and T1L σ1 protein (50 kDa). Following purification, T1L σ1 protein. T1L σ1 protein was concentrated using a 30 kDa filter (right). Filtrated solution (middle) and pellet (left) serves as the control. d, GNC conjugated with MRV σ1 protein (GNC+ σ1) or (GNC) alone, and GNS conjugated with σ1 monoclonal antibody 5C6 (GNS+5C6) or not (GNS) were incubated together and absorption was measured to identify aggregation.

3.2.2 Microfold cell (M cell) incorporated intestinal monolayer preparation

Intestinal organoids are 3-dimensional structured epithelium that are derived from small intestinal stem cells[9]. Stem cells were isolated from the small intestine of C3H/HeN conventional mice and mixed with Matrigel containing growth medium supplemented with growth factors

including R-spondin 1, EGF, and Noggin[24]. Previous studies[25,26,27,28,29] have demonstrated that adding RankL to the organoids culture medium induced the M cells appearance. The expression of M cells were confirmed by expressing M cell surface protein glycoprotein 2 (GP2) and M-cell-specific molecules annexin V (Anxa5)[5] on organoids. Additionally, biotin-conjugated lectin UEA-1 (UEA-1) binds specifically to sites of α-1,2 fucosylation on the surfaces of M cells[30].

Based on these observations, M cells were induced in 3D structured organoids by 3-day incubation in the presence of RankL. Similar to prior studies[25,26,27,28,29], we found lectin UEA-I binding (shown as red) and M cell marker GP2 expressed (shown as green) in organoids treated with RankL, but not in untreated organoids (Fig. 3.3a). For further verification, gene expression analysis was performed using RT-qPCR and primers specific for Anxa5 and GP2. Consistent with the expression of M cell markers seen by immunofluorescence, organoids treated with RankL significantly upregulated the expression of both Anxa5 and GP2 relative to untreated cells (Fig. 3.3b). Finally, Western blot was performed using antibodies specific for annexin V in which RankL induced organoids showed a specific band with the correct molecular weight that was not present in the untreated organoids (Fig. 3.3c).

Taken together, these findings strongly suggest that a 3-day incubation with RankL resulted in the induction of M cells within the organoids. While intact 3D organoids are useful for many experiments, our assay required a monolayer, and it has been demonstrated previously that organoids can be disrupted and plated on tissue culture plates to form a monolayer[10]. In order to achieve this, we treated organoids for 2 days with RankL, disrupted and re-plated the cells as a monolayer in the presence of RankL for an additional 24 hours on the top compartment of a transwell tissue culture inserts (Fig 3.3b) for further experiments. As shown in Fig. 3d,

organoid monolayers positively stained for GP2, which was absent in control samples not receiving RankL, indicating that M cells were present in the monolayer system. Additionally, E-Cadherin staining was performed to verify the presence of tight junctions within the monolayers in both control and RankL-treated groups (Fig. 3.3d). The morphology of the monolayers is further demonstrated by bright field images in supplemental Fig. 3.1.

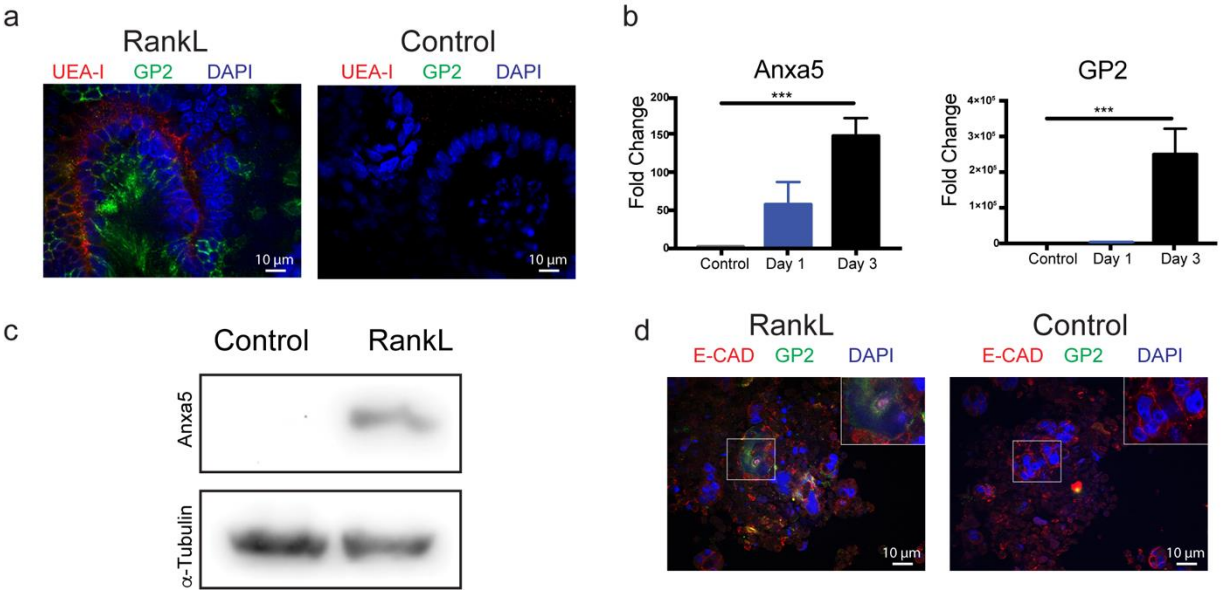

Fig 3.3: Detection of Microfold cells in 3D mouse organoids and 2D organoid-derived monolayers. a, Immunofluorescence images of untreated and 3-day RankL-treated 3D organoids with antibodies against M cell marker proteins GP2 (green) and UEA-I lectin (red). Nuclei are stained with DAPI (blue). b, RT-qPCR analysis for expression of Anxa5- and GP2-specific mRNA isolated from untreated and RankL-treated organoids. c, Western blot analysis of cell lysates from untreated and RankL-treated organoids using antibodies against Anxa5. d, Immunofluorescence images of organoid monolayers stained with antibodies against GP2 (green) and E-Cadherin (red). Nuclei are stained with DAPI (blue). The boxed region in the merged image was amplified and is shown in the inset.

3.2.3 Transport behavior of Mammalian orthoreovirus through organoid Monolayers

As proof of concept that our organoid monolayer recapitulates MRV transcytosis through M cells, experiments were conducted to measure MRV transport through intestinal organoid monolayers with or without M cells in the transwell system (Fig.3.1b). Purified MRV was added

to untreated or RankL-treated organoid monolayers plated on the top compartment of transwell. At 2, 4, 6, and 12 hour, culture medium from the bottom compartment was collected and used for virus plaque assay to examine the amount of virus that passed through the monolayer as a measure of MRV transcytosis through M cells. At each time point, there was an increase in MRV transport into the bottom transwell in RankL-treated versus control monolayers, with two of the time points showing statistically significant differences. Moreover, when measuring the transport total of MRV across the organoid monolayer, the presence of RankL significantly increased the speed at which the virus moved into the bottom compartment (Fig. 3.4b). (supplementary Note 1). To confirm M cell presence and MRV infection in these monolayers, the 4 h time point was immunostained with antibodies against GP2 and MRV (Fig. 3.4c). A noticeable overlap of GP2 and MRV staining can be observed in the RankL treated samples, further supporting MRV binding and transport through M cells in this system. Taken together, these data corroborate previously published data that MRV exploits the M cell pathway for transport into the MALT and support our hypothesis that this system can be used for measuring M cell dependent transport of AVN across the gut mucosa.

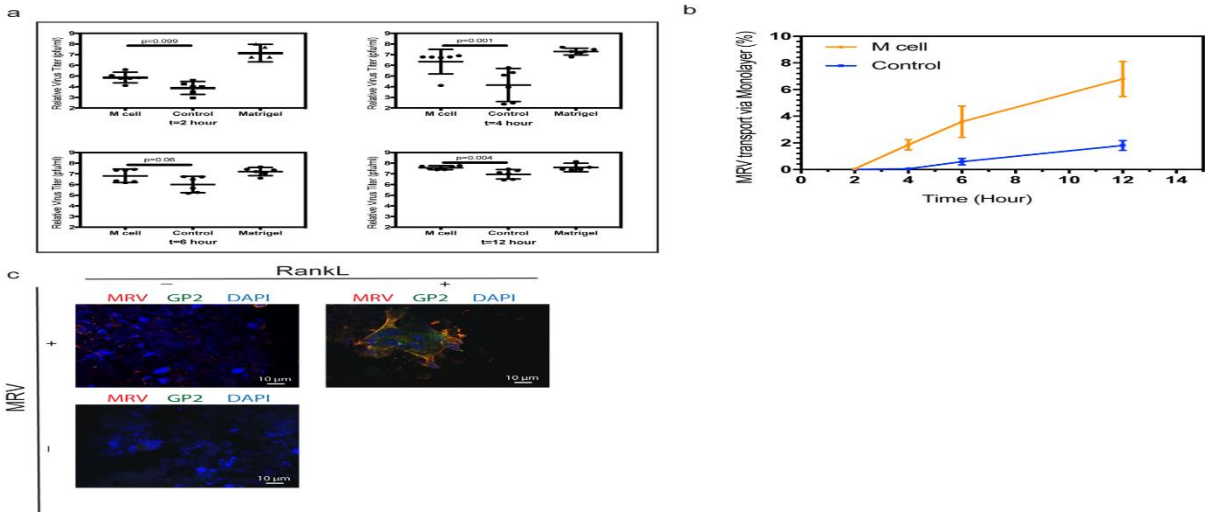

Fig 3.4 MRV Transport behavior on Organoid Monolayers. a, PFU of MRV transport through M cell induced monolayer, monolayers with M cell induction (control) and 1% Matrigel without

monolayers for 2, 4, 6 and 12 hours. p values were calculated and indicated on top of the bar line. b, MRV transport total at 2, 4, 6, and 12 hours, on monolayers with and without M cell induction. c, Immunofluorescence images of MRV-infected monolayers treated or untreated (control) with RankL using antibodies against MRV and GP2.

3.2.4 Transport of AVNs through organoid Monolayer

Following production and validation of AVNs and organoid monolayers, we tested our hypothesis that AVNs could be transported across the gut monolayer via σ1 binding and transcytosis through M cells. Using the small molecule dye Rhodamine 6G (R6G) as payload within the GNCs and AVNs, monolayers with and without M cells were overlaid with R6G (baseline for transport), R6G loaded GNCs, and R6G loaded AVNs. At 0, 0.5, 1, 2, 3, 4, 8, 12, 24, 36, and 48 hour post-treatment, samples were removed from the lower compartment of transwells and fluorescence was measured (Fig. 3.5a). These experiments demonstrated that AVNs display the highest transport across the organoid monolayer containing M cells among all four experimental groups. Moreover, while there are no differences in total transport between monolayers with and without M cells in the R6G and GNC groups, the addition of σ1 to the AVN group resulted in an increase in transport in the presence of M cells, strongly suggesting that the AVN group is using the σ1:M cell-mediated transcytosis pathway. When examining the first 8 hours, the transcytosis of AVNs across M cell containing monolayers is distinguished from the other three experimental groups, in that the transport total was higher than for AVNs across monolayers without M cells (Fig. 3.5b). As for GNCs, regardless of whether M cells were presented in the monolayers, the transport total were significantly lower than that of the AVNs. At early time points (hour 1 to 4), AVNs possessed a higher transport total than free R6G. In all four groups, some R6G payload diffused out of the nanocages throughout the experiments, and were detected in the bottom compartment. We suggest that R6G is released from the nanocages

in the top compartment and transported through the monolayers as small molecules do. When examining the UV spectra of samples collected from the bottom compartment after 48 hour, only the AVNs on monolayers with M cells contain a specific Gold nanocage absorption peak (~760 nm) in the bottom solution (Fig. 3.5c). This strongly indicates that only the AVNs can transport through the monolayer, and further only in monolayers with M cell presence, most likely via σ1-mediated transcytosis through the α2-3 sialic acid pathway. Gold nanocages otherwise cannot go through the intestinal monolayer, regardless of whether they are T1L σ1 functionalized or not. Therefore, both of the two factors, T1L σ1 and M cells, are needed for the transport of AVNs through intestinal organoid monolayers. We performed a quantitative assessment of how many payloads (R6G) inside AVNs that transported through monolayer. The overall transport of payloads in AVNs was 20% at 48 hour (Fig. 3.5d). These results strongly suggest that AVNs could be quite effective in transporting payloads through M cells in the gut mucosa, and potentially serve as promising oral vaccine carriers.

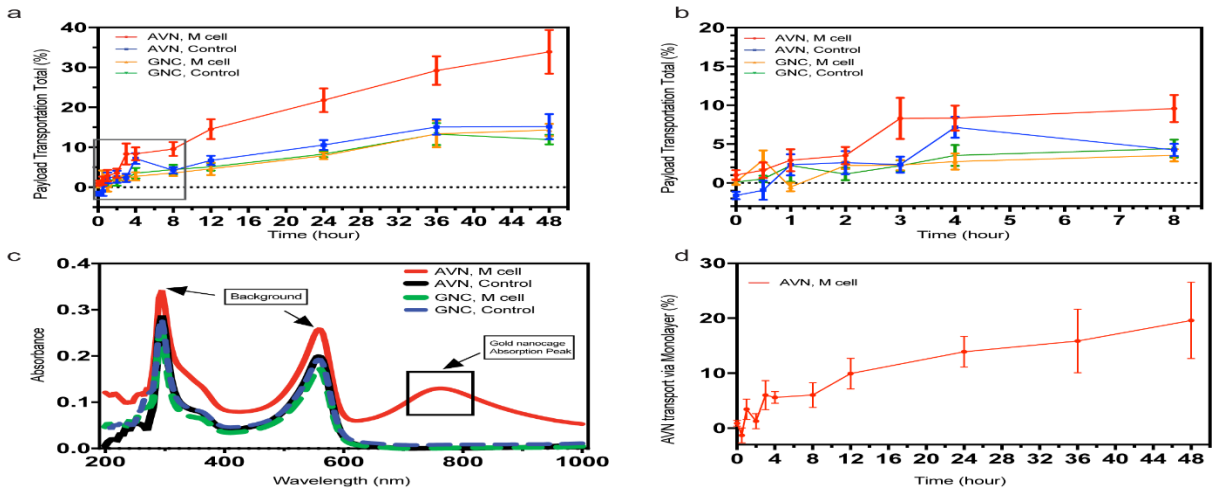

Fig 3.5: Transport behavior on monolayer platform. a, Payload (R6G) in different vaccine delivery vehicle (AVN, GNC) transport across intestinal monolayers, with and without M cell induction over time. b, First 8 hour in boxed region of Fig 5.a, c, UV absorption of each sample at 48 hour. d, AVN transport total through intestinal monolayers with M cells incorporated.

3.3 Conclusion

To summarize, artificial virus-like nanocarriers (AVNs) comprised of gold nanocages functionalized with MRV receptor binding protein σ1 were created that could effectively utilize M cells for transport across intestinal monolayers, mimicking the MRV transport pathway. Analysis revealed that both MRV σ1 functionalization of the AVNs and M cell presence in the monolayer were needed for demonstrable transport across the monolayer. The transport was reasonably efficient with ~20 % of total AVNs transported across the intestinal monolayer within 48 hour. This data suggests that AVNs, carrying an antigen or drug payload, could be used for oral delivery across the gastrointestinal mucosa into mucosal associated lymphoid sites (e.g., Peyer's patches) for enhanced vaccine effectiveness.

3.4 Experimental

3.4.1 Gold nanocage fabrication

Ethylene glycol (EG) (Sigma-Aldrich) (6 ml) was heated in 160 ˚C oil bath for 1 hour. Polyvinylpyrrolidone (PVP) (Sigma-Aldrich) (0.07 g) was added into 3.5 ml EG solution, and mixed well. $AgNO_3$ (Sigma-Aldrich) (0.12 g) was added into 2.5 ml EG solution and mixed well. Well mixed 3 mM $NaSO_4$ (Acros) EG solution was made by adding 70 μl of the sodium sulfide solution to EG solution in oil bath. 10 minutes later, 1.5 ml PVP solution and 0.5 ml Silver Nitrate solution were added into the reaction system and reacted for 10-15 mins. At the end of this incubation, 6 ml of acetone were added to cool down the reaction mix. The silver nanocube solution obtained from the above steps was centrifuged at 1,300 rpm for 30 min. The supernatant was removed, and 1 ml of deionized water was added. The nanocubes were then re-suspended in DI water in a sonicator for at least 1 hour. Then the nanocubes were washed twice,

collected by centrifugation at 9,000 rpm, before re-dispersed de-ionized water.

PVP (20 mg) was dissolved in 20 ml of deionized water. The PVP solution was then heated to 245 ˚C and stirred at 220 rpm. Once the PVP solution started to boil, 200 µL of Silver nanocubes were added into it. The combined solution was stirred and heated for an additional 10 minutes. 10 µL of $HAuCl_4$ (Sigma-Aldrich) was then added in 2-minute increments until desired concentration was attained (determined by solution color). Further verification of the concentration was done using UV-Vis spectrometry. The solution was then boiled down to 1 ml to concentrate the gold nanocages and NaCl was added in excess into solution until saturation[17,18]. The GNC solution was centrifuged for 30 minutes at 2000 g to form a pellet. The supernatant was removed, and 1 mL of distilled water was added. The solution was sonicated for 1hour to re-disperse the pellet back into a stable solution. Then the nanocages were centrifuged at 9000 g for 10 minutes and re-dispersed in in sonicator for 1hour. This last step was repeated one more time. The washed gold nanocages were stored at 4˚C.

3.4.2 T1L σ1 isolation and purification

L929 mouse fibroblast cells were maintained in Joklik modified minimum essential medium (Sigma-Aldrich) supplemented with 2 % fetal bovine serum, 2 % bovine calf serum (HyClone), 2 mM L-glutamine (Mediatech), and penicillin (100 IU/ml)–streptomycin (100 µg/ml) solution. MRV strain type 1 Lang (T1L) was propagated in spinner adapted L929 cells, the cells were harvested by centrifugation at 3000 x g for 10 min, resuspended in HO buffer (250 mM NaCl, 10 mM Tris, pH 7.4), and frozen at -80ºC [19]. Virus was purified as described [19] with the substitution of Vertrel® XF (DuPont) in place of Freon [21]. Purified MRV was then digested with α-hymotrypsin and purified to produced ISVPs [20], and then heated to 52 ºC for 30 min to release σ1 [19]. The ISVPs were pelleted at 35,000 rpm and the supernatant containing free σ1 was concentrated in a Centricon-30 microconcentration unit (Amicon Corp.) as described[19].

3.4.3 Gold nanocage functionalization

GNC functionalization was achieved using (1-ethyl-3-(3-dimethylaminopropyl) carbodiimide hydrochloride) (EDC) (Thermo scientific) /N-hydroxysulfosuccinimide (NHS) (Sigma-Aldrich) procedure. 4-Aminothiophenol was linked onto GNC by shaking overnight. The solution was centrifuged at 9,000 g for 10 minutes, then add DI-water was added, and GNC were re-dispersed in sonicator for 30 minutes to remove excess 4-Aminothiophenol. Freshly made EDS/NHS solution was added to GNC for 30 mins at room temperature. MRV T1L σ1 protein aqueous solution was added and incubated 2 hours at room temperature, and the reaction was stopped with 1 ml PBS with Tween-20 (PBST) to stop reaction. Finally, the solution was centrifuged at 6,500 x g for 30 mins, the supernatant was removed, and 2 ml of deionized water were added to re-disperse the nanocages [22,23].

3.4.4 High-resolution immunofluorescence microscopy

Organoids were grown in 4-well chamber slides and were fixed with 4% paraformaldehyde for 1 hour at room temperature. Sections were permeabilized with 0.5 % TritonX buffer (250 µL Triton-X100 in 50 mL PBS) for 30 minutes, after PBS washes for 3 times, 1% PBSA was used for making primary antibodies' solution then stained overnight at 4 °C. Then, at day 2, secondary antibodies were added and incubated at room temperature for 2 hours. After 3 times PBS washes, 4', 6-Diamidino-2-phenylindole (DAPI) (EMD Millipore) was used to stain nuclei and stick cells under cover slips. After drying the slides for 1 day in dark, slides were ready to use for observation under microscope. Fluorescence staining images were acquired with the Olympus®IX81 laser scanning confocal microscope using a 100X oil-immersion objective.

For staining with UEA-1, Lectin *Ulex europaeus*(biotinylated UEA-1, Sigma) and rabbit anti-biotin (Rockland) were used with a suggested concentration of 10 µg/ml. For secondary antibody, goat anti-rabbit antibody– Texas Red X (Invitrogen) were used at a 1:250 dilution. For staining GP2, primary antibody Rat anti-GP2 (MBL International Corporation) was used with a concentration of 2.5 µg/ml, secondary antibody goat anti-rat FITC (ThermoFisher) was used at a 1:250 dilution. For staining E-Cadherin, primary antibody rabbit anti-E-cadherin (Invitrogen) was used at a 1:250 dilution, followed with a secondary antibody Donkey Anti-Rabbit IgG H&L (Alexa Fluor® 594) (Abcam) at a 1:250 dilution. For MRV staining, Rabbit T1L anti-virion antibody, Mouse anti-σ3 5C3, Mouse anti-σ3 10C1 and Mouse anti-µ1 4A3 were used at a 1:250 dilution[31,32]. The following day, secondary antibody donkey anti-mouse Alexa Fluor® 594 (Invitrogen) and Donkey Anti-Rabbit IgG H&L (Alexa Fluor® 594) at a 1:250 dilution was used.

3.4.5 Quantitative RT-PCR for verifying microfold cells development

Matrigel was removed from organoids by treating them with 1000 µl of Cell Recovery Solution (Corning Life Sciences) with shaking for 1 h at 4°C, followed by two PBS washes. RNA was extracted by using RNeasy Mini Kit (Qiagen) following the manufacturer's procedure. Concentration and purity of the extracted RNA were checked by NanoDrop spectrophotometer. Three primer pairs were purchased from the DNA facility, Iowa State University, Ames, IA: Anxa5 (F: 5'-ATCCTGAACCTGTTGACATCCC-3'; R: 5'-AGTCGTGAGGGCTTCATCATA-3'), GP2 (F:5'-CTGCTACCTCGAAGGGGACT-3'; R: 5'-CATTGCCAGAGGGAAGAACT-3') and a primer for housekeeping gene Gapdh (F: 5'-TTCACCACCATGGAGAAGGC-3'; R: 5'-GGCATGGACTGTGGTCATGA-3'). Power SYBR™ Green RNA-to-CT™ 1-Step Kit was used. Gene expression levels were normalized against that of the housekeeping genes.

3.4.6 Western blot for verifying presence of M cell related proteins and σ1 protein

Matrigel was removed from organoids by treating them with 1000 µl of Cell Recovery Solution (Corning Life Sciences) with shaking for 1 h at 4°C, followed by PBS washes. For □1 identification, MRV was collected in protein loading buffer. Cells or MRV was denatured by heating 5 to 10 mins at 100 °C. Proteins were separated on a 4% Tris-HCl SDS-PAGE gel. Gels were transferred to nitrocellulose membrane and Western blotting was performed with Rabbit Anti-Anxa5 antibody (Abcam) at a dilution of 1:500; anti-□-tubulin monoclonal mouse antibody (ThermoFisher Scientific) at a dilution of 1:1000. For σ1 protein, Western blotting was performed with Rabbit T1L virion antibody at a dilution of 1:1000. Blots were washed 3X in Tris-buffered saline (20 mM Tris, 137 mM NaCl [pH 7.6]) with 0.25% Tween 20 (TBST) buffer, and then incubated with secondary goat anti-rabbit IgG (BioRad, 170-6518) at a dilution of 1:2500. After three additional washes, membranes were subjected to PhosphaGLO AP (SeraCare) to image detected proteins[3].

3.4.7 Minigut monolayer development

Murine organoids were cultured for 3 days using well established methods[9]. At day 3, for M cell differentiation, 200 ng/ml RankL was added and incubated for an additional 2 days. Resulting 3D structured organoids were disrupted and pipetted into buffer containing 0.5 mM EDTA, and centrifuged at 200 x g at 4 °C for 5 mins. 500 µl of 0.05 % trypsin/0.5 mM EDTA was added to the pellet for dissociation. After incubating for 4 mins at 37 °C, 1 ml DMEM/F12 with 10% FBS was added to inactivate trypsin. The cell suspension was filtered through a 40 µm cell strainer and filtered cells were dropped on solidified 1% Matrigel coated wells to form a monolayer. 100 µl of culture medium was added on top of the cell layer, and 500 µl of culture

medium were added to the bottom. Monolayers were used for experiments after 24 hours. For M cell development, RankL 200 ng/ml was added in both top and bottom compartments.

3.4.8 Transport of Mammalian orthoreovirus across intestinal monolayer in transwell model system

Purified virus was serially diluted and subjected to a modified plaque assay analysis[19,33]. In brief L929 cells were seeded at 1.2 $x10^6$ cells/mL (or per well) in 6-well plates and upon monolayer formation, the medium was removed and virus diluted in phosphate-buffered saline (PBS) (137 mM NaCl, 3 mM KCl, 8 mM Na_2HPO_4, 1.5 mM KH_2PO_4, pH 7.4) with 2 mM $MgCl_2$. Virus was incubated on monolayers for 1 h at room temperature, then bottom solution was collected at 2 hour, 4 hour, 6 hour, and 12 hour after the addition of virus to the top of the transwell system. Then, 10 µl of the culture medium from the bottom chamber was collected and overlaid with 2 ml of 1 % Bacto Agar (Becton Dickinson), 1x Medium 199 (Life Technologies) supplemented with 2.2 g/L sodium bicarbonate (Fisher Scientific), and 12 µg/ml trypsin (Worthington Biochemical) solution. Dilutions were made for 10^{-3}, 10^{-4},10^{-5}, and 10^{-6} by using the previously made solution. Once the overlay solidified, the 6-well plates were placed at 37ºC and 5% CO_2 and plaques were counted 2 days later. The means and standard deviations were determined from two biological replicates done in triplicate.

3.4.9 Transport of AVNs across intestinal monolayer in transwell model system

Rhodamine 6G (Sigma-Aldrich) (15 µl, 10 mM) was incubated with 1.5 ml of OD=3.0 GNCs and AVNs overnight by shaking at 4 °C to allow loading of R6G into the nanocages via diffusion. R6G loaded nanocages were collected by centrifugation at 9,000 x *g*. Supernatants were removed, and the nanocages were re-dispersed in 1 ml of deionized water under sonication.

Initial R6G fluorescence intensities were recorded, and 150 µl of R6G-loaded AVNs or nanocages were added to each transwell. At 0, 0.5, 1, 2, 3, 4, 8, 12, 24, 36, and 48 hour, 50 µl was collected from the lower compartment of the transwell setup, and R6G fluorescence intensities were recorded. Each experiment was conducted in triplicate.

Data availability

The data that support the plots and other findings of this study are available from the corresponding authors upon reasonable request.

Author Contributions

T.T. fabricated GNC, isolated σ1 protein, assembled σ1 protein and Gold nanocage together to fabricate AVN, characterization of GNC, σ1 protein, AVN transporting on monolayer. Y.Q. prepared the ISC monolayer system and the characterization of M cell in 3D and 2D system. Y.Q. preformed MRV transporting tests. T.T. and Y.Q. performed in imaging, analysis of data. co-wrote the paper. L.D.B, assisted in isolated σ1 protein, assisted in MRV transporting tests, and assisted in imaging. M.W., C.L.M., Q.W. and C.Y. provided the laboratory and equipment and assisted in editing the paper. C.Y. and Q.W. provided the financial support for the research, C.L.M., Q.W. and C.Y. supervised the experiment design and execution, and provided materials.

Conflict of Interest

There is no conflict of interest to declare.

Acknowledgements

Finical support: Dr. Wang is grateful for the support from Crohn's & Colitis Foundation of America (CCFA) Career Award (No. 348137), PhRMA Foundation Research Starter Award (No. RSGTMT17). Dr. Yu would like to acknowledge USDA-NIFA (grant no. 2016-07802) and USDA-ARS (award no. 019636-00001) for partially funding this research.

The authors thank D. Rollins for assistance with data analysis, K. Yoon for assistance in T1L σ1 purification and qPCR, B. Bellaire and N. Peroutka-Bigus for assistance in immunofluorescence.

3.5 References

[1] Lycke, N. Recent progress in mucosal vaccine development: Potential and limitations. Nature Reviews Immunology (2012). doi:10.1038/nri3251

[2] Giudice, E. L. & Campbell, J. D. Needle-free vaccine delivery. Advanced Drug Delivery Reviews (2006). doi:10.1016/j.addr.2005.12.003

[3] Bussiere, L. D., Choudhury, P., Bellaire, B. & Miller, C. L. Characterization of a Replicating Mammalian Orthoreovirus with Tetracysteine-Tagged μNS for Live-Cell Visualization of Viral Factories. J. Virol. (2017). doi:10.1128/jvi.01371-17

[4] Wolf, J. L. et al. Determinants of reovirus interaction with the intestinal M cells and absorptive cells of murine intestine. Gastroenterology (1983).

[5] Wang, M., Gao, Z., Zhang, Z., Pan, L. & Zhang, Y. Roles of M cells in infection and mucosal vaccines. Human Vaccines and Immunotherapeutics (2014). doi:10.4161/hv.36174

[6] Helander, A. et al. The Viral 1 Protein and Glycoconjugates Containing 2-3-Linked Sialic Acid Are Involved in Type 1 Reovirus Adherence to M Cell Apical Surfaces. J. Virol. (2003). doi:10.1128/jvi.77.14.7964-7977.2003

[7] Lee, P. W. K. & Leone, G. Reovirus protein σ1: From cell attachment to protein oligomerization and folding mechanisms. BioEssays (1994). doi:10.1002/bies.950160311

[8] Knoop, K. A. et al. RANKL Is Necessary and Sufficient to Initiate Development of Antigen-Sampling M Cells in the Intestinal Epithelium. J. Immunol. (2009). doi:10.4049/jimmunol.0901563

[9] Sato, T. et al. Single Lgr5 stem cells build crypt-villus structures in vitro without a mesenchymal niche. Nature 459, 262–265 (2009).

[10] Altay, G. et al. Self-organized intestinal epithelial monolayers in crypt and villus-like domains show effective barrier function. Sci. Rep. (2019). doi:10.1038/s41598-019-46497-x

[11] Barton, E. S. et al. Junction adhesion molecule is a receptor for reovirus. Cell (2001). doi:10.1016/S0092-8674(01)00231-8

[12] Kanaya, T. et al. Development of intestinal M cells and follicle-associated epithelium is regulated by TRAF6-mediated NF-κB signaling. J. Exp. Med. (2018). doi:10.1084/jem.20160659

[13] Gregory, A. E., Titball, R. & Williamson, D. Vaccine delivery using nanoparticles. Frontiers in Cellular and Infection Microbiology (2013). doi:10.3389/fcimb.2013.00013

[14] Zhao, L. et al. Nanoparticle vaccines. Vaccine (2014). doi:10.1016/j.vaccine.2013.11.069

[15] Pokharkar, V. et al. Gold nanoparticles as a potential carrier for transmucosal vaccine delivery. J. Biomed. Nanotechnol. (2011). doi:10.1166/jbn.2011.1200

[16] Almeida, J. P. M., Figueroa, E. R. & Drezek, R. A. Gold nanoparticle mediated cancer immunotherapy. Nanomedicine: Nanotechnology, Biology, and Medicine (2014). doi:10.1016/j.nano.2013.09.011

[17] Skrabalak, S. E. et al. Gold nanocages: Synthesis, properties, and applications. Acc. Chem. Res. (2008). doi:10.1021/ar800018v

[18] Skrabalak, S. E., Au, L., Li, X. & Xia, Y. Facile synthesis of Ag nanocubes and Au nanocages. Nat. Protoc. (2007). doi:10.1038/nprot.2007.326

[19] Furlong, D. B., Nibert, M. L. & Fields, B. N. Sigma 1 protein of mammalian reoviruses extends from the surfaces of viral particles. J. Virol. (1988).

[20] Dryden, K. A. et al. Internal structures containing transcriptase-related proteins in top component particles of mammalian orthoreovirus. Virology (1998). doi:10.1006/viro.1998.9146

[21] Mendez, I. I., Hermann, L. L., Hazelton, P. R. & Coombs, K. M. A comparative analysis of Freon substitutes in the purification of reovirus and calicivirus. J. Virol. Methods (2000). doi:10.1016/S0166-0934(00)00217-2

[22] Fischer, M. J. E. Amine coupling through EDC/NHS: a practical approach. Methods Mol. Biol. (2010). doi:10.1007/978-1-60761-670-2_3

[23] Ivanov, M. R., Bednar, H. R. & Haes, A. J. Investigations of the mechanism of gold nanoparticle stability and surface functionalization in capillary electrophoresis. ACS Nano (2009). doi:10.1021/nn8005619

[24] Fatehullah, A., Tan, S. H. & Barker, N. Organoids as an in vitro model of human development and disease. Nature Cell Biology (2016). doi:10.1038/ncb3312

[25] de Lau, W. et al. Peyer's patch M cells derived from Lgr5(+) stem cells require SpiB and are induced by RankL in cultured 'miniguts'. Mol. Cell. Biol. 32, 3639–47 (2012).

[26] Rouch, J. D. et al. Development of functional microfold (M) cells from intestinal stem cells in primary human enteroids. PLoS One (2016). doi:10.1371/journal.pone.0148216

[27] Yin, Y. & Zhou, D. Corrigendum: Organoid and Enteroid Modeling of Salmonella Infection. Frontiers in cellular and infection microbiology (2018). doi:10.3389/fcimb.2018.00257

[28] Wood, M. B., Rios, D. & Williams, I. R. TNF-α augments RANKL-dependent intestinal M cell differentiation in enteroid cultures. Am. J. Physiol. - Cell Physiol. 311, C498–C507 (2016).

[29] Gehart, H. & Clevers, H. Tales from the crypt: new insights into intestinal stem cells. Nature Reviews Gastroenterology and Hepatology (2019). doi:10.1038/s41575-018-0081-y

[30] Mabbott, N. A., Donaldson, D. S., Ohno, H., Williams, I. R. & Mahajan, A. Microfold (M) cells: Important immunosurveillance posts in the intestinal epithelium. Mucosal Immunology (2013). doi:10.1038/mi.2013.30

[31] Virgin, H. W., Bassel-Duby, R., Fields, B. N. & Tyler, K. L. Antibody protects against lethal infection with the neurally spreading reovirus type 3 (Dearing). J. Virol. (1988).

[32] Virgin IV, H. W., Mann, M. A., Fields, B. N. & Tyler, K. L. Monoclonal antibodies to reovirus reveal structure/function relationships between capsid proteins and genetics of susceptibility to antibody action. J. Virol. (1991).

[33] Middleton, J. K. et al. Thermostability of Reovirus Disassembly Intermediates (ISVPs) Correlates with Genetic, Biochemical, and Thermodynamic Properties of Major Surface Protein 1. J. Virol. (2002). doi:10.1128/jvi.76.3.1051-1061.2002

CHAPTER 4. EFFECTIVE TRANSPORT AND SLOW RELEASE OF RHODAMINE 6 G BY SIGMA 1 FUNCTIONALIZED ORAL VACCINE DELIVERY VEHICLE (OVDV) VIA MICROFOLD CELL-MEDIATED TRANSCYTOSIS

Tianjian Tong, Yijun Qi, Luke D. Bussiere, Cathy L Miller, Qun Wang* and Chenxu Yu*

[1]Department of Agricultural Biosystem and Engineering, Iowa State University, Ames, Iowa

[2]Department of Chemical and Biological Engineering, Iowa State University, Ames, Iowa

[3]Department of Veterinary Microbiology and Preventive Medicine, College of Veterinary Medicine, Iowa State University, Ames, Iowa

[4]Interdepartmental Microbiology Program, Iowa State University, Ames, Iowa

Proposed to submit to *Chemical Engineering Journal*

Abstract

Compared to intramuscular/intravenous injection as the delivery pathway for vaccines, oral delivery through gastrointestinal mucosa has its advantages of high patient acceptance (e.g., no-pain) and easy administration. However, delivery efficiency and protection of medically effective payloads (i.e., immunogens) against gastric damage during the process are critical factors limiting the efficacy of the oral delivery system and limiting oral delivery systems' effectiveness. In this study, hollowed silicon nanospheres with poly-l-lysine (PLL) coating and σ1 protein functionalization (HSS-pLL-σ1) were explored as oral vaccine delivery vehicles (OVDV). The transport of these OVDVs to mucosal lymphoid tissues could be facilitated by the

σ1-induced transcytosis targeting microfold cells (M-cells) in gastrointestinal epithelia. PLL coating provided protection and slow-release control of rhodamine 6 G, a model payload. The transport effectiveness of these OVDVs was tested on intestinal organoid monolayers *in vitro*. When compared with other experimental groups, the HSS-σ1-PLL OVDV system demonstrated two significant advantages: a significantly higher transport efficiency (a 29% net additional payload transport compared to blank control); and protection of payloads which led to both better transport performance (a 61% improvement over the no-coating control) and extended-release of payloads which could enhance vaccine efficacy. The strategy of producing OVDVs via σ1 protein functionalization and PLL coating on hollowed nanoparticles could be an effective method to have oral vaccine/drug delivery vehicles utilizing M cell-mediated transcytosis pathway for better transport performance.

4.1 Introduction

Oral vaccination delivery specifically aiming intestinal mucosa layer is viewed as patient-friendly[1,2] as it generally supports pain-free administration. In addition, oral delivery could also have advantages over intravenous injection and subcutaneous injection on cost efficiency, convenience, and increased safety[1–3]. The development of oral vaccine needs to face some specific challenges that do not exist for injection-based vaccine. Namely, the vaccine needs to survive the harsh gastric environment and be transported across the GI mucosal epithelia effectively[2,3]. Vaccine delivery vehicles hold the key to overcoming both challenges, they will protect the vaccines against gastric degradation, and they need to be effective in transporting the vaccines to their target areas (for example, mucosal-associated lymphoid tissues (MALT) like Peyer's patches) and release them there to trigger strong immune responses.

Previously we reported a strategy to use σ1 protein from mammalian reovirus to functionalize gold nanocages into artificial virus-like nanocarriers (AVN) that utilize σ1:Microfold cells (M cells) transcytosis pathway to improve nanocarrier transport across intestinal cell monolayer that mimics gastrointestinal wall[2]. But the AVNs reported earlier were not protected, and the release of payloads from the AVNs was not controlled. Hence, the payload could freely diffuse out of the AVNs, limiting the system's effectiveness. In this study, we further explored the σ1:M cell transcytosis strategy by utilizing a different nanocarrier system, the hollowed silicon nanospheres. The abundance of silicon makes it a much more economically feasible option over gold. To test the hypothesis that coating could be put outside the nanocarriers, which could then be conjugated with σ1 proteins to further improve the effectiveness of the nanocarriers for vaccine delivery, we developed a coating method using poly-l-lysine (PLL), a nontoxic polymer, to create a protective layer outside the nanocarriers which also serve as a diffusion barrier to slow down the release of payloads from the nanocarriers. σ1 proteins were then conjugated to the PLL coating for specific M cell binding. We aimed to provide a complete strategy to address both of the oral delivery challenges more effectively and achieve an oral vaccine delivery vehicle (OVDV) that could offer further enhanced vaccine efficacy.

σ1 protein was extracted from type 1 Lang mammalian reovirus (T1L-MRV). T1L-MRV has a diameter of 85 nm[4]. MRV is a non-enveloped virus consist of 5 structural proteins (λ1, λ2, λ3, σ2, and μ2), and the viral genome is enclosed by a core particle formed with the five structural proteins[4]. Outside the core are three (σ1, μ1, and σ3) outer capsid proteins all play critical roles in virus cell entry[4]. Among them, the σ1 protein is instrumental in recognizing and

interacting with M cells. M cells are specialized cells in the follicle-associated epithelium (FAE) of Peyer's patchesd[5,6]. M cells can endocytose foreign antigens in the lumen, then transport them from the apical surface to the basolateral surface (Fig. 4.1a[2]). For MRV, σ1 can adhere to α2–3-linked sialic acids on the apical surface of M cell and facilitate the transcytosis of MRV into MALT to create infection on the basolateral surface of enterocytes[7]. Our previous development of gold nanocage AVN was inspired by MRV transcytosis across M cells, and σ1 proteins were the key to exploring this M cell pathway[2]. It was reasonable to believe that σ1-induced functionalities would work on nanocarriers other than gold nanocages. With σ1: M cell pathway, we can build a universal oral drug/vaccine delivery strategy regardless of the types of nanocarriers. It should be noted that surface-functionalization with σ1 proteins is a vital part of our design for the nano delivery system, which means, solid nanoparticles that can only carry medically-effective payloads (i.e., vaccines) on the surface (2-D loading) would not be the best choices, as the surface sites occupied by the σ1 proteins could not be used for payload anymore which would limit the loading capacity on the nanocarriers. Hence, hollowed shell nanoparticles with interior space available for payload would be preferred. In this study, we chose hollowed silicon spheres (HSS) as our nanocarriers. These particles were easy to make, and with inert chemical properties that make them nontoxic for medical applications[8–11]. As these particles have void internal space, loading/unloading of medically effective payloads can be readily carried out via diffusion-driven processes. To protect the payloads against the harsh gastric environment, poly-l-lysine (PLL), a widely used non-toxic polymer[12], was used in this study as a soft coating to seal the payloads inside the HSS, which would also provide release control (i.e., extended-release) for the payloads as the nanocarriers reached their destination since the diffusion of the

payloads through the PLL coating would be much slower than that in naked nanocarriers as the gold nanocage AVN from our previous report[2].

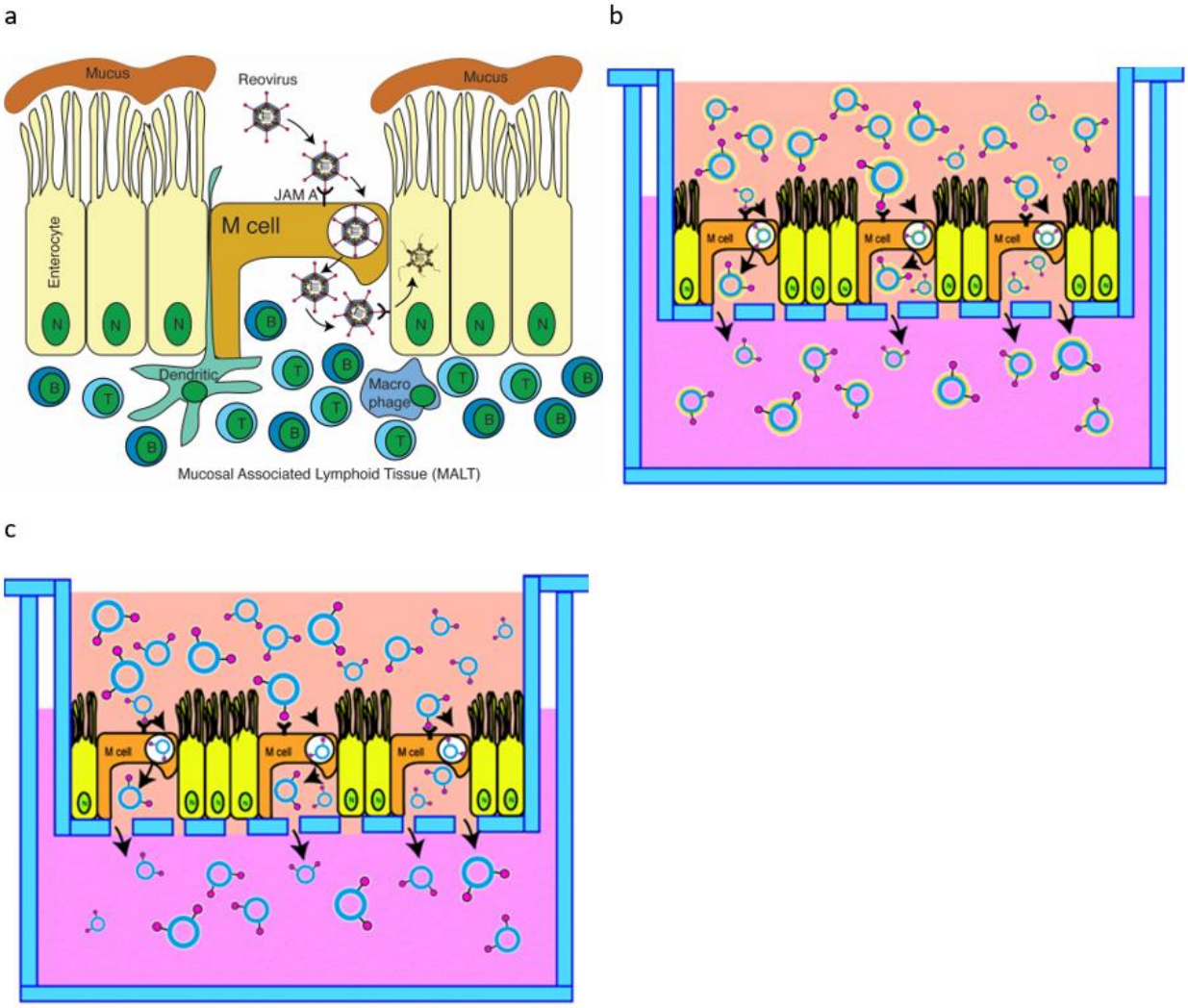

Fig 4.1 Scheme: T1L σ1 functionalized OVDVs (HSS-PLL-σ1 and HSS-σ1) exploit the M cell transcytosis pathway. (a) Model of MRV infection of MALT. (b) Schematic of the transport of R6G loaded OVDVs (HSS-PLL-σ1) nanocarriers through M cells incorporated to intestinal organoid monolayers. (c) Schematic of the transportation of R6G loaded HSS-σ1 through M cells incorporated to intestinal organoid monolayers.

To validate the effectiveness of the HSS-σ1 based OVDV system and evaluate the differences in terms of payload protection and release with and without the PLL coating, we used

the same intestinal monolayer system reported in our previous work[2] as an *in vitro* mimic to the gastrointestinal epithelia, transwell plates containing organoid monolayer with M cells, which were cultivated from differentiated small intestinal stem cells, were used, in which intestinal mucosal layer was modeled on the top inserts, and MALT sites were modeled by the bottom compartment, as shown in Fig. 4.1b and Fig. 4.1c. Utilizing this M cell monolayer system, we aimed to compare the capacity of both HSS-PLL-σ1 and HSS-σ1 nanocarrier systems to transport the payload (e.g., R6G) across the monolayer via M cell-mediated transcytosis pathway, which can serve as an excellent simulation to evaluate the potential performance of the nanocarriers as oral vaccine delivery vehicles.

4.2 Results and discussion

4.2.1HSS- σ1 DDV: HSS, Poly-L-lysine, and MRV σ1

Hollowed silicon nanospheres (HSS) have been used as drug delivery tools[8–11]. HSS has superior properties compared to solid nanoparticles[13], as its hollowed interior significantly increased the loading capacity of targeted payloads (vaccine and drugs). HSS were synthesized by a simple one-step reverse microemulsion method at room temperature by mixing oil phase and the water phase for just 24 hours[13]. The HSS made was characterized using transmission electron microscopy (TEM). As shown in fig. 4.2a, the particles had an average diameter of xx nms. They were hollow inside as evidenced by the light color of the interior in comparison to the darker shell which was the silicon.

MRV σ1 proteins were extracted and purified from MRV as previous described[2,14–16]. The protein preps from MRV were enriched via centrifugation, then filtrated using 30 kDa cut-off molecular weight filter. The identity of the obtained purified protein samples was confirmed by western blot using T1L virion anti-sera, which can recognize σ1 protein[2]. As shown in Fig. 4.2b, the band at 50 kDa represented σ1 protein (left lane). No band was detected in the middle section of the western blot, which was the filtrate. These results confirmed that after 30kDa filtration, there was no unconjugated σ1 protein existed in the filtrate. In the meantime, the right section of the western blot showed all structural proteins from MRV.

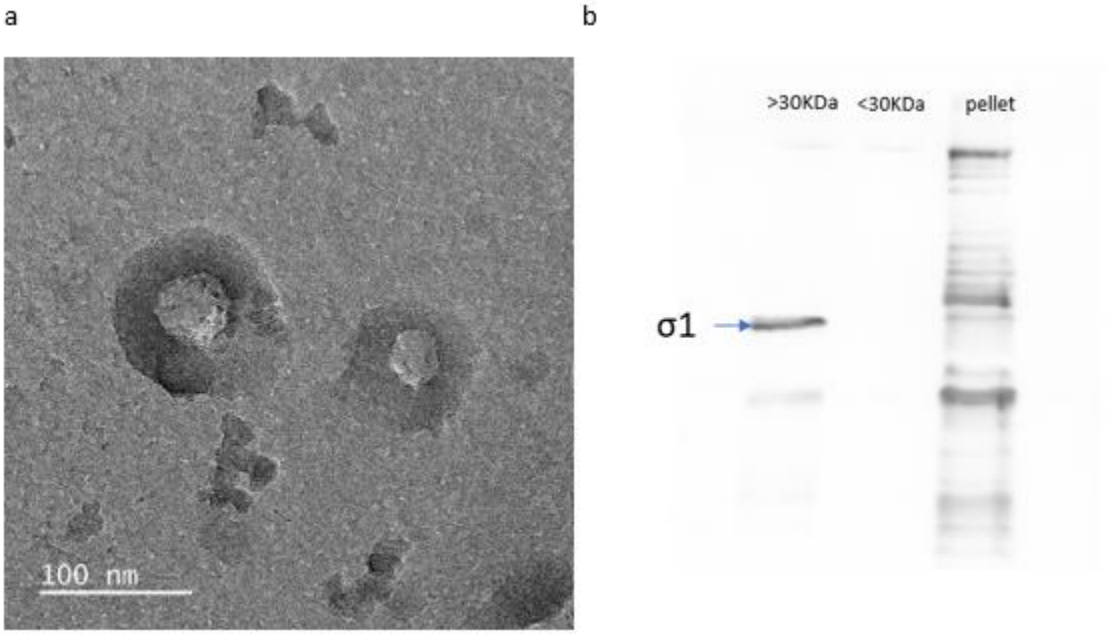

Fig 4.2 MRV σ1 functionalization of HSSs. (a) TEM image of HSSs showing an average diameter of 50 nm. (b) Western blot for pellets after last centrifugation, control group, and T1L σ1 protein (50 kDa). Following purification, T1L σ1 protein was concentrated using a 30 kDa filter (left). Filtrated solution (middle) and pellets (right) serve as the control.

4.2.2 Preparation of M cell incorporated intestinal monolayer from small intestinal organoids

3-dimensional structured small intestinal organoids were derived from mice's small intestinal stem cells[2,17] as described elsewhere. Briefly, Stem cells were harvested from C3H/HeN mice's small intestine[18]. Then growth medium and growth factors (R-spondin 1, Noggin, and EGF) included Matrigel, were added to stem cells[18]. Previous works[2,19–23] indicated that M cell presence can be induced by Rank L to the culture medium of the small intestinal organoids. As shown in fig. 4.3b, glycoprotein 2 (GP2) was a marker that confirmed the expressing of M cell in the organoids (fig. 4.3a) as well as the monolayer samples (fig. 4.3C)[2].

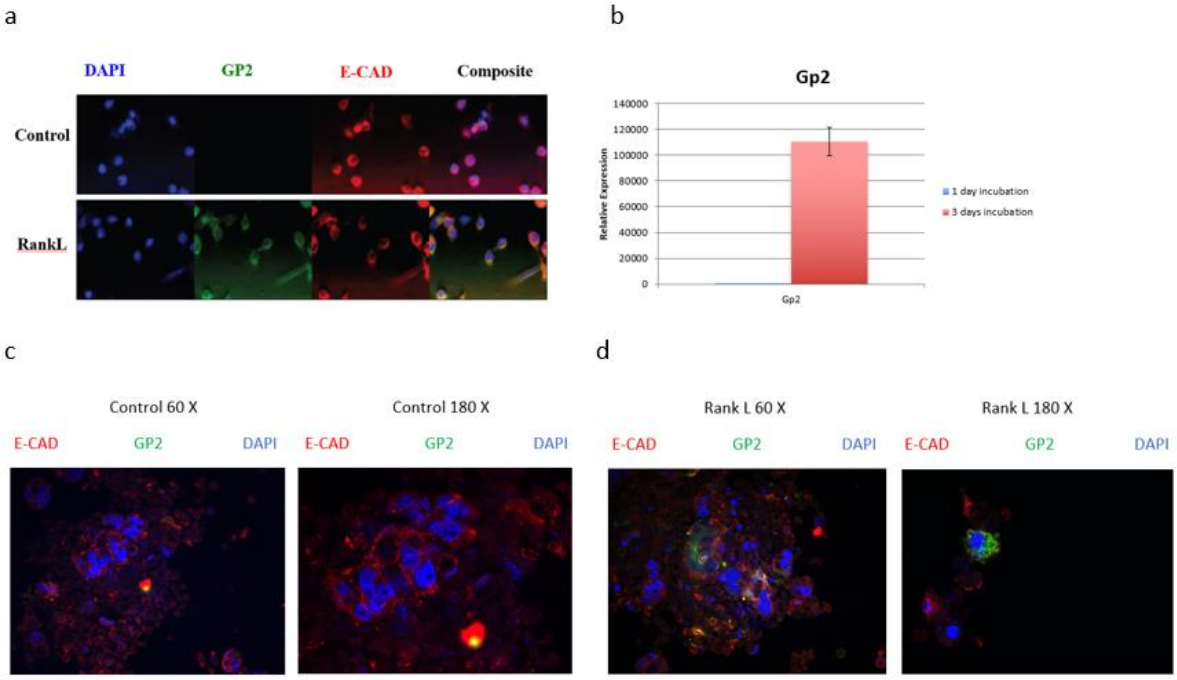

Fig 4.3 Detection of microfold cells in 3D mouse organoids and 2D organoid-derived monolayers. (a)Immunofluorescence images of untreated and three-day Rank L-treated 3D organoids stained with antibodies against GP2 (green) and E-Cadherin (red). Nuclei are stained with DAPI (blue). (b) RT-qPCR analysis for expression of GP2-specific mRNA isolated from untreated and Rank L-treated organoids. (c) Immunofluorescence images of untreated organoid

monolayers stained with antibodies against GP2 (green) and E-cadherin (red). Nuclei are stained with DAPI (blue). (d) Immunofluorescence images of Rank L-treated organoid monolayers stained with antibodies against GP2 (green) and E-cadherin (red). Nuclei are stained with DAPI (blue).

In Fig. 4.3a, we can only find GP2 maker expressed (green) in the Rank L treated organoids, not in the control groups with untreated organoids. These results suggested that only Rank L treated organoids contained M cells in agreement with the previous reports[2,19–23]. RT-qPCR with GP2 specific primers was utilized to verify the M cells presence. The RT-qPCR results (Fig. 4.3b) confirmed the immunofluorescence results (Fig. 4.3a) of M cell presence in only the Rank L treated organoids. Again, our work confirmed that by adding Rank L into organoids with 3-day incubation, M cells were induced in the organoids.

Once the M cell containing organoids were produced and grown to the proper size (two days after Rank L was introduced), their 3-D structure was carefully broken up, and the cells were re-cultured in transwells. Rank L was introduced again into the growth media. A. After incubation of 24 hours, a stable cellular monolayer was formed, which was a mimic of the gastrointestinal epithelia reported before[2,24]. Again, GP2 expressions were only detected in Rank L treated monolayers, as shown in fig. 4.3d, and not in the control group, which received no Rank L treatment (Fig. 4.3c).

4.2.3 Transportation of HSS nanocarriers through intestinal monolayers

Transport of both HSS-PLL-σ1 and HSS-σ1 with a small molecule dye (rhodamine 6G, R6G) serving as a model payload was tested with the transwell organoid monolayer system. As mentioned earlier, the transport of these nanocarriers was facilitated by σ1 binding to M cells, which triggered transcytosis through M cells. As σ1 protein and M cells both were needed for the elevated transport across the monolayer to materialize, samples with R6G-loaded HSS without

σ1 functionalization were used as HSS control, and small intestinal organoid monolayer without M cells was used as monolayer control.

The cross-monolayer transport was then monitored by measuring the movement of R6G, which is a fluorophore and can be readily quantified by measuring the fluorescence intensity. This was also the main reason why we chose it to be our model payload. We first compared the performance of HSS-σ1 and HSS transport on organoid monolayers with/without M cells. At time points of 0, 1, 2, 3, 4, 8, 12, 24, 36, and 48 hours, from initial addition of HSS-σ1 or HSS into the transwells, samples were taken from the lower compartments of each of the transwell, and the fluorescence from R6G was measured. The fluorescence intensity data were normalized against the initial samples' full R6G fluorescence intensity, and the percentage represented the percentage of payloads moved across the monolayers. Similar patterns for gold nanocage AVNs in our previous work[2] were observed. As shown in Fig. 4.4a, transport of R6G by HSS-σ1 across the organoid monolayer with M cells was the highest among the four groups. No significant differences in transport were seen among the three groups with controls, as at least one of the two required conditions (σ1 proteins or M cells) was missing from these groups. Thus, it was again confirmed that both σ1 and M cell were needed to trigger the M-cell transcytosis pathway. A quantitative assessment of the payload (R6G) effectively carried by HSS-σ1 through the M cells was conducted by subtracting out the baseline, which was the R6G transported by HSS- σ1 through monolayer without M cells. At 48 hours (Fig. 4.4b), around 18% of the payload (R6G) was delivered by HSS-σ1 nanocarriers into the bottom compartment of our transwell setup, which was slightly less than transport of the payload (R6G) by gold nanocage AVNs through M cell monolayers (~20%) from our previous study. Given the differences in the shape and size of the nanocarriers, such discrepancy was to be expected. Nonetheless, we can conclude

that the delivery vehicles utilizing the σ1-M cell pathway were effective means to enhance the transport efficiency for drugs/vaccines, regardless of the materials of the nanocarriers.

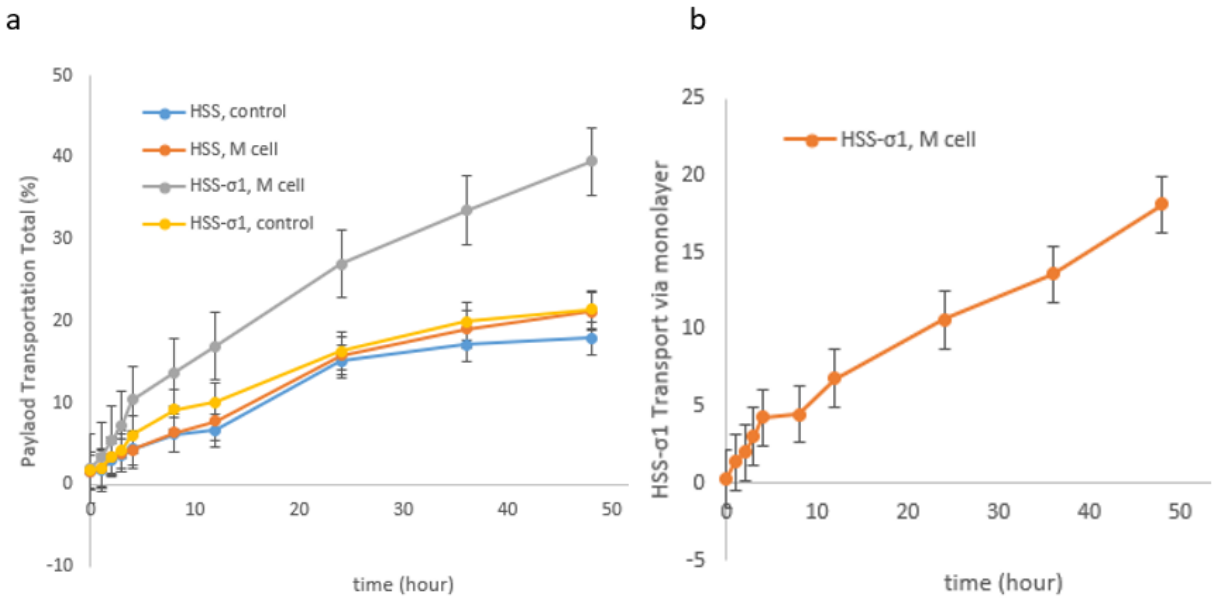

Fig 4.4 a Payload (R6G) in different vaccine delivery vehicles (HSS- σ1, HSS) transport across intestinal monolayers, with and without M cell induction over time. b HSS- σ1 transport total through intestinal monolayers with M cells incorporated.

Next, we tested our hypothesis that HSS-PLL-σ1 nanocarriers be more effective in transporting cargoes across the monolayer with PLL coating. Here we compared transporting performance of HSS-PLL-σ1 and HSS-σ1. At time points of 0, 1, 2, 3, 4, 8, 12, 24, 36, and 48 hours the transport of the payloads (R6G) was measured as before. As shown in fig. 4.5a, the σ1 functionalized HSS nanocarriers clearly transported more R6G payloads through the M-cell monolayers, showing the σ1:M cell-mediated transcytosis pathway was at work.

It should be noted that consistently higher R6G levels were observed in HSS-σ1/monolayer control groups than in HSS-PLL-σ1/monolayer control groups. The baseline level of R6G transport in monolayer control systems (i.e., without M-cells) was determined by free diffusion of released R6G in the top compartment of the transwell across the monolayers. The

higher baseline level was caused by more R6G being released from unprotected HSS-σ1 system throughout the experiments, which was evidence showing the release control effects of the PLL coating.

Furthermore, fig. 4.5a appeared to show that the HSS-σ1 system transported more R6G across the M-cell monolayer in the first 8 hours. However, when the net transport of R6G (normalized against baseline levels with no M cells) was calculated, a different picture emerged. As shown in fig. 4.5b, the net transport went up significantly in the HSS-PLL-σ1 system, at 4 hours and beyond. Within the first 4 hours, the higher level of R6G was most likely due to its faster release from the uncoated HSS-σ1 system as the nanocarriers were not protected. The data suggested that the presence of the PLL coat provided good protection for the R6G and significantly slowed down its release within the first 4 hrs. In addition, as shown in fig. 4.5a, at 36 hours and beyond, more payload (R6G) was released in the bottom compartment from the HSS-PLL-σ1 OVDVS, which further confirmed the extended-release achieved in the coated OVDVs.

Quantitatively, as shown in fig. 4.5c, HSS-PLL-σ1 nanocarriers transported the payloads effectively across the M-cell monolayer via the σ1-M cell α2–3 sialic acid transcytosis pathway. Compared with the HSS-σ1 nanocarriers, the net transport of R6G went up from 18% to 29% at the 48 hour time mark. These results strongly suggested that PLL coating could slow down the diffusion of payload out of the nanocarriers, which the r would protect payloads against the harsh gastric environment and could serve as a control mechanism to extend the duration of the payload release at the targeted destination of the delivery. Thus, we concluded that the PLL coating conjugated with σ1 proteins could provide a complete strategy to make 3-D loaded nanocarriers into more effective OVDVs that displayed delay release patterns and better delivery

efficiency (61% improvement when compared against uncoated OVDVs). These characteristics of HSS-PLL-σ1 nanocarriers could make them an auspicious oral vaccine delivery system to transport immunogens into the gut mucosa.

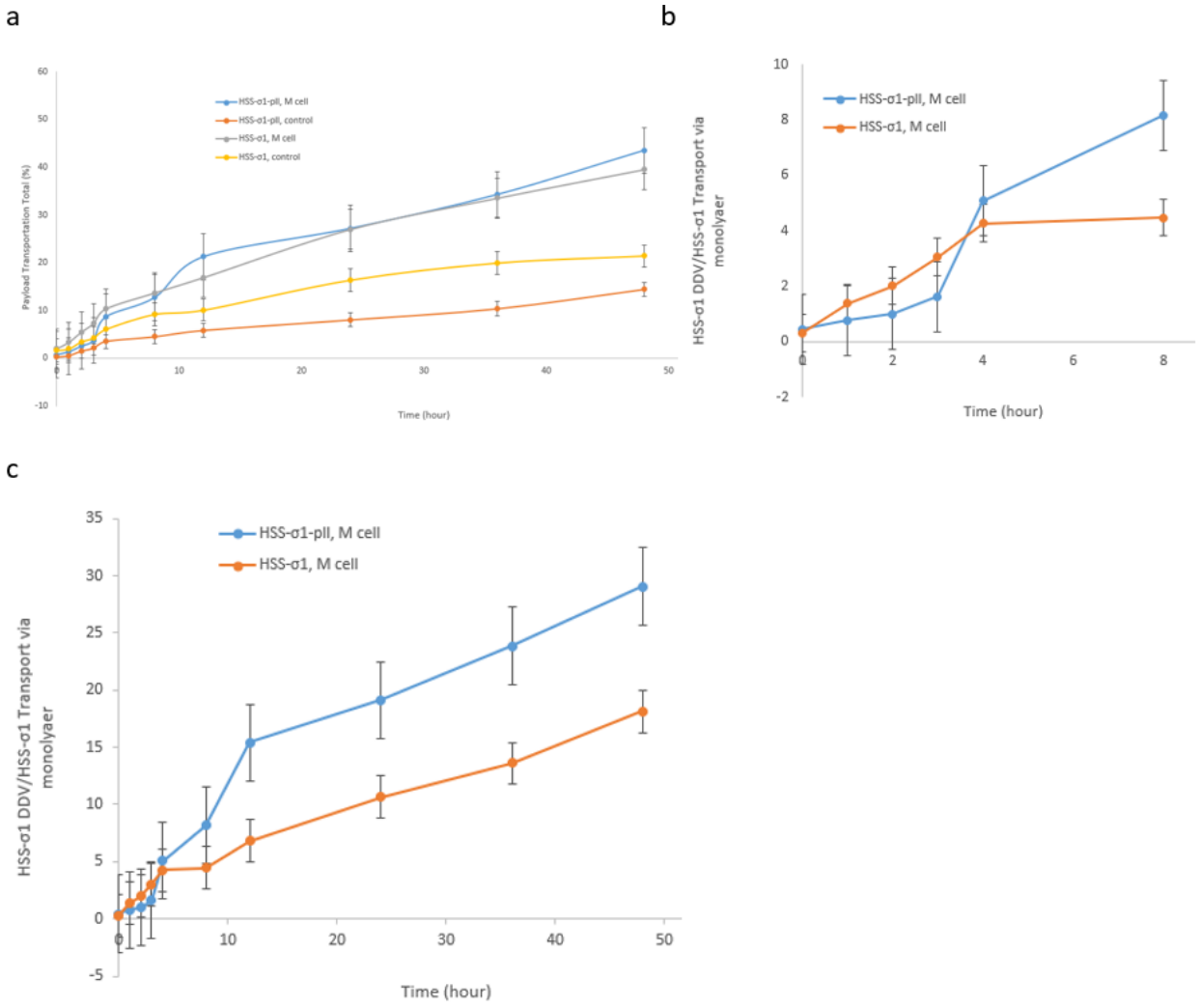

Fig 4.5 a. Payload (R6G) in different vaccine delivery vehicles (HSS- σ1DDV, HSS- σ1) transport across intestinal monolayers with and without M cell induction over time. b. Amplified version for first 8 hours of Fig. 4.5a, across intestinal monolayers, with and without M cell induction at early times only. c. HSS- σ1 DDV and HSS- σ1 transport total through intestinal monolayers with M cells incorporated. d. Amplified version for first 8 hours of Fig. 4.4c, HSS- σ1 DDV and HSS- σ1 transport total through intestinal monolayers with M cells incorporated at the early time only.

4.3 Conclusion

To summarize, our OVDVs (HSS-PLL-σ1) composed of hollowed silicon nanosphere functionalized with MRV receptor binding protein σ1 with Poly-L-Lysine coating were shown to be able to utilize M cells mediated transcytosis effectively to transport model payloads across intestinal epithelia mimic (i.e., organoid monolayers), and the PLL coating provided an effective diffusion barrier that could protect the payload inside, as well as slow down and extended its release. Overall a much-improved delivery performance (61%) was achieved in the PLL coated OVDVs vs. uncoated systems. With the σ-1:M-cell-mediated transcytosis pathway and the PLL payload protection/control release, the HSS-PLL-σ1 OVDVs are more complete drug delivery vehicles with better-transporting efficiency. Potentially, they can offer enhanced vaccine effectiveness by orally delivering antigens across the gastrointestinal mucosa into mucosal-associated lymphoid sites (e.g., Peyer's patches).

4.4 Experimental

4.4.1 HSS fabrication

(3-aminopropyl) triethoxysilane (APS), tetraethylorthosilicate (TEOS), and Triton X-100 were purchased from Acros Organics. Cyclohexane was purchased from Fisher.

The water phase of this experiment was made by adding 3 μL of APS into 1.1 mL DI water. For Oil phase of this experiment, 4.47g of Triton X-100 and 3.64g of n-octanol were added to 14.5 g of cyclohexane. The reaction needs to be carried at the high-speed stirring of the oil phase. The water phase was added to the oil phase. Then 200 μL of NH_4OH and (TEOS) were

added into water-oil microemulsion. These two agents. These two agents will trigger polymerization reaction these two agents will trigger polymerization reaction. Twenty-four hours of reaction time at room temperature were required to make HSS. Acetone needs to be added after 24 hours to stop the reaction. Washing steps first with ethanol and then with DI-water will be carried three times for each[13].

4.4.2 T1Lσ1 isolation and purification

L929 mouse fibroblast cells were maintained in Joklik modified minimum essential medium (Sigma-Aldrich) supplemented with 2 mM L-glutamine (Mediatech), 2% bovine calf serum (HyClone), 2% fetal bovine serum, and penicillin (100 IU ml−1)–streptomycin (100 μg ml−1) solution[2]. Type 1 ang (T1L) MRV was propagated in the L929 cells in spinner[2]. These cells were then harvested by centrifuged at 3,000g for 10 min. And then, they were resuspended in HO buffer (250 mM NaCl, 10 mM Tris, pH 7.4) and frozen at −80 °C[2,16]. Then the virus was purified as described in our previous work[2]. Substitution of Vertrel® XF (DuPont) in place of Freon was utilized to achieve the purification[2]. After this purification step, digesting with α-chymotrypsin was necessary to produce ISVPs[2]. After purification of ISVPs, we heated ISVPs to 52 °C for 30 min to release σ1[2]. Specifically, ISVPs were centrifuged at 35 000 rpm, and σ1 will be in the supernatant after centrifuge[2,16]. Then σ1 was concentrated by Centricon-30 micro concentration unit (Amicon Crop.)[2,16].

4.4.3 HSS functionalization

HSS- σ1 DDV: 2 ml HSS was first incubated with poly-l-lysine (PLL) (w/v 0.1%) and 200 μl R6G. The solution was centrifuged at 9,000g for 10 minutes, then DI-water was added to

re-disperse HSS-PLL. Then (1-ethyl-3-(3-dimethyl aminopropyl) carbodiimide hydrochloride) (EDC) (Thermo scientific)/N-hydroxysulfosuccinimide (NHS) (Sigma-Aldrich) mix solution was added to HSS-PLL, the solution was incubated for 30 min. The solution was centrifuged at 6,500g for 30 min to remove the excessive EDC/NHS. Then σ1 was added and incubated with HSS-PLL at 4°C overnight.

HSS- σ1: HSS the first used EDC/NHS procedure to link σ1 protein onto HSS. Then HSS- σ1 was incubated with R6G at 4°C overnight. Wash with DI water to get rid of excessive R6G.

HSS: incubated with R6G at 4°C overnight. Wash with DI water to get rid of excessive R6G.

4.4.4 High-resolution immunofluorescence microscopy

Small intestinal organoids were fixed with 4% paraformaldehyde for 1 hour at room temperature. Then were permeabilized for 30 minutes with 0.5% TritonX bugger (250 μL Triton-X100 in 50 mL PBS). Triple PBS washes were needed. The primary antibody solution was made with 1% PBSA, organoids were stained with primary antibody at 4 °C overnight. On day 2, secondary antibodies were added to the solution and incubated for 2 hours at room temperature. Then triple wash with PBS. To stain nuclei of organoids, 4′,6-diamidino-2-phenylindole (DAPI) (EMD Millipore) was used. Fluorescence staining images were acquired by an Olympus®IX81 laser scanning confocal microscope using a 100× oil-immersion objective. Primary antibody Rat anti-GP2 (MBL International Corporation) was used with a concentration of 2.5 μg ml^{-1}, and secondary antibody goat anti-rat FITC (ThermoFisher) was used at a 1 : 250 dilution to stain GP2. Primary antibody rabbit anti-E-cadherin (Invitrogen) was used at a 1 : 250 dilution,

followed by a secondary antibody donkey anti-rabbit IgG H&L (Alexa Fluor® 594) (Abcam) at a 1 : 250 dilution to stain E-cadherin.

4.4.5 Quantitative RT-qPCR for verifying microfold cell development

Treatment with 1000 µl of Cell recovery solution (Corning Life Sciences) at 4 °C for 1 hour of organoids was carried to remove Matrigel. Then washes with PBS twice. RNA extraction was carried using an RNeasy Mini Kit (Qiagen) and following the kit's procedure. NanoDrop spectrophotometer was used to check the concentration and purity of the RNA. For primers, pairs were used. Three of them were purchased from the DNA facility, Iowa State University, Ames, IA: Anxa5 (F: 5′-ATCCTGAACCTGTTGACATCCC-3′; R: 5′-AGTCGTGAGGGCTTCATCATA-3′), GP2 (F: 5′-CTGCTACCTCGAAGGGGACT-3′; R: 5′-CATTGCCAGAGGGAAGAACT-3′) and a primer for the housekeeping gene Gapdh (F: 5′-TTCACCACCATGGAGAAGGC-3′; R: 5′-GGCATGGACTGTGGTCATGA-3′). A Power SYBR™ Green RNA-to-CT™ 1-Step Kit was utilized to complete RT-qPCR.

4.4.6 Western blot for verifying the presence of σ1 protein

For σ1 protein identification, western blotting was used. Rabbit T1L virion antibody at a dilution of 1 : 1000 was used as the primary antibody. Followed by triple-wash with Tris-buffered saline (20 mM Tris, 137 mM NaCl [pH 7.6]) with 0.25 % Tween 20 (TBST) buffer. We choose goat anti-rabbit IgG (BioRad, 170-6518) at a dilution of 1 : 2500. Then again followed by triple-washes. PhoshpaGLO AP (SeraCare) were added to the membranes to be ready for image[4].

4.4.7 Organoid monolayer development

Organoids were cultured for three days using well-established methods[17]. On the 3rd day, 200 ng ml−1 RankL was added and incubated for an additional two days to differentiate M cells. Then, 3D structured organoids were disrupted and pipetted into a buffer containing 0.5 mM EDTA. Then the solution was centrifugated at 200g at 4 °C for 5 min. Dissociation of the pellet was achieved by adding 500 µl of 0.05% trypsin/0.5 mM EDTA. Incubation at 37 °C for 4 min was required. To inactivate the trypsin, 1 ml DMEM/F12 with 10% FBS was added. The cell suspension went through a 40 µm cell strainer, and then filtered cells were added on solidified 1% Matrigel-coated wells to set up a monolayer. For monolayer setup: on top of the cell layer, 100 µl of culture medium was added; at the bottom and 500 µl of culture medium were added. Monolayers will be ready for experiments after 24 hours. For M cell development, 200 ng ml^{-1} RankL was added in both top and bottom compartments.

4.4.8 Transport of HSS- σ1 DDV, HSS- σ1 and HSS across intestinal monolayers in a Transwell model system

HSS- σ1 DDV, HSS- σ1, and HSS all loaded with R6G. Initial R6G fluorescence intensities were recorded. 150 µl R6G loaded HSS- σ1 DDV, HSS- σ1, and HSS were added to each Transwell. At 0, 1, 2, 3, 4, 8, 12, 24, 36, and 48 hours, 50 µl of each sample was collected from the lower compartment of the Transwell setup. Then R6G fluorescence intensities were recorded by GLOMAX MULTI DETECTION SYSTEM (EX 525, EM 580-640). Each experimental group was conducted in triplicate.

Author contributions

T. T. wrote the paper, fabricated HSSs, isolated σ1 protein, assembled HSS- σ1 drug delivery vehicles: σ1 protein and HSS with PLL coating and performed characterization of HSSs, σ1 protein, and HSS- σ1 drug delivery vehicles transport on monolayers. Y. Q. prepared the ISC monolayer system and characterized M cells in 3D and 2D systems. T. T. and Y. Q. performed imaging and analysis of data. L. D. B. assisted in isolating σ1 protein and imaging. C. L. M., Q. W., and C. Y. provided the laboratory and equipment and edited the paper. C. Y. and Q. W. provided financial support for the research. C. L. M., Q. W., and C. Y. supervised the experiment design and execution and provided materials.

Conflicts of interest

There are no conflicts of interest to declare.

Acknowledgments

Finical support: Dr. Wang is grateful for the support from Crohn's & Colitis Foundation (CCF) Career Award (No. 348137) and PhRMA Foundation Research Starter Award (No. RSGTMT17). Dr. Yu would like to thank USDA-NIFA (grant no. 2016-07802) and USDA-ARS (award no. 019636-00001) for partially funding this research.

The authors thank K. Yoon for assistance in T1L σ1 purification and qPCR, B. Bellaire, and N. Peroutka-Bigus for immunofluorescence.

4.5 References

[1] N. Lycke, *Nat. Rev. Immunol.*, , DOI:10.1038/nri3251.

[2] T. Tong, Y. Qi, L. D. Bussiere, M. Wannemuehler, C. L. Miller, Q. Wang and C. Yu, *Nanoscale*, , DOI:10.1039/D0NR03680C.

[3] A. A. Date, J. Hanes and L. M. Ensign, *J. Control. Release*, , DOI:10.1016/j.jconrel.2016.06.016.

[4] L. D. Bussiere, P. Choudhury, B. Bellaire and C. L. Miller, *J. Virol.*, , DOI:10.1128/JVI.01371-17.

[5] J. L. Wolf, R. S. Kauffman, R. Finberg, R. Dambrauskas, B. N. Fields and J. S. Trier, *Gastroenterology*, , DOI:10.1016/0016-5085(83)90313-X.

[6] M. Wang, Z. Gao, Z. Zhang, L. Pan and Y. Zhang, *Hum. Vaccin. Immunother.*, , DOI:10.4161/hv.36174.

[7] A. Helander, K. J. Silvey, N. J. Mantis, A. B. Hutchings, K. Chandran, W. T. Lucas, M. L. Nibert and M. R. Neutra, *J. Virol.*, , DOI:10.1128/JVI.77.14.7964-7977.2003.

[8] S. Wang, *Microporous Mesoporous Mater.*, , DOI:10.1016/j.micromeso.2008.07.002.

[9] M. Sasidharan, H. Zenibana, M. Nandi, A. Bhaumik and K. Nakashima, *Dalt. Trans.*, , DOI:10.1039/c3dt51267c.

[10] R. K. Singh, T.-H. Kim, C. Mahapatra, K. D. Patel and H.-W. Kim, *Langmuir*, , DOI:10.1021/acs.langmuir.5b03436.

[11] S. Kwon, R. K. Singh, T.-H. Kim, K. D. Patel, J.-J. Kim, W. Chrzanowski and H.-W. Kim, *Acta Biomater.*, , DOI:10.1016/j.actbio.2013.10.028.

[12] M. Stobiecka and M. Hepel, *Biomaterials*, , DOI:10.1016/j.biomaterials.2010.12.064.

[13] N. Jatupaiboon, Y. Wang, H. Wu, X. Song, Y. Song, J. Zhang, X. Ma and M. Tan, *J. Mater. Chem. B*, , DOI:10.1039/C5TB00194C.

[14] K. A. Dryden, D. L. Farsetta, G. Wang, J. M. Keegan, B. N. Fields, T. S. Baker and M. L. Nibert, *Virology*, , DOI:10.1006/viro.1998.9146.

[15] I. I. Mendez, L. L. Hermann, P. R. Hazelton and K. M. Coombs, *J. Virol. Methods*, , DOI:10.1016/S0166-0934(00)00217-2.

[16] D. B. Furlong, M. L. Nibert and B. N. Fields, *J. Virol.*, , DOI:10.1128/jvi.62.1.246-256.1988.

[17] T. Sato, R. G. Vries, H. J. Snippert, M. van de Wetering, N. Barker, D. E. Stange, J. H. van Es, A. Abo, P. Kujala, P. J. Peters and H. Clevers, *Nature*, , DOI:10.1038/nature07935.

[18] A. Fatehullah, S. H. Tan and N. Barker, *Nat. Cell Biol.*, , DOI:10.1038/ncb3312.

[19] J. D. Rouch, A. Scott, N. Y. Lei, R. S. Solorzano-Vargas, J. Wang, E. M. Hanson, M. Kobayashi, M. Lewis, M. G. Stelzner, J. C. Y. Dunn, L. Eckmann and M. G. Martín, *PLoS One*, , DOI:10.1371/journal.pone.0148216.

[20] W. de Lau, P. Kujala, K. Schneeberger, S. Middendorp, V. S. W. Li, N. Barker, A. Martens, F. Hofhuis, R. P. DeKoter, P. J. Peters, E. Nieuwenhuis and H. Clevers, *Mol. Cell. Biol.*, , DOI:10.1128/MCB.00434-12.

[21] Y. Yin and D. Zhou, *Front. Cell. Infect. Microbiol.*, , DOI:10.3389/fcimb.2018.00257.

[22] M. B. Wood, D. Rios and I. R. Williams, *Am. J. Physiol. Physiol.*, , DOI:10.1152/ajpcell.00108.2016.

[23] H. Gehart and H. Clevers, *Nat. Rev. Gastroenterol. Hepatol.*, , DOI:10.1038/s41575-018-0081-y.

[24] G. Altay, E. Larrañaga, S. Tosi, F. M. Barriga, E. Batlle, V. Fernández-Majada and E. Martínez, *Sci. Rep.*, , DOI:10.1038/s41598-019-46497-x.

CHAPTER 5. MICROFOLD CELL MODULATED BY RANK L LEVELS IN INTESTINAL MONOLYAERS AFFECTING TRANSPORT EFFICIENCY OF SIGMA-1 FUNCTIOINALIZED NANOCARRIERS

Tianjian Tong[1], Yijun Qi[2], Debarpan Dhar[3,4], Cathy L Miller[3,4], Qun Wang[2]* and Chenxu Yu[1]*

[1]Department of Agricultural Biosystem and Engineering, Iowa State University, Ames, Iowa

[2]Department of Chemical and Biological Engineering, Iowa State University, Ames, Iowa

[3]Department of Veterinary Microbiology and Preventive Medicine, College of Veterinary Medicine, Iowa State University, Ames, Iowa

[4]Interdepartmental Microbiology Program, Iowa State University, Ames, Iowa

Proposed to submit to *Material Science and Engineering C*

Abstract

In this work, we discovered that Microfold cell presence in intestinal organoid monolayers modulated by Rank L levels could dictate transport behaviors of σ1 functionalized nanocarriers. Both gold nanocage with poly-l-lysine (PLL) coating (GNC-PLL-σ1) and hollowed silica nanosphere with poly-l-lysine (PLL) coating (HSS-PLL-σ1) were shown to follow the same trend: when Rank L amount added in intestinal organoids monolayers was higher, Microfold cells (M-cells) developed out of the mouse small intestinal stem cells which were used to construct the organoid monolayers showed characteristics that supported higher transport

efficiency for model payload (rhodamine 6g, R6G) via both σ1 functionalized nanocarriers. To a less content, PLL coating was another factor that impacted the transport behaviors. The synergistic effect of PLL coating and modulated M cell presence contributed to the effective transport of the nanocarriers as potential oral vaccine and/or drug delivery vehicles.

5.1 Introduction

Oral vaccine delivery method has several advantages over traditional injection-based methods (intravenous and subcutaneous)[1–3], including less pain for patients, easier to administer, and better safety assurance[1–3]. From our previous research[1], we developed two functional nanocarriers for oral drug/vaccine delivery that could specifically target microfold cells (M cells) in gastrointestinal epithelia. These hollow nanocarriers (e.g., gold nanocage (GNC) and hollow silica sphere (HSS)) offered better loading capacity than solid particles[1]. To provide protection for the payloads against harsh gastric environment, and to impart release control after the nanocarriers have transported into the mucosal associated lymphoid tissues (MALTs), we introduced poly-l-lysine (PLL) coating which was non-cytotoxic[4], which was shown in the previous chapter to improve the performance of the nanocarriers effectively.

In developing the nanocarrier systems, we explore the MRV transcytosis across M cells pathway (Fig. 5.1a) by functionalizing oral drug delivery vehicles with T1L σ1 protein and with poly-l-lysine coating (PLL). We understand that T1L σ1 protein were critical for oral drug delivery vehicles to explore M cells. The next question is, how the transport efficiency will be affected by M cell. As the M cells were induced in the intestinal organoids monolayer[1] by the

addition of Rank L, it is reasoned that their characteristics will be affected by the Rank L level used. Rank L can express multiple M cell-related genes: Spib, Chemokine (C-C motif) ligand 9, Tnfapi2 (TNF- α-induced protein 2), Anxa5 (annexin A5), and Marcksl1 (myristoylated alanine-rich protein kinase C substrate)[5]However, no research has been done on checking how Rank L level can affect the transport behaviors of nanoparticle-based oral drug delivery vehicles through altering the M cell presence in the organoid monolayer. We hypothesized that higher the Rank L level added to intestinal organoids monolayer, better the M-cell mediated transcytosis pathway would work to facilitate the transport of σ1-functionalized nanocarriers.

To test this hypothesis, we constructed our monolayer testing systems similarly as reported in previous chapters, to mimic the gastrointestinal epithelia. As shown in Fig. 1b, and 1c, we tested gold nanocage (GNC) based nanocarriers functionalized with σ1 protein with/without PLL coating. We also tested a different type of nanocarriers: hollowed silica nanospheres (HSS) with PLL coating functionalized with σ1 protein. All three groups (GNC-σ1, GNC-PLL- σ1, and HSS-PLL- σ1) were loaded with rhodamine 6g (R6G) as model payloads. We tested the transport performance of these three systems on monolayers with three different Rank L levels (200 µl, 100 µl, and 0 µl). To be specific, Rank L level refers to the amount of Rank L incubated with organoids at the preparation stage of small intestinal organoids monolayers. In this way, we can have a better understanding of how Rank L level, PLL coating, and types of nanocarriers would affect the transport performance of our oral drug delivery systems. We will also evaluate the three factors' weight on affecting the OVDV transport performance.

a

b

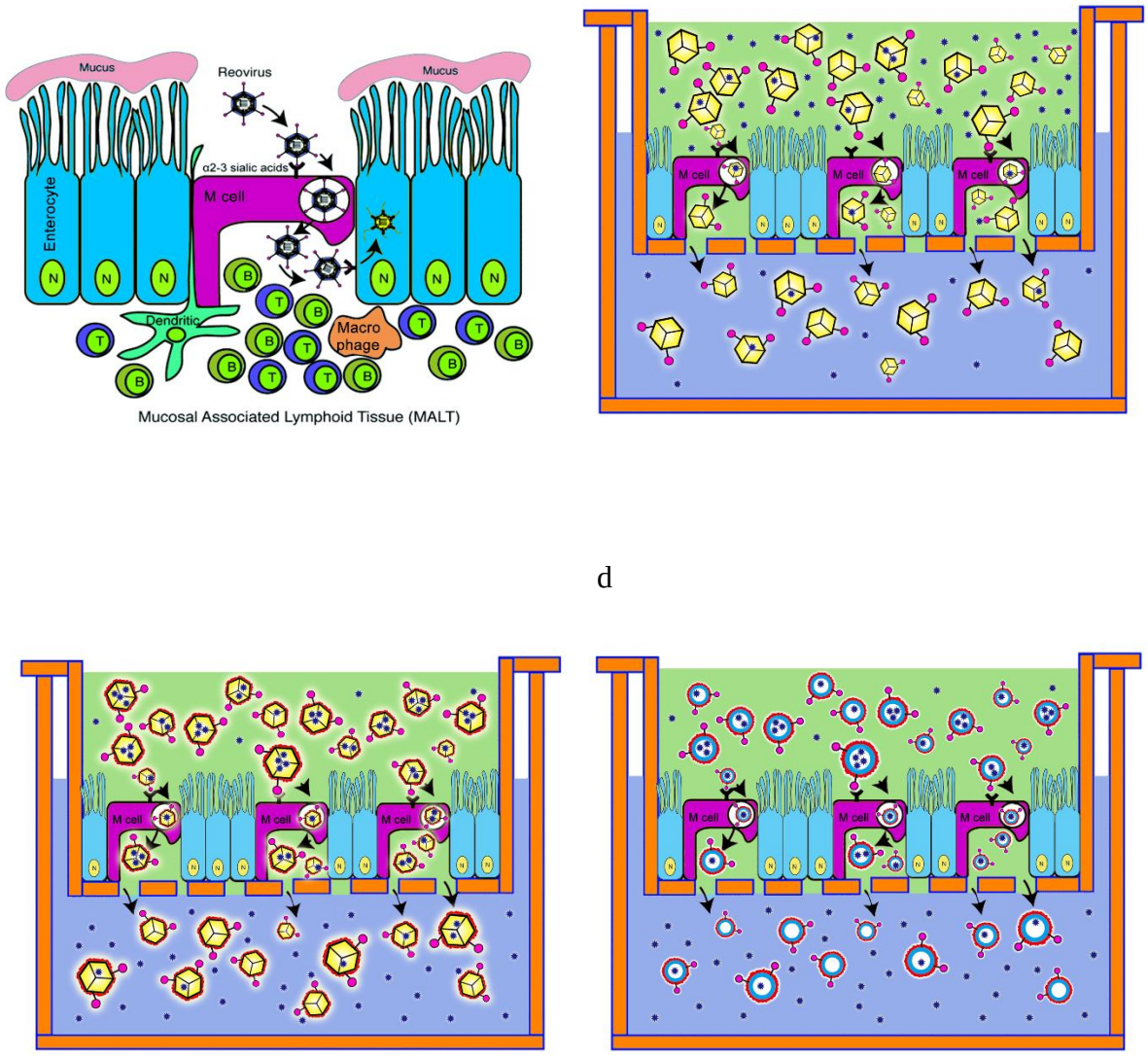

c

d

Fig 5.1: T1L σ1 functionalized GNC-PLL, GNC and HSS-PLL explore M cell transcytosis pathway inspired by MRV infection of MATL. (a) How MRV infection MALT. (b) Transport of R6G loaded GNC-PLL nanocarriers across M cells imbedded intestinal organoid monolayers with different Rank L levels (200 µl, 100 µl, 0 µl). (c) Transport of R6G loaded GNC-PLL-σ1 nanocarriers across M cells imbedded intestinal organoid monolayers with different Rank L levels (200 µl, 100 µl, 0 µl). (d) Transport of R6G loaded HSS-PLL-σ1 nanocarriers across M cells imbedded intestinal organoid monolayers with different Rank L levels (200 µl, 100 µl, 0 µl).

5.2 Results and discussion

5.2.1 GNC and HSS nanocarriers: σ1 functionalization and poly-L-lysine coating

Both gold nanoparticles and silica nanoparticles were very commonly used in oral drug and vaccine delivery research[6–14]. To improve the oral drug/vaccine delivery vehicles, something with hollowed structures were desired, because of the superior loading capacities compares to the 2D structures[1,15]. Gold nanocage (GNC) were synthesized by galvanic replacement reaction consist of two stages[14,16]. In stage one, silver nanocubes were synthesized to serve as templates. Then, in stage two galvanic replacement reaction was utilized to exchange gold into the sacrificing templates (silver nanocubes). As shown in Fig. 5.2a, from transmission electron microscopy (TEM) image, GNC thus fabricated showed an average size of 40 nm with holes on the surface. The holes were visible as color difference between the interior of GNC and the shell. Synthesis of Hollowed silica nanospheres (HSS) was conducted with reverse microemulsion as templates[15]. The microemulsion templates were produced by mixing water phase and oil phase together for 24 hours at room temperature as described in the previous chapter[15]. Fig. 5.2b showed the transmission electron microscopy (TEM) image of the HSS. The average size of the particles was about 100 nm. Hollowed interior was also observed in the HSS. T1L MRV σ1 protein was obtained from the previously purified MRV as descried in the previous chapters[1,17–19]. Western blot by using T1L virion antibody was carried out to verify the exist of σ1 protein. In Fig. 5.2c, we can clear see that the band at ~52 KDa which is the σ1 protein (left lane).

a b

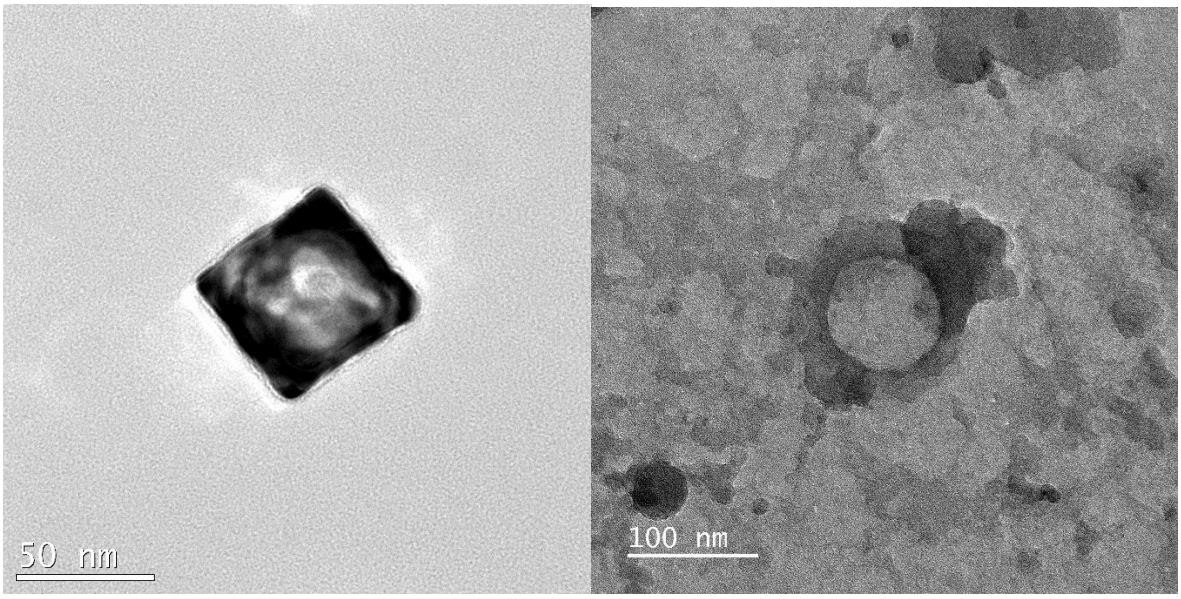

c

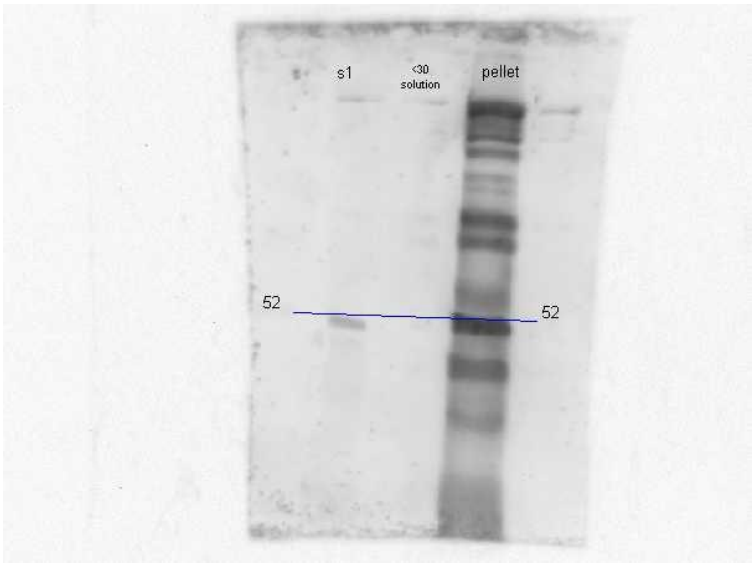

Fig 5.2 MRV σ1 functionalization of GNCs and HSSs. (a) TEM image of GNCs showing an average diameter of 40 nm. (b) TEM image of HSSs showing an average diameter of 100 nm. (c) Western blot for pellets after last centrifugation, control group, and T1L σ1 protein (50 kDa). Following purification, T1L σ1 protein was concentrated by a 30 kDa filter (left lane). Both 30 KDa Filtrated solution (middle lane) and pellets (right lane) are served as the control group.

5.2.2 Transportation of nanocarriers through Rank L modulated organoids monolayers

The transport behaviors of HSS- σ1-PLL, GNC- σ1-PLL, and GNC- σ1, with small molecule dye (rhodamine 6G, R6G) as payload, were tested on all three types of transwell organoid monolayer systems treated with Rank L at three levels (i.e., 0 µl, 100 µl, 200 µl Rank L). A fourth level (400 µl Rank L) was also investigated. However, at this level the organoid could not grow normally, hence it was not pursued further.

The transport of the nanocarriers was facilitated via the σ1-M cell transcytosis pathway, as described in previous chapters. Both σ1 and M cells were required for this transcytosis to happen. As pervious mentioned, Rank L was added to organoids to induce M cells.

The transport of various nanocarriers was monitored by measuring the movement of the payloads, R6G, across the organoid monolayers. At time points of 0, 1, 2, 3, 4, 8, 12, 24, 36, and 48 hours, from initial addition of R6G-loaded HSS- σ1-PLL, GNC-σ1-PLL, and GNC-σ1 into the top compartment of transwells, samples were taken from the lower compartments of each of the transwell to quantify the delivered payload R6G via its fluorescence intensity. The fluorescence intensity data were then normalized against each group's total initial R6G fluorescence intensity. The percentage delivered for each group represented how much of payloads were transported across the organoids monolayers in each case.

As showed in Fig 5.3, when 0 µl of Rank L added, all three groups showed low baseline transport. To be more specific, HSS- σ1-PLL and GNC- σ1-PLL had similar performance (14%), while GNC- σ1 had a slight edge over the other two groups (17%). With 0 µl Rank L, no M cell

was induced in the organoid monolayer, hence, no σ1-M cells mediated transcytosis could have happened. It was reasoned that the payloads that crossed over were indeed the ones that leaked out (via diffusion) of the nanocarriers in the upper compartment, then diffused through the monolayer as small molecules do. The difference between coated (i.e., the –PLL groups) and uncoated group was an indication of the different leakage level: PLL coating apparently cut that down.

At 100 µl Rank L level, all three groups (HSS-σ1-PLL, GNC- σ1-PLL, and GNC- σ1) showed similar transport performance again at ~26%, went up significantly from the control groups (with no Rank L). At 200 µl Rank L level, the transport performance was further improved across all groups: HSS-σ1-PLL and GNC-σ1-PLL showed similar transport performance around 44%, and GNC-σ1 group was lower at 36.7%.

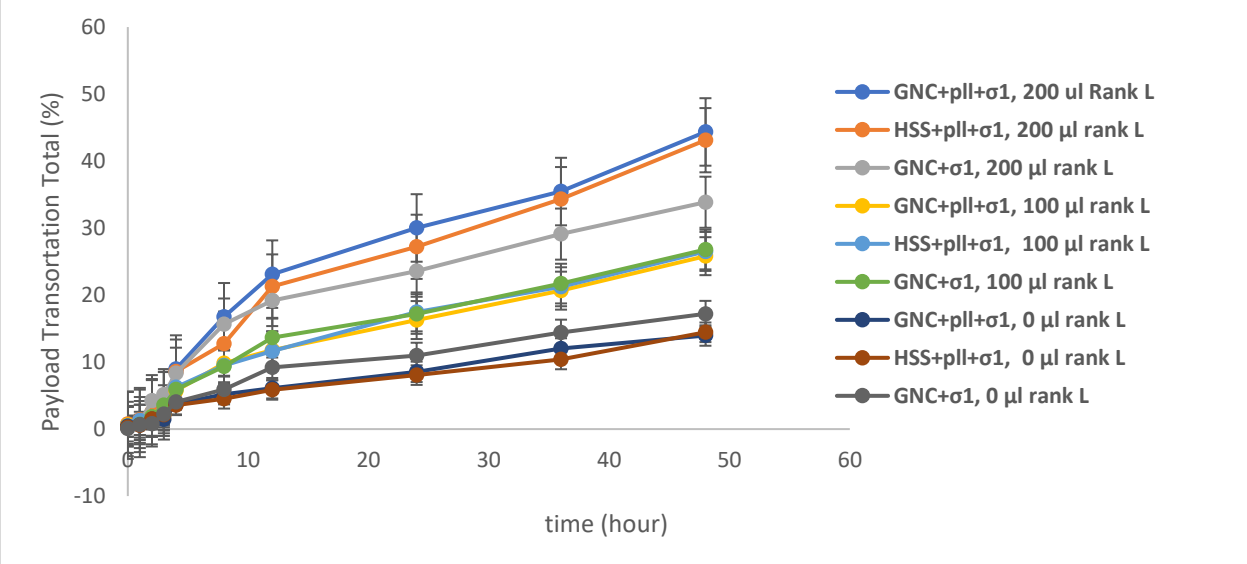

Fig 5.3 Payload (R6G) in different vaccine delivery vehicle (GNC-PLL- σ1, GNC- σ1, HSS-PLL-σ1) transport across intestinal monolayers with different Rank L level (200 µL, 100 µL, 0 µL).

In additional, when we checked the net transport of R6G for organoid monolayer with both 100 μL and 200 μL Rank L levels (by subtracting out the baseline transport at level of 0 μL Rank L), we had an interesting situation at our hand. As showed in Fig. 5.4a, at 100 μL Rank L level, the net transport of GNC- PLL-σ1 went up significant at 8 hours and beyond compared to GNC- σ1. For the first 8 hour, the higher level of R6G of GNC- σ1 system was very likely due to the lack of PLL coating. At 200 μL Rank L level, the transport of GNC- PLL-σ1 went up significant at 4 hours and beyond compared to GNC- σ1, this result was similar to what was reported in the previous chapter for HSS based nanocarriers. The reason of higher level of R6G of GNC- σ1 group was also likely due the lack of PLL coating. As to the difference between the timing for GNC-PLL- σ1 overtaking GNC- σ1 for the groups with different Rank L levels, it is likely caused by the different transport efficiency between these two cases that was tied to the M cell behavior modulated by the Rank L, which would require further investigation. These results indicated that both Rank L level and PLL coating are factors that affect the transport behavior of our nanocarriers.

When we take a look at the whole picture, as show in Fig. 5.4b, GNC-PLL-σ1 group at 200 μL Rank L level had the most efficacy transporting payload across the organoid monolayers, through the σ1-M cell α2–3 sialic acid transcytosis pathway. Compared with GNC-σ1 group at 200 μL Rank L level, the net transport of our payload increased from 20% to 30% at the 48-hour time mark. This result is similar to our previous work for HSS nanocarriers, indicating that PLL coating could slow down the diffusion rate of the payload out of the nanocarriers. The PLL coating can not only protect the payloads from the tough gastric environment, but also extend the release of payload at the desired destination of the delivery. When we do the same comparison at 100 μL Rank L level, the net transport of our payload only increased from 10% to 12%. This

indicated that the PLL coating's effect can be limited by decreasing Rank L level, which was affecting the M cell behavior in a more direct way.

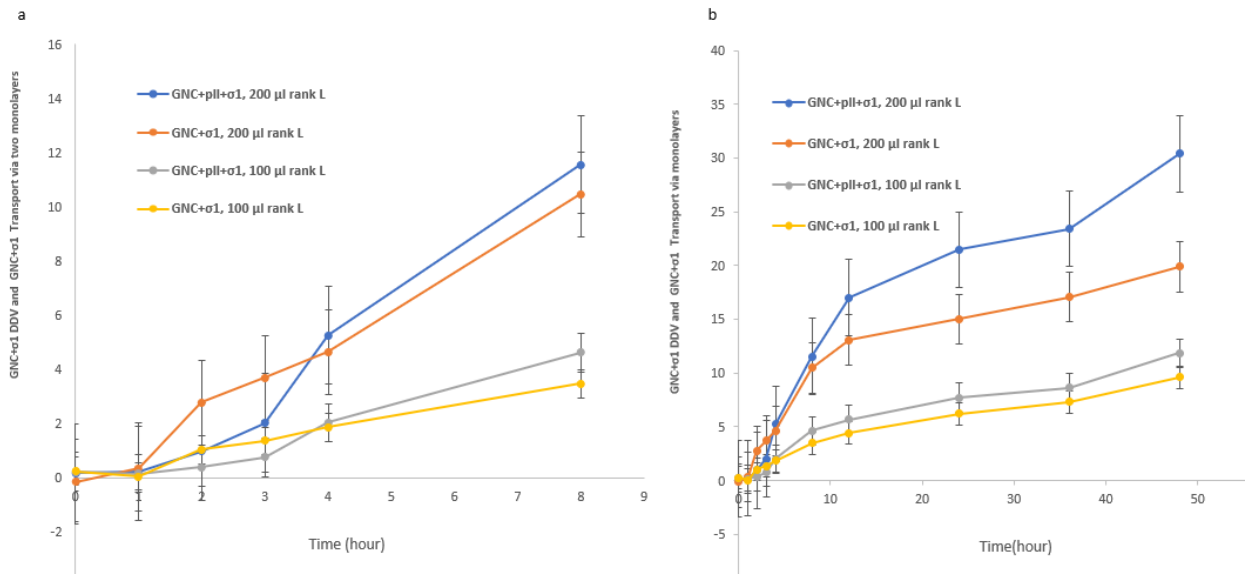

Fig 5.4 (a) GNC-PLL-σ1, GNC-σ1 transport total through intestinal monolayers with different Rank L level (200 µL, 100 µL) from time point 0-8 hour (b) GNC-PLL-σ1, GNC-σ1 transport total through intestinal monolayers with different Rank L level (200 µL, 100 µL) from 0-48 hour.

From Fig. 5.3 we can conclude the transport behaviors of GNC-PLL-σ1 and HSS-PLL-σ1 are similar. To further check if this conclusion stands, we check the net transport of both GNC-PLL-σ1 and HSS-PLL-σ1 at different Rank L levels (200 µL, 100 µL). We used the same methods by using 0 µL Rank L case as our baseline. Then we get the normalized net transport of GNC-PLL-σ1 and HSS-PLL-σ1. In Fig. 5.5, we can see that the net transport of GNC-PLL-σ1 and HSS-PLL-σ1 at both Rank L levels was similar. At 200µL Rank L level, for both cases results showed much better net transport comparing to those cases at 100 µL Rank L level. To be specific, GNC-PLL-σ1 at 200 µL Rank L level had a net transport of 30% at 48-hour time point, comparing to 11.8% at 100 µL Rank L level. HSS-PLL-σ1 at 200 µL Rank L level have a net

transport of 28.6% at 48-hour time point, comparing to 12% at 100 µL Rank L level. Extra 100 µL Rank L improved the net transport by 154% for GNC-PLL-σ1 and 138% for HSS-PLL-σ1. This indicated that the key to the M cell mediated transport was the M cells themselves. These results clearly suggested that the discrepancy in transport of payloads caused by different nanocarriers systems was the least affected by the type of nanoparticles used. Whether the nanocarriers are GNC or HSS, our strategy of utilizing the σ1-M cell mediated transcytosis pathway worked equally effectively, as long as the M cell characteristics dictated by the Rank L level remained the same.

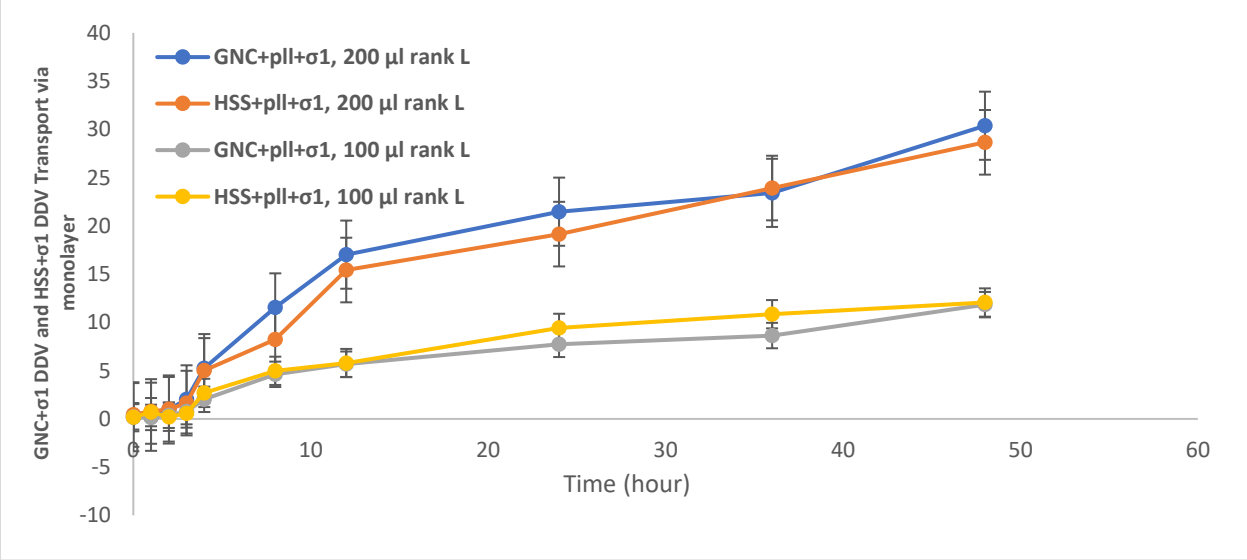

Fig 5.5 GNC- PLL-σ, HSS-PLL-σ1 transport total through intestinal monolayers with different Rank L level (200 µL, 100 µL).

5.3 Conclusion

To summarize, we are reporting universal set up of oral drug delivery vehicles utilizing σ1-M cell mediated transcytosis pathway for payload transport across gastrointestinal epithelia. By testing different types of nanocarriers' (GNC-PLL-σ1 and HSS-PLL-σ1) at different Rank L levels, it was established that higher (200 μL) Rank L treatment triggered changes in M cell behavior in the intestinal organoids monolayer which significantly changed the effectiveness of the transcytosis pathway, net transport went up by 154% and 138%, respectively for the two coated nanocarriers comparing to the cases with lower (100 μL) Rank L treatment. PLL can improve the net transport of payloads by 66.7% at 200 μL Rank L level, and 20% at 100 μL Rank L level for GNC systems. For the three factors that played determining roles in this oral drug delivery system, Rank L level (i.e., M cell characteristics) was more significant than PLL coating, and types of nanocarriers were almost a non-factor. Future research is needed to further enlighten how M cell presence was affected by Rank L that led to these changes in σ1-M cell mediated transcytosis pathway.

5.4 Experimental

5.4.1 GNC and HSS fabrication

GNCs Step one: Ethylene glycol (EG) (Sigma-Aldrich) (6 ml) was heated four 1 hour in a 160 °C oil bath with stirring. Polyvinylpyrrolidone (PVP) (Sigma-Aldrich) (0.07 g) was added into 3.5 ml EG solution, mixture was required. AgNO3 (Sigma-Aldrich) (0.12 g) was solved into 2.5 mg EG solution and mixture was required.

Then 3 mM NaSO4 (Acros) was solved EG solution. Then 70 μl of sodium sulfide solution was added into the ethylene glycol EG solution which are in the oil bath. After 15 minutes, 1.5 ml PVP solution and 0.5 ml silver nitrate solution was added. After 10-15 minutes of reaction, acetone was added into the solution to stop the reaction. Then the solution was centrifuged for 30 minutes at 1,300 rpm. 1 mL of DI-water were added to the pellet. Then re-disperse the pellet by sonicating for 1 hour. This wash step needs to be repeated for two more times.

GNCs step two: 20 mL of DI-water is put into a glass vile, 20 mg of PVP was added to DI-water. Then heat and stir the PVP solution to 245 °C and 220 rpm. When PVP solution were heated to boil, add 200 μL of silver nanocubes made in step one. After 10-15 minutes, adding 2 μL of HAuCl4 (Sigma-Aldrich) every 2 minute, until the mixture solution turns to blue. The wash step is also required. Centrifuge at 2,000 g for 30 minutes at room temperature, then get rid of the supernatant and add new DI-water in. Then re-disperse the pellet by sonicating for an hour. Then centrifuge at 9,000 g for 10 minutes, get rid of the supernatant and re-disperse. The last step needs to be repeated once.

HSSs: HSSs synthesis consists of two phases mixing together at room temperature. Water phase was prepared by mix 3 μL of (3-aminopropyl) triethoxysilane (APS) (Acros Organics) and 1.1 ML DI-water together. Oil phase was prepared by mixing 4.47 or Triton X-100 (Acros Organics), 3.64g of n-octanol (Fisher) and 14.5 g of cyclohexane (Fisher) together. Then the water phase was collected and added into the oil phase. After mixing for 30 minutes, 200 μL of NH4OH and tetraethylorthosilicate (TEOS) (Acros Organics) were add into water-oil mixing. The reaction was stirred at room temperature for 24 hours. Acetone was added into the solution

to stop the reaction. Then three times wash with ethanol and three times wash with DI-water was needed[15].

5.4.2 T1Lσ1 isolation and purification

Type 1 Lang (T1L) MRV was grown in the L929 cells inside of a spinner [1]. Then the cells were collected by centrifuge 10 minute at 3,000g. HO buffer (250 mM NaCl, 10 mM Tris, pH 7.4) was added into the pellet to re-disperse the cells. The solution was then store at −80 °C[1,17]. The purification of the virus was followed same protocol as our previous work[1]. The purification was achieved by replace Freon by substitution of Vertrel ® XF (DuPont)[1]. Following purification step, we use α-chymotrypsin digestion method to get ISVPs After the purification of ISVPs, ISVPs was heated for 30 minutes at 52 °C[1]. Then the heated ISVPs were centrifuged for 4 hours at 35,000 rpm. The σ1 protein were expected to in the supernatant[1,17]. Then Centricon-30 microconcentration unit (Amicon Crop.)[1,17] were untilized to concentrate the σ1 protein.

5.4.3 GNC and HSS functionalization

GNC-σ1: GNC was linked to σ1 protein with (1-ethyl-3-(3-dimethylaminopropyl) carbodiimide hydrochloride) (EDC) (Thermo scientific)/N-hydroxysulfosuccinimide (NHS) (Sigma-Aldrich) procedure. 4- Aminothiophenol were added to the GNC solution and shaking overnight. Then the mix solution was centrifuged for 10 minutes at 9,000g. After getting rid of the supernatant, Di-water was added to re-dispersed the pellet. EDC/NHS solution was added to GNCs and incubated for 30 minutes at room temperature. Then T1L MRV σ1 protein was added to GNC solution and incubated 4°C overnight. Then solution was centrifuged at 6,500g for 30 minutes. Then R6G were added into the GNC-σ1 solution, incubation at 4 °C is required.

GNC-PLL-σ1: poly-l-lysine (PLL) (w/v 0.1%) and 200 µl R6G were added into 2ml GNC solution, incubation at 4 °C. Then the solution was centrifuged for 10 minutes at 9,000 g.

Then we get rid of the supernatant and add DI-water to re-disperse GNC-PLL. Then we use (1-ethyl-3-(3-dimethylaminopropyl) carbodiimide hydrochloride) (EDC) (Thermo scientific)/N-hydroxysulfosuccinimide (NHS) (Sigma-Aldrich) mix solution to link T1L MRV σ1 protein ono GNC-PLL. After EDC/NHS were added to GNC-PLL, 30 minutes of incubation were required. And the centrifuge for 30 minutes at 6,500g. After the excessive EDC/NHS were removed. T1L MRV σ1 protein were then added to HSS-PLL and incubation needs to be carried at 4°C overnight.

HSS-PLL-σ1: poly-l-lysine (PLL) (w/v 0.1%) and 200 μl R6G were added into 2ml HSS solution, and incubation at 4 °C. Then the solution was centrifuged for 10 minutes at 9,000 g. Then we get rid of the supernatant and add DI-water to re-disperse HSS-PLL. Then we use (1-ethyl-3-(3-dimethylaminopropyl) carbodiimide hydrochloride) (EDC) (Thermo scientific)/N-hydroxysulfosuccinimide (NHS) (Sigma-Aldrich) mix solution to link T1L MRV σ1 protein ono HSS-PLL. After EDC/NHS were added to HSS-PLL, 30 minutes of incubation were required. And the centrifuge for 30 minutes at 6,500g. After the excessive EDC/NHS were removed. T1L MRV σ1 protein were then added to HSS-PLL and incubation needs to be carried at 4°C overnight.

5.4.4 Western blot for verifying the presence of σ1 protein

We used western blotting method to identify the presence of σ1 protein. For primary antibody, we used Rabbit T1L virion antibody (1:1000) and secondary antibody of goat anti-rabbit IgG (1:2500). After wash with TBST for three times, we take the image[20].

5.4.5 Minigut monolayer development

We used the method that have been previous reported[21]. 200 ng ml^{-1} was added at the third day, and extra 2 days of incubation is carried out. Then we disrupted and pipetted 3D structures organoids and added onto transwell, we then added 200 ng ml^{-1}, 100 ng ml^{-1}, and 0 Rank L into the top and lower compartment of transwell system.

5.4.6 Transport of GNC-PLL-σ1, HSS-PLL-σ1, and GNC-σ1 across intestinal monolayers in a Transwell model system

GNC-PLL-σ1, HSS-PLL-σ1, and GNC-σ1 all loaded with R6G as our payload in this test. Before adding, the R6G fluorescence intensities were recorded. 150 μl of each R6G loaded oral drug devilry vehicles were added to the top compartment of the transwell systems. We took 50 μl of each sample was sampled from the lower compartment of the transwell systems to test fluorescence intensities at time point of 0, 1, 2, 3, 4, 8, 12, 24, 36, and 48 hours. Triplicate groups were tested for all three oral drug delivery vehicles.

Author contributions

T. T. wrote the paper, fabricated GNCs, HSSs, isolated σ1 protein, assembled GNC-σ, GNC-PLL-σ1 and HSS-PLL-σ1 as drug delivery vehicles, and performed characterization of GNCs, HSSs, σ1 protein, testing all three oral drug delivery vehicles: GNC-σ, GNC-PLL-σ1, and HSS-PLL-σ1 transporting performance on monolayers. Y. Q. prepared the ISC monolayer system. T. T. and Y. Q. performed imaging and analysis of data. D.D. assisted in isolating σ1 protein and imaging. C. L. M., Q. W. and C. Y. provided the laboratory and equipment and assisted in editing the paper. C. Y. and Q. W. provided the financial support for the research. C. L. M., Q. W. and C. Y. supervised the experiment design and execution and provided materials.

Conflicts of interest

There are no conflicts of interest to declare.

Acknowledgements

Financial support: Dr. Wang is grateful for the support from Crohn's & Colitis Foundation (CCF) Career Award (No. 348137) and PhRMA Foundation Research Starter Award (No. RSGTMT17). Dr. Yu would like to thank USDA-NIFA (grant no. 2016-07802) and USDA-ARS (award no. 019636-00001) for partially funding this research.

The authors thank K. Yoon for assistance in T1L σ1 purification and qPCR, B. Bellaire, and N. Peroutka-Bigus for immunofluorescence.

5.5 References

[1] T. Tong, Y. Qi, L. D. Bussiere, M. Wannemuehler, C. L. Miller, Q. Wang and C. Yu, *Nanoscale*, , DOI:10.1039/D0NR03680C.

[2] N. Lycke, *Nat. Rev. Immunol.*, , DOI:10.1038/nri3251.

[3] A. A. Date, J. Hanes and L. M. Ensign, *J. Control. Release*, , DOI:10.1016/j.jconrel.2016.06.016.

[4] M. Stobiecka and M. Hepel, *Biomaterials*, , DOI:10.1016/j.biomaterials.2010.12.064.

[5] M. B. Wood, D. Rios and I. R. Williams, *Am. J. Physiol. Physiol.*, , DOI:10.1152/ajpcell.00108.2016.

[6] S. Wang, *Microporous Mesoporous Mater.*, , DOI:10.1016/j.micromeso.2008.07.002.

[7] M. Sasidharan, H. Zenibana, M. Nandi, A. Bhaumik and K. Nakashima, *Dalt. Trans.*, , DOI:10.1039/c3dt51267c.

[8] R. K. Singh, T.-H. Kim, C. Mahapatra, K. D. Patel and H.-W. Kim, *Langmuir*, , DOI:10.1021/acs.langmuir.5b03436.

[9] S. Kwon, R. K. Singh, T.-H. Kim, K. D. Patel, J.-J. Kim, W. Chrzanowski and H.-W. Kim, *Acta Biomater.*, , DOI:10.1016/j.actbio.2013.10.028.

[10] A. E. Gregory, R. Titball and D. Williamson, *Front. Cell. Infect. Microbiol.*, , DOI:10.3389/fcimb.2013.00013.

[11] L. Zhao, A. Seth, N. Wibowo, C.-X. Zhao, N. Mitter, C. Yu and A. P. J. Middelberg, *Vaccine*, , DOI:10.1016/j.vaccine.2013.11.069.

[12] V. Pokharkar, D. Bhumkar, K. Suresh, Y. Shinde, S. Gairola and S. S. Jadhav, *J. Biomed. Nanotechnol.*, , DOI:10.1166/jbn.2011.1200.

[13] J. P. M. Almeida, E. R. Figueroa and R. A. Drezek, *Nanomedicine Nanotechnology, Biol. Med.*, , DOI:10.1016/j.nano.2013.09.011.

[14] S. E. Skrabalak, J. Chen, Y. Sun, X. Lu, L. Au, C. M. Cobley and Y. Xia, *Acc. Chem. Res.*, , DOI:10.1021/ar800018v.

[15] N. Jatupaiboon, Y. Wang, H. Wu, X. Song, Y. Song, J. Zhang, X. Ma and M. Tan, *J. Mater. Chem. B*, , DOI:10.1039/C5TB00194C.

[16] S. E. Skrabalak, L. Au, X. Li and Y. Xia, *Nat. Protoc.*, , DOI:10.1038/nprot.2007.326.

[17] D. B. Furlong, M. L. Nibert and B. N. Fields, *J. Virol.*, , DOI:10.1128/jvi.62.1.246-256.1988.

[18] K. A. Dryden, D. L. Farsetta, G. Wang, J. M. Keegan, B. N. Fields, T. S. Baker and M. L. Nibert, *Virology*, , DOI:10.1006/viro.1998.9146.

[19] I. I. Mendez, L. L. Hermann, P. R. Hazelton and K. M. Coombs, *J. Virol. Methods*, , DOI:10.1016/S0166-0934(00)00217-2.

[20] L. D. Bussiere, P. Choudhury, B. Bellaire and C. L. Miller, *J. Virol.*, , DOI:10.1128/JVI.01371-17.

[21] T. Sato, R. G. Vries, H. J. Snippert, M. van de Wetering, N. Barker, D. E. Stange, J. H. van Es, A. Abo, P. Kujala, P. J. Peters and H. Clevers, *Nature*, , DOI:10.1038/nature07935.

CHAPTER 6. FUTURE PERSPECTIVE

As shown in this research, σ1 protein can interact with α 2-3 sialic acids and explore transcytosis through M cells. We use both gold nanocages and hollowed silica spheres as our drug delivery vehicles. σ1 protein was used to modify gold nanocages and hollowed silica spheres. In this way, our gold AVN and silica AVN can both explore the transcytosis through M cells in small intestinal organoids. Thus, we established universal drug delivery vehicles with σ1 protein on the surface. These drug delivery vehicles shown high potential of providing universal oral drug/vaccine delivery solutions *in vitro*.

Next step of this research will be to test the protection of the PLL coating of AVNs in harsh acidic gastric environment. As a first step, we can setup simulated gastric/intestinal digestion models and evaluate whether the PLL coating can effectively reduce degradation of payloads. Throughout this study we used r6g as our model payload due to its easily trackable nature as a fluorophore. The next testing step is to use a more real immunogen mimic, such as ovalbumin, to serve as payload and track its uploading/unloading dynamics to better understand the potential of the AVNs as vaccine delivery vehicles.

In vivo test will be the ultimate test. Instead of using R6G as the payload in vitro monolayer test, certain antigen will be loaded into our AVNs, and the immune response will be tested on mice/rabbit, to evaluate whether the efficacy of the immunogens was indeed elevated. With positive *in vivo* test results, the AVNs would truly be proven to be effective oral vaccine delivery vehicles that can be further explored for novel vaccine development. Given what the world just went through during the COVID19 pandemic, vaccine is more important than ever for the general benefit of human beings. Immunoglobulin A (IgA) is a specific antibody existed in the guts and mucosal space, we can utilize the Secret IgA inside mucosal space and oral vaccine delivery

methods to trigger Covid-19 specific SIgAs and trigger better immunes defense for Covid-19 for the human body.